2009

New scorpionate ligands for catalysis and synthesis of oligocholate foldamers with various spacers using " click " chemistry

Jiachun Su
Iowa State University

New scorpionate ligands for catalysis and synthesis of oligocholate foldamers with various spacers using " click " chemistry

by

Jiachun Su

A thesis submitted to the graduate faculty

in partial fulfillment of the requirements for the degree of

MASTER OF SCIENCE

Major: Organic Chemistry

Program of Study Committee:
Yan Zhao, Major Professor
Aaron D. Sadow
Nichola L. Pohl

Iowa State University

Ames, Iowa

2009

TABLE OF CONTENTS

ABSTRACT

This thesis contains two chapters. The first chapter describes the design and synthesis of new oxazoline-based scorpionate ligands: the achiral compound hydrogen *tris*(4,4-dimethyl-2-oxazolinyl)phenylborate (H[To^{M}]) as well as the chiral compound lithium *tris*((4*S*)-4-isopropyl-2-oxazolinyl)phenylborate (Li[To^{P}]) and its protonated form hydrogen *tris*((4*S*)-4-isopropyl-2-oxazolinyl)phenylborate (H[To^{P}]). A series of ruthenium ((4*S*)-4-isopropyl-2-oxazolinyl) phenylborate complexes with different co-ligands, including {ruthenium(II)[κ^3–*tris*((4*S*)-4-isopropyl-2-oxazolinyl)phenylborate]*tris*(acetonitrile)}*tetra*phenylborate {[Ru(κ^3–To^{P})(CH$_3$CN)$_3$]}BPh$_4$, [ruthenium(II)*tris*((4*S*)-4-isopropyl-2-oxazolinyl)phenylborate (η^6-*p*-cymene)]chloride [Ru(κ^3–To^{P})(η^6–*p*-cymene)]Cl and ruthenium(II)[κ^3–*tris*((4*S*)-4-isopropyl-2-oxazolynyl)phenylborate](η^4-cyclooctadiene)hydride Ru(κ^3–To^{P})(η^4-COD)H were designed and synthesized. The structure of [Ru(κ^3–To^{P})(CH$_3$CN)$_3$]BPh$_4$ has been determined through NMR analysis and single-crystal X-ray diffraction. The κ^3 coordination mode of ligand To^{P} was conformed in [Ru(κ^3–To^{P})(CH$_3$CN)$_3$]BPh$_4$, which is similar to *tris*(pyrozolyl)borate ligand Tp. Acetonitrile ligands in [Ru(κ^3–To^{P})(CH$_3$CN)$_3$]BPh$_4$ are labile and could be replaced by pyridine, triphenylphosphine and trimethylphosphine. Reactivity of [Ru(κ^3–To^{P})(CH$_3$CN)$_3$]BPh$_4$ has been systematically explored in several catalytic reactions, including allylic alkylation, dimerization of phenylalkynes and hydroamination. [Ru(κ^3–To^{P})(CH$_3$CN)$_3$]BPh$_4$ was found to be effective in catalyzing dimerization of phenyl alkynes. All the compounds: {[Ru(κ^3–To^{P})(CH$_3$CN)$_3$]}BPh$_4$, [Ru(κ^3–To^{P})(η^6–*p*-cymene)]Cl and Ru(κ^3–To^{P})(η^4-COD)H require further characterizations.

The second chapter describes the design and attempted synthesis of several oligocholate foldamers. Extended oligocholates with various spacers in between the second and third cholate units were to be constructed through “click” chemistry, and labeled with 1-naphthylamine and dansyl chloride at the chain ends. The synthesis route has been paved out through the careful synthesis and characterization of different building blocks. New

approaches to monomer synthesis and new ways to construct the oligomers, which are expected to speed up the research in the future, were established during the exploration. Further efforts in the synthesis and fluorescence energy resonances transfer FERT studies on the conformation change are needed to complete the project. Experimental conditions of FERT and possible results of conformation changes are discussed.

CHAPTER 1. INTRODUCTION

This thesis consists of two chapters. The first chapter describes the preparation and characterization of two scorpionate ligands and the attempted synthesis and application in several catalytic reactions of their ruthenium complexes. The research was conducted in Prof. Aaron Sadow's Lab. The synthesis of the ligands contributed to two publications. The second chapter presents the attempted synthesis of a series of spaced cholate foldamers using "click" chemistry for the purpose of studying chain flexibility tolerance in the conformation change. The second part was under Prof. Yan Zhao's guidance. Preceding the first chapter is the general introduction. Following each chapter is the acknowledgments section.

CHAPTER 2. NEW SCORPIONATE LIGANDS FOR CATALYSIS

1. Abstract

This chapter describes the design and synthesis of new oxazoline-based scorpionate ligands: the achiral compound hydrogen *tris*(4,4-dimethyl-2-oxazolinyl)phenylborate (H[To^{M}]) and the chiral lithium/hydrogen *tris*(4*S*-isopropyl-2-oxazolinyl)phenylborate (Li/H[To^{P}]). Synthesis of initial characterization of {ruthenium(II)[κ^3–*tris*((4*S*)-4-isopropyl-2-oxazolinyl)phenylborate]*tris*(acetonitrile)}*tetra*phenylborate {[Ru(κ^3–To^{P})(CH$_3$CN)$_3$]}BPh$_4$, [ruthenium(II)*tris*((4*S*)-4-isopropyl-2-oxazolinyl)phenylborate (η^6-*p*-cymene)]chloride [Ru(κ^3–To^{P})(η^6–*p*-cymene)]Cl and ruthenium(II)[κ^3–*tris*((4*S*)-4-isopropyl-2-oxazolynyl)phenylborate](η^4-cyclooctadiene)hydride Ru(κ^3–To^{P})(η^4-COD)H compounds are discussed. {[Ru(κ^3–To^{P})(CH$_3$CN)$_3$]}BPh$_4$ was applied as a catalyst in several allylic alkylation reactions, hydroamination reactions, and the dimerization of phenylalkynes. It was found that {[Ru(κ^3–To^{P})(CH$_3$CN)$_3$]}BPh$_4$ is effective in catalyzing the dimerization of phenylalkynes.

2. Introduction

Poly(pyrozolyl)borates were first introduced by Trofimenko in the 1960's.[1] This family of ligands has drawn much attention ever since,[2] due to its unique coordination features. Poly(pyrozolyl)borates are anionic, which makes them more electrostatically attracted to the metal center, and they are capable of donating six electrons to the metal through the pyridine-like coordination of the 2-N (Chart 1B) on the pyrazoles or substituted pyrazoles. Their coordination ability resembles the well-established cyclopentadiene system (Chart 1A), and has even more potential for development. However, it was found that in a range of transition metal complexes, ligand isomerization via 1,2-sigmatropic shifts and decomposition through the B-N bond hindered their possible utility in catalysis.[3] In order to overcome these problems, the Sadow group prepared a related scorpinate ligand system by

replacing the pyrazole with oxazoline, in hope that the C-B bond would be able to avoid the reported isomerization and decomposition.[3] (Chart 1C)

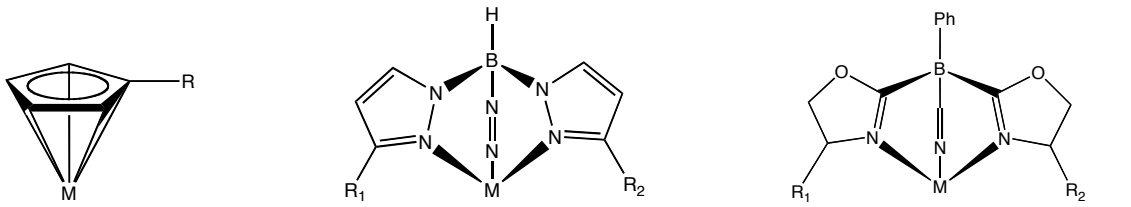

A B C

Chart 1. (A) cyclopentadiene metal compound (B) *tris*-pyrozolylborate metal compound (C) *tris*-oxazolinylborate metal compound

Research on C_3-symmetric trisoxazolines was initiated in the 1990's by Sorrell's group.[4] The first reported tripodal trisoxazoline, *tris*[4,4-dimethyl-2-(5-dihydrooxazolyl)]methylamine employed the nitrogen atom as a core for the three oxazoline units. (Chart 2A, $R_1 = R_2 = CH_3$.) Two years later, the first chiral *tris*(oxazolyl)methylamine, derived from nitrilotriacetate, was developed by Katsuki's group.[5] (Chart 2A, R_1 = H, R_2 = ^{i}Pr, ^{t}Bu, Bn, *p*-(*t*-Bu)C_6H_4, *p*-$MeOC_6H_4$, *p*-ClC_6H_4, 2-Naphthyl.) It was found that the core nitrogen atom of trisoxazoline in Chart 2A did not coordinate to the metal centre (e.g. copper) or influence the structure of the catalytic species. Another type of C_3-symmetric *tris*(oxazoline) ligand (Chart 2B), similar to *tris*(oxazolyl)methylamine but with a carbon atom as the core, was also developed by Katsuki's group in 2000.[6] (Chart 2B, R_1 = H, R_2 = 4-$CF_3OC_6H_4$, ^{i}Pr or R_1 = Ph, 4-$MeOC_6H_4$, R_2 = H.). Gade et. al.[7] later developed modular synthesis of 1,1,1-*tris*(oxazolinyl)ethane derivatives (Chart 2C, $R_1 = {}^{i}Pr$, $R_2 = {}^{t}Bu$ or ^{i}Pr, $R_1 = {}^{t}Bu$, $R_2 = {}^{i}Pr$ or ^{t}Bu.) by coupling lithiated bisoxazolines with 2-bromooxazolines. The strategy established the lithiated bisoxazolines as a potential useful tool in the synthesis of homochiral as well as heterochiral *tris*oxazolines (as shown in Scheme 1). The core was further replaced with a rigid C_3-symmetric cyclohexane[8], benzene[9] and cyclopropane[10]. The trisoxazoline ligands with different cores have applied in several reactions such as Kharash–Sosnovsky reaction,[5,6,8,11] allylic amination,[12] Friedel-Crafts,[14] Michael addition,[15] 1,3-dipolar

cycloaddition,[17] Diels-Alder reaction,[16] addition of diethylzinc to aldehydes[8,13] and cyclopropanation[7]. However, the successful application of chiral *tris*oxazoline ligands in asymmetric catalysis is still very limited.[18]

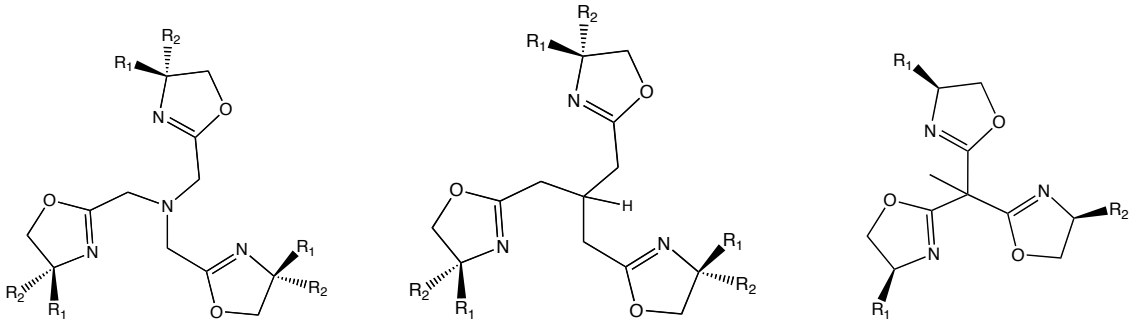

Chart 2. (A) *tris*(oxazolinyl)methylamine ligand. (B) *tris*(oxazolinyl)methane ligand. (C) 1,1,1-*tris*(oxazolinyl)ethane ligand.

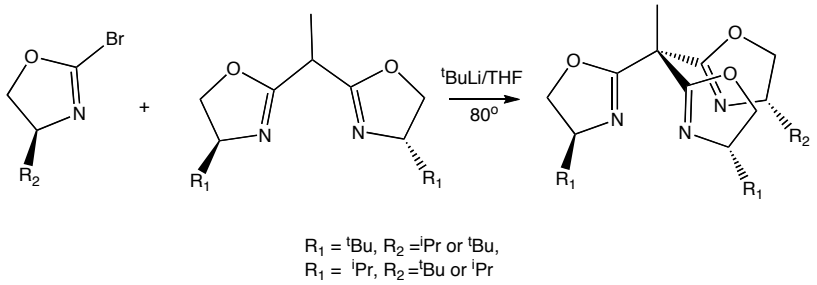

Scheme 1. A modular synthesis of 1,1,1-*tris*(oxazolinyl)ethane derivatives by coupling lithiated bisoxazolines with 2-bromooxazolines.

The anionic poly(oxazolinyl)borates were therefore developed in order to combine the features of the poly(pyrozolyl)borates and *tris*oxazolines, and unique properties of this family of ligands are expected. Pfaltz's group recently introduced an anionic boron-bridged bisoxazolines (borabox) ligand (Figure 1) for the enantio- and diastereoselective formation of nitroalcohols derived from nitropropane and aliphatic aldehydes, known as the Henry reaction.[19] Comparison with the corresponding dimethylmethylene-bridged bisoxazoline and other privileged ligands showed that borabox was the most suitable ligand system for the

Henry reaction.[19] The preparation of the boron-bridged bisoxazolines (borabox) ligand shows the synthetic potential of other poly(oxazolinyl)borates ligand. The first *tris*(oxazolinyl)borates ligand, *tris*(4,4-dimethyl-2-oxazolinyl)phenylborate [To^{M}], was reported by the Sadow group in 2008.[3] Li[To^{M}] was readily prepared through a one pot synthesis from the commercially available 4,4-dimethyl-2*H*-oxazoline (Scheme 2).[3] The chiral version of the ligand, *tris*((4*S*)-4-isopropyl-2-oxazolinyl)phenylborate [To^{P}], was synthesized and characterized by Sadow group in 2009.[20]

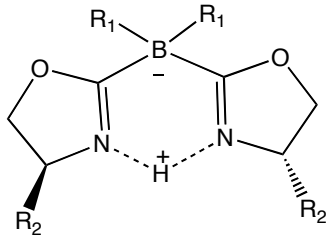

Figure 1. Anionic boron-bridged bisoxazolines (borabox) ligand

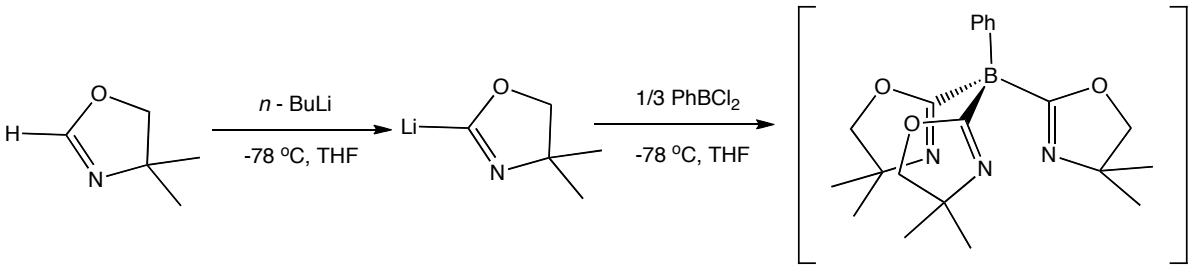

Scheme 2. Preparation of 4,4-dimethyl-2*H*-oxazoline.

Herein, the preparations of protonated achiral ligand H[To^{M}], chiral ligand Li[To^{P}] and H[To^{P}] are described in detail. A series of ruthenium complexes with the chiral ligand [To^{P}] were synthesized for potential applications in catalysis.

Ruthenium complexes have broad applications in the field of catalysis.[21] Trost and coworkers explored the application of ruthenium catalysis for the formation of carbon-carbon bonds, and found that Ru(κ^3-Cp*)(CH$_3$CN)$_3$PF$_6$ (Cp* = η^5-C$_5$Me$_5$) catalyzes allylic alkylations starting from unsymmetrically substituted substrates to yield branched product.[22] Bruneau and other groups further developed this system[23] and found that Ru(κ^3-Cp*) complexes bearing nitrogen ligands such as acetonitrile or bipyridine activated allylic halides

and carbonates to generate [Ru(κ^3-Cp*)(η^3-allyl)] complexes, which were isolated and fully characterized. The catalytic allylation reactions take place at room temperature and are easy to transfer to applications in fine chemistry to form C-C, C-O, C-S and C-N bonds which could be obtained from the allylation of various types of nucleophiles (Scheme 3). In most cases, the formation of the branched isomers is favored. However, this reaction strongly depends on the nature of the allylic starting material, the nucleophile, the catalyst precursor, the solvent and the temperature. Satisfactory enantioselectivities were obtained for the allylation of phenols in the presence of either modified planar chiral ruthenium catalyst[24] or the bisoxazoline ligands[25]. It still remains a big challenge to find the proper catalysts suitable for the preparation of enantiomerically branched allylic derivatives with high regioselectivity, and at the same time, applicable to a large range of nucleophiles.[23] Our chiral ligand [To^P]$^-$ which ensembles [Cp*]$^-$ system in its design, opens opportunity to this field.

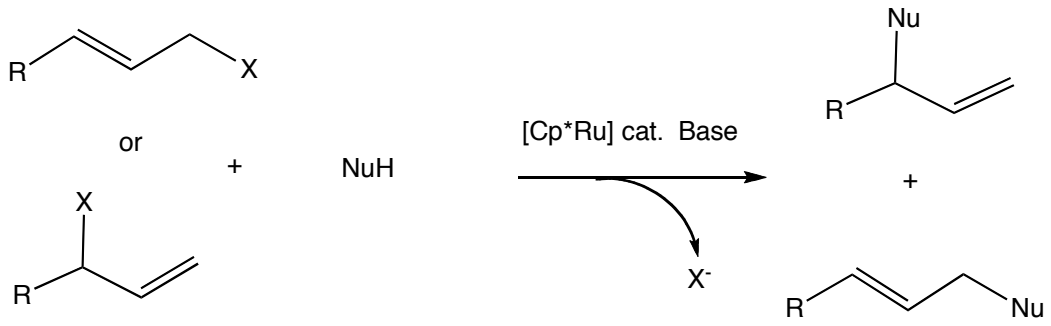

R = Ph, $PhCH_2$, *n*-Pr; NuH = alcohol, amine, phenol, YCR'Z^1Z^2, Base = NaH, K_2CO_3, (Z^1 = CO_2Me, Z^2 = CO_2Me, COMe, Z^1 = Z^2 = COMe; R' = H, Me; Y = H, Na)

Scheme 3. Ru(Cp*)$^+$ catalyzed allylic alkylation

Ruthenium complexes also play an important role in hydroamination. Hartwig and coworkers reported an Ru(COD)(methylallyl)$_2$ / 1,5-bis(diphenylphosphino)pentane ligand (DPPPent) / CF_3SO_3H catalyzed anti-Markovnikov hydroamination of vinylarenes in a very high yield.[26] (Scheme 4A) The following mechanism studies[27] of this reaction revealed that a new (η^6-styrene) ruthenium complex is generated *in situ* as the result of a combination of

protonolysis of the allyl groups, a replacement of COD by the DPPPent ligand, metalation of the central carbon of the pentane backbone of the DPPPent ligand, and coordination of the arene to the PCP-ruthenium fragment (Scheme 4B). Nucleophilic addition of amine on the (η^6-styrene) ruthenium complex affords the anti-Markovnikov adduct, and followed with arene exchange of free styrene for the coordinated arene in (η^6-(2-phenylethyl)morpholine)ruthenium complex to free the products and regenerate catalysts. It was notable that DPPPent serves as a tridentate ligand in the intermediate complex. We hypothesized that our tridentate ligand system [To]$^-$ could also serve as the ligand in the hydroamination reaction.

A

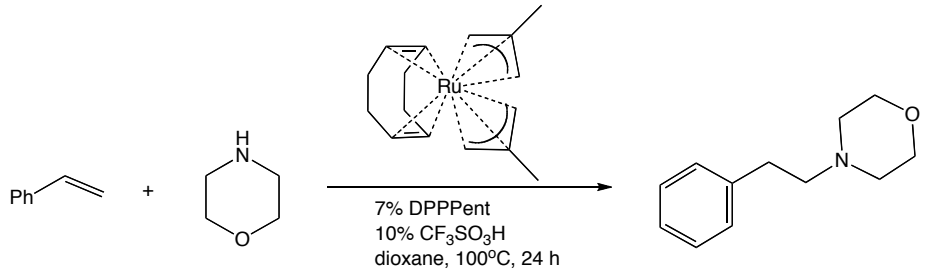

B

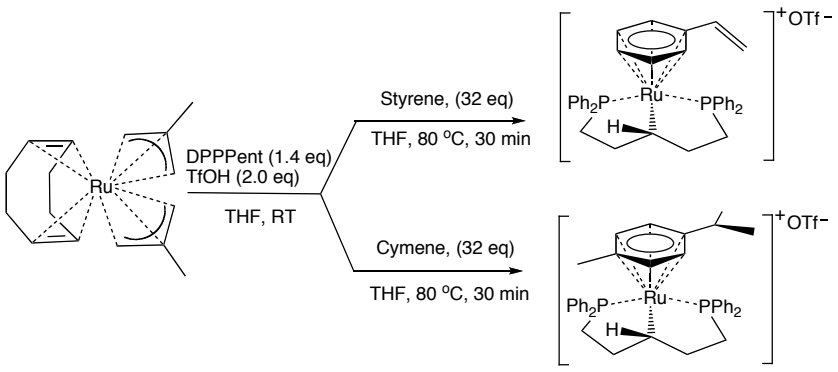

Scheme 4. (A) Ru(COD)(methylallyl)$_2$ catalyzed hydroamination. (B) Proposed intermediate

and cymene substitute in Ru(COD)(methylallyl)$_2$ catalyzed hydroamination.

Ruthenium complexes are also employed in C—H functionalization. Gunnoe synthesized TpRu^{II} complexes with nondative-heteroatomic ligands (e.g. amido, hydroxo, methoxo, and aryloxo ligands), and found that for such complexes, the disruption of ligand-to-metal π-donation due to a filled dπ manifold could enhance the nucleophilic and/or basic reactivity at the nondative-heteroatomic ligand relative to transition-metal complexes in high oxidation states.[28] (Scheme 5) As a result, these substrates were highly reactive in catalytic polymerizations and transformations of small molecules.[29] (Scheme 6**)** Using well-defined RuTp^{II} system, Gunnoe and coworkers demonstrated controlled stoichiometric and catalytic N–C bond formation using polar substrates, N–C and O–C bond formation using olefins as well as metal-mediated activation of dihydrogen and carbon–hydrogen bonds.[28] Further efforts need to be directed into stereoselective C—H activation, to which our chiral ligands might contribute.

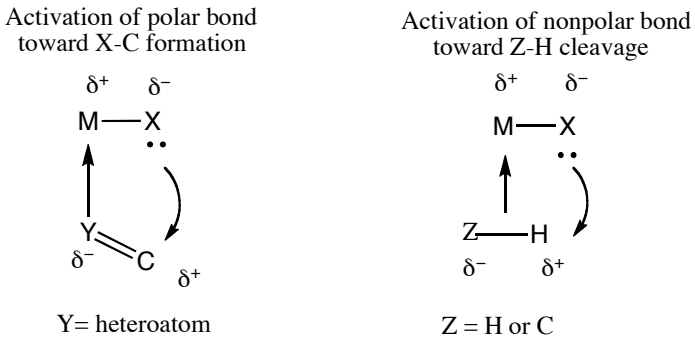

Scheme 5. Potential use of Lewis acidic metal centers with the basic anionic ligand "X" (X = NR_2, OR, SR, etc.) to activate substrates with polar and non-polar bonds.

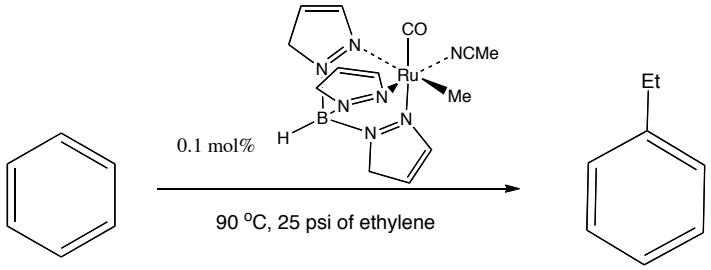

Scheme 6. Ru(Tp)($NCCH_3$)(CO)(Me) catalyzed aromatic C—H activation

Inspired by the above examples, we designed a series of ruthenium *tris*((4*S*)-4-isopropyl-2-oxazolinyl)phenylborate complexes with different co-ligands, including [ruthenium(II)*tris*((4*S*)-4-isopropyl-2-oxazolinyl)phenylborate*tris*(acetonitrile)]$^+$ {[Ru(To^P)(CH_3CN)$_3$]$^+$}, [ruthenium(II)*tris*((4*S*)-4-isopropyl-2-oxazolinyl)phenylborate(*p*-cymene)]chloride [Ru(To^P)(*p*-cymene)]Cl, ruthenium(II)*tris*((4*S*)-4-isopropyl-2-oxazolinyl)phenylborate(cyclooctadiene)hydride Ru(To^P)(COD)H, and systematically explored the reactivity of these compounds. The structure of [Ru(To^P)(CH_3CN)$_3$]$^+$ has been determined through NMR analysis and single crystal X-ray diffraction. The κ^3 coordination mode of ligand To^P was conformed in [Ru(To^P)(CH_3CN)$_3$]$^+$, which is similar to ligand Tp. [Ru(To^P)(CH_3CN)$_3$]$^+$ has been applied in several catalytic reactions and was found to be effective in catalyzing the dimerization of alkynes.

3. Results and Discussion

3.1. Synthesis of Ligands

3.1.1. Synthesis of achiral ligand H[To^M]:

The protonated ligand H[To^M] is prepared by flash chromatography of Li[To^M] on silica gel in hexane:isopropanol:triethylamine (15:1:0.5), giving the product as an off-white solid. In contrast to the broad resonances observed for Li[To^M] in benzene-d_6,[3] the ^{1}H NMR spectrum of H[To^M] in benzene-d_6 contains sharp singlet resonances at 1.02 (Me) and 3.55 ppm (CH_2). The oxazoline peaks are shifted downfield by 0.1 and 0.3 ppm (to 1.29 and 3.90 ppm) in comparison to Li[To^M] when the ^{1}H NMR spectrum is taken in acetonitrile-d_3.[3]

Crystals of H[To^M] were obtained from the slow evaporation of the chromatography solvent mixture. Despite the weak diffraction, the solved single-crystal structure confirmed the constitution and connectivity of [To^M]$^-$, in particular the formation of a tetrahedral borate

center containing four B-C bonds (Figure 2). Although all three oxazoline groups are equivalent in the ^{1}H NMR spectrum of H[To^M] in solution (benzene-d_6 or acetonitrile-d_3), the symmetry of [To^M]$^-$ in the solid state is C_s, as two of the oxazolines' C=N were coplanar (N1=C7-C17=N3 dihedral = 0^o), oriented toward each other as if to form a bidentate chelate, and related by a mirror plane. The mirror plane contains the phenyl group and the third oxazoline ring.

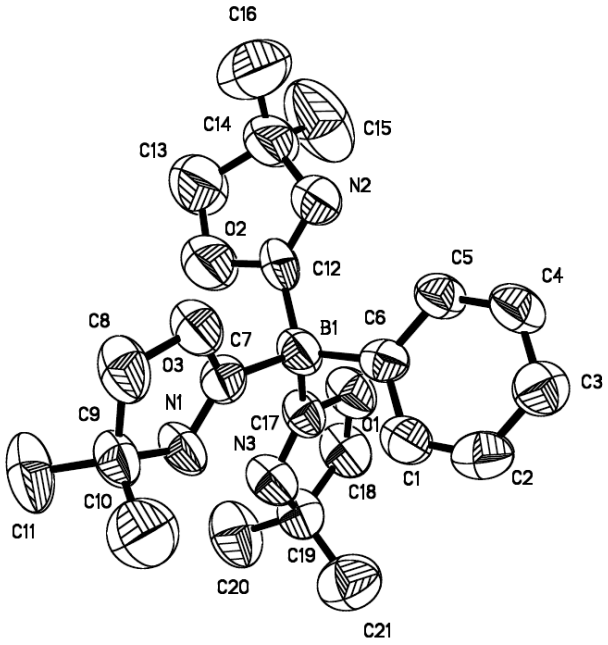

Figure 2. ORTEP diagram of H[To^M] at 50% probability. Hydrogen atoms were omitted for clarity.[3]

3.1.2. Synthesis of chiral ligand [To^P]:

Synthesis of the chiral ligand Li[To^P] and H[To^P] was developed by Jiachun Su. The ^{1}H NMR study of the isolated 2-lithium-4*S*-4-isopropyl-2-oxazolide {Li[Oxa$^{i\text{Pr}}$]} at 200K was conducted by Dr. Andrew Pawlikowski. Elemental analysis of Li[To^P] was accomplished by Benjamin Baird. Material Solid-State NMR and ^{15}N NMR were carried out by Dr. Jerzy W. Wiench and Dr. Marek Pruski. Other characterizations related to Li[To^P] and

H[To^{P}] were conducted by Jiachun Su. The results were published on *Inorganic Chemistry* in 2009.[20]

A one pot synthesis, which is similar to the synthesis of Li[To^{M}], was attempted at first in the synthesis of Li[To^{P}]. However, it led to multiple products according to the ^{1}H NMR spectrum. Silks and coworkers reported deprotonation of isopropyloxazoline using *n*-butyllithium led to inconsistent yield.[30] In their research, metalation of the oxazolines was accomplished using lithium diisopropylamide (LDA) or lithium hexamethyl disilazine (LHMDS).[30] As a result, the deprontonation of 4*S*-isopropyl-2*H*-oxazoline H[Oxa$^{i\text{Pr}}$] was attempted with lithium hexamethyl disilazine (LHMDS) or lithium diisopropylamide (LDA) in THF. LHMDS/LDA is first generated at 0 °C, and the base solution is then transferred to the THF solution of H[Oxa$^{i\text{Pr}}$], which is chilled to -78°C. Phenylborondichloride is added dropwise to the reaction mixture in hope that the desired product could be obtained. It was found that both LHMDS and LDA react quantitatively with H[Oxa$^{i\text{Pr}}$] to give Li[Oxa$^{i\text{Pr}}$], however, the byproduct of the deprotonation, HN(SiMe$_3$)$_2$ and HN[CH(CH$_3$)$_2$]$_2$, also react rapidly with PhBCl$_2$ and inhibited B-C bond formation. Fortunately, the analytically pure Li[Oxa$^{i\text{Pr}}$] is isolated in near-quantitative yield by the reaction of LiN(SiMe$_3$)$_2$ and H[Oxa$^{i\text{Pr}}$] followed by removal of the volatile materials and an ether wash (Scheme 7). The synthesis of K[Oxa$^{i\text{Pr}}$] from H[Oxa$^{i\text{Pr}}$] and KHMDS in THF failed, because the potassium salt is not stable and can not be isolated.

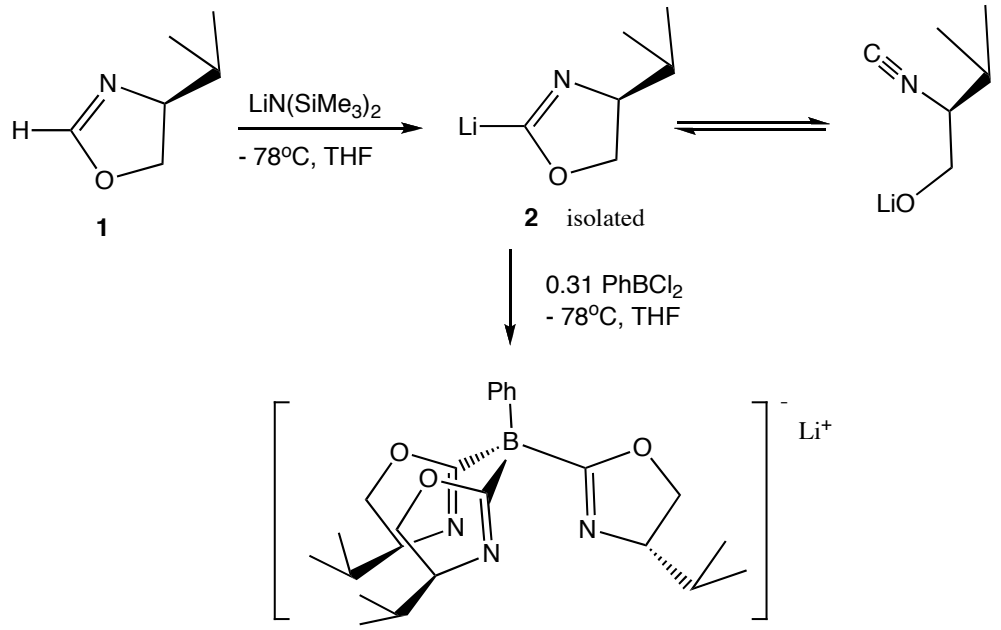

Scheme 7. Synthesis route of the chiral ligand Li[To^{P}]

In a previous study of the deprotonation of oxazolines, Meyers *et al.* reported that under carefully controlled conditions the lithiated carbanion is in equilibrium with the open-chain isonitrile, when 4,4-dimethyl-2-oxazoline is treated with *n*-butyllithium to generate the C-2 carbanion.[31] Silks' group studied the metalation of a number of chiral oxazolines including H[Oxa$^{i\text{Pr}}$], and found the same equilibrium existing in the deprotonation of chiral oxazolines.[30] Silks further ruled out the possibility of deprotonation at C-4 position in H[Oxa$^{i\text{Pr}}$] and therefore the possibility of racemization by the study of solution NMR.[30] However, Li[Oxa$^{i\text{Pr}}$] has never been isolated and characterized in its pure form.

Sadow's group first reported the synthesis and purification of Li[Oxa$^{i\text{Pr}}$]. The ^{1}H NMR spectrum of Li[Oxa$^{i\text{Pr}}$] in THF-d_6 shows broad peaks at room temperature, which was suspected to be caused by the equilibrium between lithiated carbanion and open-chain isonitrile. ^{1}H and ^{13}C{^{1}H} NMR spectroscopy down to 200 K was carried out in order to confirm our hypothesis, however, only the cyclic form of lithiated carbanion was observed. IR spectrum of the solid sample shows both isocyanide ν_{CN} (2173 cm^{-1}) and oxazolinyl ν_{CN} (1629 cm^{-1}), indicating that the two isomers are rapidly exchanging on the NMR time scale.[8]

Despite potential complications due to lithium alkoxide/isocyanide interconversion, the reaction of 3.3 equiv. of isolated Li[Oxa$^{i\text{Pr}}$] and $PhBCl_2$ in THF affords the desired Li[To^{P}] in excellent yield (92%, Scheme 4). It should be noted that a slight excess of Li[Oxa$^{i\text{Pr}}$] is required in order to achieve the high yield, less amount (< 3.3 equiv.) results in low yield (< 50%) and inseparable impurities based on the ^{1}H NMR spectrum. The identity of the Li[To^{P}] is supported by a series of characterization. In the ^{1}H NMR spectrum of Li[To^{P}], only one set of oxazoline resonances is observed, which shows that all three oxazoline rings in the ligand are equivalent. The calibration of oxazoline peaks and that of phenyl peaks has a 3:1 ratio, which means the ligand contains three oxazoline rings and one phenyl ring. ^{11}B NMR spectroscopy shows a single peak (δ -16.8 ppm), which is consistent with a four-coordinate borate center according to literature.[32] Therefore, all three oxazoline rings and the phenyl group are connected to the borate center, and the ligand adopts a C_3-symmetry with the phenyl group rapidly rotate in the NMR time-scale. The enantiopurity of [To^{P}]$^{-}$ is proven by the ^{1}H NMR spectrum of a single diastereomer (*S*,*S*,*S* enantiomers). The oxazoline rings connected to the borate center are rather stable with no ring opening, which is supported by the IR spectrum, where oxazoline C=N stretches are observed at 1589 cm^{-1}, while isocyanide peaks are not detected.

Li[To^{P}] is not hydrolyzed in wet methanol. The protonated ligand H[To^{P}] is not able to be obtained through chromatography either, due to the decomposition of the ligand on silica gel. However, Li[To^{P}] reacts with a mild acid [Et_3NH]Cl in THF to give the ivory solid product H[To^{P}]. The ^{1}H NMR of H[To^{P}] is quite similar to Li[To^{P}], in which only one set of resonances of oxazoline ring is observed and the ratio of oxazoline to phenyl integral signals is 3:1. In contrast to Li[To^{P}], the resonances of oxazoline ring in H[To^{P}] shift up field and the resonances of phenyl shift down field. In the IR spectrum, oxazoline C=N stretches are observed 1594 cm^{-1}, while isocyanide peaks shows at 2137 cm^{-1}, which indicates the equilibrium of oxazoline ring opening in H[To^{P}].

3.2. Synthesis of Ruthenium Complexes with Chiral Ligand [To^{P}]

$[Ru(To^P)(CH_3CN)_3]^+$ was designed as an analog of $[Ru(Tp)(CH_3CN)_3]^+$[34] and $[Ru(Cp^*)(CH_3CN)_3]^+$[35]. A mixture of $[RuCl_2(COD)]_n$ and $Li[To^P]$ is heated in acetonitrile-d_3 at 60 °C under argon in a Teflon-sealed NMR tube for 24 hours, and a brownish yellow solution is formed. The ^1H NMR spectrum reveals a single C_3-symmetric product in which three oxazoline groups are equivalent. However, the scaled up reaction turn from brownish yellow to green upon cooling or purification, and attempts to isolate the material by heating in a sealed flask results in green solutions upon evaporation of solvent (even in the glovebox). Interestingly, although the compound may change color, there are no noticeable changes in the ^1H NMR spectrum. ^1H NMR spectra of the green substance are identical to the yellow solutions from NMR-scale reactions, except for variation in the integration of the acetonitrile peak.

The $[To^P]$-containing species that is suitable for X-ray diffraction could not be isolated from the reaction mixtures. Instead, we obtained a ruthenium (II) pentaacetonitrile salt, $\{[RuCl(NCCH_3)_5]Cl\}CH_2Cl_2$, and identified its structure by X-ray crystallography. The ruthenium center sits in a distorted octahedron environment with one chloride ion and five acetonitrile molecules around the coordination sphere. Another chloride ion is out of the coordination sphere to balance the charge. (Figure 3) The species of $[RuCl(NCCH_3)_5]^+$ were reported to be very sensitive toward oxidation and could be easily oxidized to Ru(III), which is apparently responsible for facile formation of green solutions. [33]

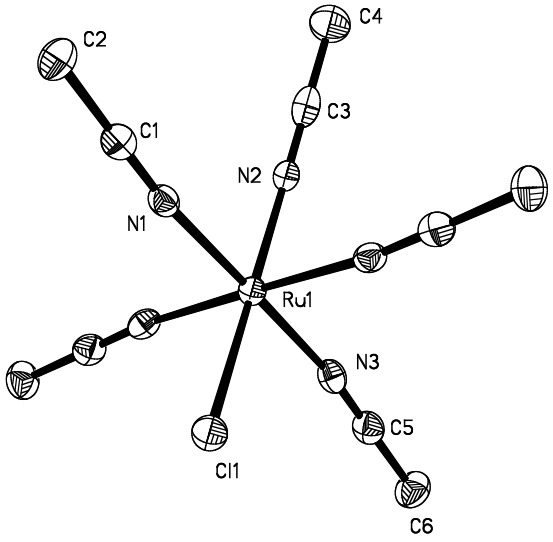

Figure 3. ORTEP diagram of $[Ru(CH_3CN)_5Cl]Cl$ at 50% probability. Hydrogen atoms were omitted for clarity. Hydrogen atoms are omitted for clarity.

In order to isolate single crystals containing $[Ru(\kappa^3\text{-}To^P)(CH_3CN)_3]^+$ that are suitable for structure analysis, the counter ion Cl^- was exchanged with BPh_4^-, PF_6^-, or SbF_6^-, through the addition of $NaBPh_4$, $NaPF_6$ or $NaSbF_6$ as a reactant in the reaction mixture (Scheme 8). The new species' ^1H NMR spectra of $[Ru(\kappa^3\text{-}To^P)(NCCH_3)_3]X$ (X = BPh_4^-, PF_6^-, or SbF_6^-) are identical to the species observed in the absence of the new counter ions $[Ru(\kappa^3\text{-}To^P)(NCCH_3)_3]Cl$, suggesting that all of the $[Ru(To^P)(CH_3CN)_3]L$ compounds (L=Cl^-, BPh_4^-, PF_6^-or SbF_6^-) exist as solvent separated ions in acetonitrile. Acetonitrile solutions of $[Ru(\kappa^3\text{-}To^P)(NCCH_3)_3]L$ (L= BPh_4^-, PF_6^-or SbF_6^-) remain yellow upon exposure to air (and the ^1H NMR spectrum is unchanged) indicting its resistance to oxidation. The solubility test of $[Ru(\kappa^3\text{-}To^P)(CH_3CN)_3]L$ compounds (L=Cl^-, BPh_4^-, PF_6^-or SbF_6^-) shows that this type of compounds are not soluble at all in hexane, slightly soluble in ether or benzene, and fairly soluble in acetonitrile, tetrahydrofuran, and methylene chloride. With this knowledge in mind, we fortunately obtained X-ray quality crystals of $[Ru(\kappa^3\text{-}S\text{-}To^P)(NCCH_3)_3]BPh_4$ from methylene chloride/diethyl ether mixtures. The acetonitrile solution of $[Ru(\kappa^3\text{-}S\text{-}To^P)(NCCH_3)_3]BPh_4$ is amazingly stable to air, moisture and high temperature. There are no

obvious changes in either the color of the compound or the ^{1}H NMR spectrum under those conditions.

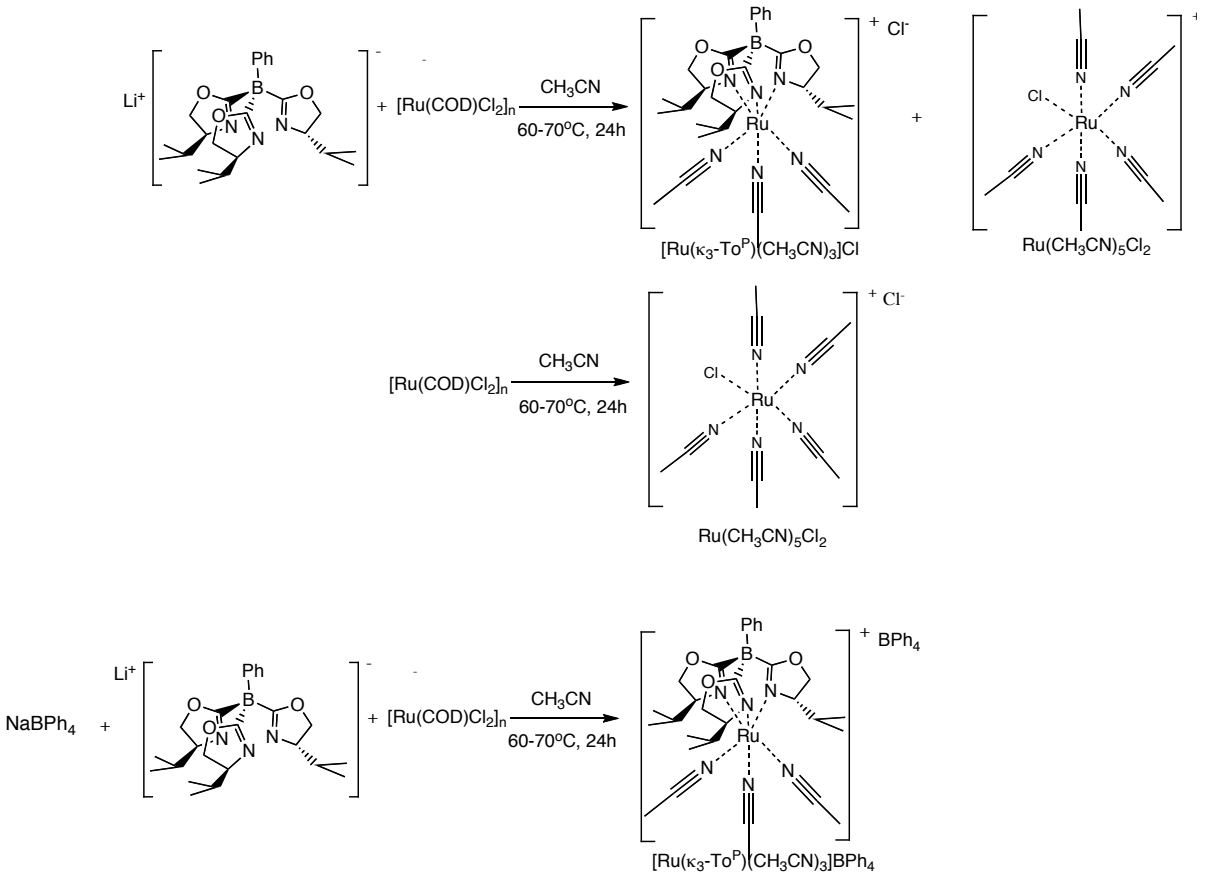

Scheme 8. Synthesis of $[Ru(To^P)(NCCH_3)_3]BPh_4$ and the formation of the byproduct $[Ru(CH_3CN)_5Cl]Cl$

Yellow crystals of $[Ru(\kappa^3\text{-}S\text{-}To^P)(NCCH_3)_3]BPh_4$ were obtained by layering diethyl ether on top of a dichloromethane solution. Crystals diffracted X-rays very weakly and it was clear from the very beginning that data would be of a very poor quality; however, the results of X-ray structure analysis proved the reaction path and confirmed our hypothesis about the structure of the $[Ru(\kappa^3\text{-}S\text{-}To^P)(NCCH_3)_3]BPh_4$. Structure was refined in isotropic approximation for all atoms except of Ru and lead to reasonable molecular geometry and

crystal packing mode. All geometrical parameters are for reference because of high values of ESD.

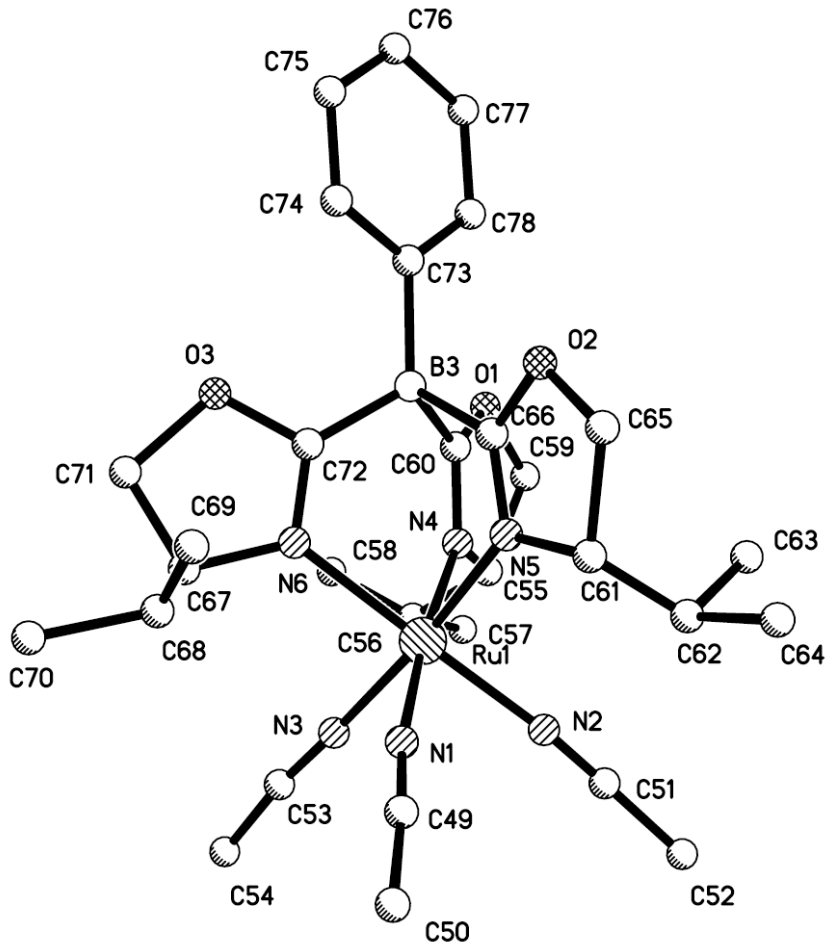

Figure 4. ORTEP diagram of $Ru(To^{P})(CH_3CN)_3^{+}$. Hydrogen atoms are omitted for clarity.

Figure 4 shows the coordination geometry around the ruthenium ions. Each ruthenium ion is coordinated to the three nitrogens on the oxazoline rings of the $[To^{P}]^{-}$ ligand and to three acetonitrile molecules. The overall coordination geometry of $[Ru(\kappa^3\text{-}S\text{-}To^{P})(NCCH_3)_3]^{+}$ is approximately octahedral. The isopropyl groups on the 4-position are positioned in a distorted modern Vestas windmill fashion. This unique feature creates an

asymmetric pocket for the ruthenium center with the potential of promoting interesting transformations and catalysis. The cone angle[21] of the $[To^P]^-$ is determined from the angle $(C\mathbf{H}_3)_2CH$---**Ru**---**B**. The vertex is enclosed by the ray from ruthenium center and between the methyl hydrogen (CH_3) on the isopropyl group, and the ray from ruthenium center to the borate center. Based on current crystallographic data, the cone angle of $[To^P]$ is larger than 200°. This value shows that the asymmetric pocket offers great protection for the ruthenium center. Although the sterically congested metal center might provide good substrate selectivity, it might also cause lower reactivity for bulky substrates.

The structure of $[Ru(\kappa^3\text{-}S\text{-}To^P)(NCCH_3)_3]^+$ is compared with the known compounds $[Ru(\kappa^3\text{-Tp})(NCCH_3)_3]^+$ [34] and $[Ru(\eta^5\text{-Cp})(NCCH_3)_3]^+$ [35] (Chart 3). The $Ru(CNCH_3)_3^{2+}$ moieties in the three compounds are very similar; the acetonitrile ligands, the legs of the piano stool, are slightly curved away from their linear structure. However, the ruthenium center in the $[Ru(\kappa^3\text{-}S\text{-}To^P)(NCCH_3)_3]^+$ sits in a chiral environment, which is unique among the three compounds.

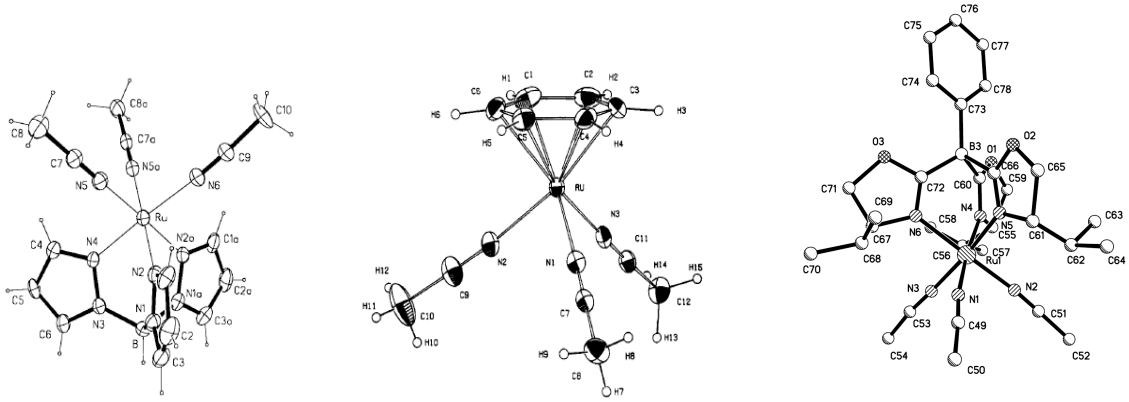

A B C

Chart 3. Crystal structures of (A) $[Ru(\kappa^3\text{-Tp})(NCCH_3)_3]^+$ [34], (B) $[Ru(\eta^5\text{-}C_5H_5)(NCCH_3)_3]^+$ [35], (C) $[Ru(\kappa^3\text{-}S\text{-}To^P)(NCCH_3)_3]$

$[Ru(\kappa^3\text{-Tp})(NCCH_3)_3]^+$, $[Ru(\eta^5\text{-}C_5H_5)(NCCH_3)_3]^+$ and $[Ru(\kappa^3\text{-}S\text{-To}^P)(NCCH_3)_3]$ are very different in reactivity. The piano-stool complexes $[Ru(\eta^5\text{-}C_5R_5)(NCCH_3)_3]^+$ (R = H, Me)[35] are highly active catalysts for alkyne coupling,[36] allylic alkylation,[22] etc., and their reactivities depend partially on the high lability of the nitrile ligands.[35] In contrast, the nitrile ligands in the scorpionate complex $[Ru(\kappa^3\text{-Tp})(NCCH_3)_3]^+$ are not labile, which could be explained by the strong d-π^* back bonding.[34] To our surprise, the nitrile ligands in $[Ru(\kappa^3\text{-To}^P)(NCCH_3)_3][BPh_4]$ are quite reactive despite the structural resemblance of $[Ru(\kappa^3\text{-To}^P)(NCCH_3)_3][BPh_4]$ with $[Ru(\kappa^3\text{-Tp})(NCCH_3)_3]^+$. Thirty percent of the CH_3CN ligands exchange with CD_3CN at room temperature within 24 hours, and the complete exchange of the CH_3CN ligands with CD_3CN takes place in 7 hours when the reaction is heated to 60-70°C. Further study shows that the nitrile ligands in $[Ru(\kappa^3\text{-To}^P)(NCCH_3)_3][BPh_4]$ can also be replaced by other L-typed ligands, as observed by changes in the ^1H NMR spectra. Considering that the steric bulk of the $[\kappa^3\text{-To}^P]^-$ ligand is much larger than its analogs, $[\eta^5\text{-}C_5R_5]^-$ and $[\kappa^3\text{-Tp}]^-$, the substitution reaction was first tested with some small nitrogen containing ligands. For example, reaction of $[Ru(\kappa^3\text{-To}^P)(NCCH_3)_3][BPh_4]$ and 1.0 equivalent of pyridine gives $[Ru(\kappa^3\text{-To}^P)(Pyridine)(NCCH_3)_2][BPh_4]$, while reaction of $[Ru(\kappa^3\text{-To}^P)(NCCH_3)_3][BPh_4]$ and 1.0 equivalent of PMe_3 (with a cone angle of 118°) yields the similar compound $[Ru(\kappa^3\text{-To}^P)(PMe_3)(NCCH_3)_2][BPh_4]$. An even bulkier ligand PPh_3 (with a cone angle of 145°) is then added to react with $[Ru(\kappa^3\text{-To}^P)(NCCH_3)_3][BPh_4]$, and a singly substituted product $[Ru(\kappa^3\text{-To}^P)(PPh_3)(NCCH_3)_2][BPh_4]$ is successfully obtained. When the amount of the PPh_3 is increased to 6.0 equivalent, no further substituted compounds are formed. The result is consistent with our calculated size of the asymmetric pocket.

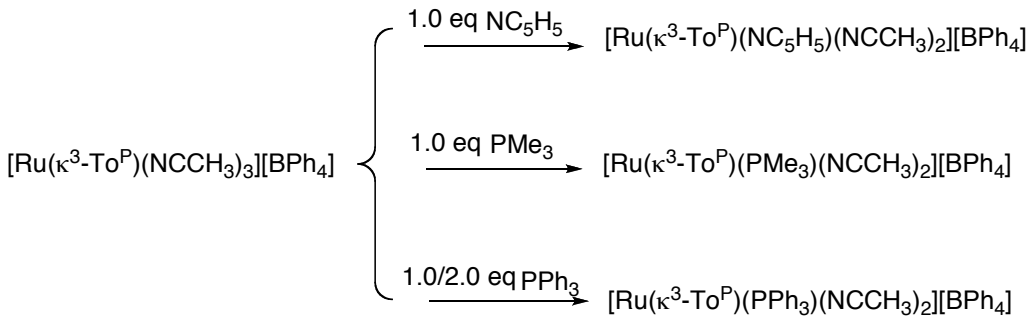

Scheme 9. Substitution reactions of $[Ru(\kappa^3\text{-To}^P)(NCCH_3)_3][BPh_4]$

The catalysis potential of $[Ru(\kappa^3\text{-To}^P)(NCCH_3)_3][BPh_4]$ was investigated and it was found that $[Ru(\kappa^3\text{-To}^P)(NCCH_3)_3][BPh_4]$ is an active catalyst for phenyl alkyne dimerization. Phenyl alkynes (MW=112) were mixed with 10% $[Ru(\kappa^3\text{-To}^P)(NCCH_3)_3][BPh_4]$ catalyst in C_6D_6 at room temperature, the solution immediately turned yellow upon mixing. The solution then turned brown after sitting at room temperature for 12 hours, and the GC analysis indicated the formation of three compounds with the molecular weight of 224, with the ^1H NMR spectrum displaying the hydrogen peak on the double bond. All of this evidence supported the formation of *cis*- and *trans*-1,4-disubstituted enynes PhCH=CHCCPh and 1,3-disubstituted enynes CH_2=C(Ph)CCPh (Scheme 10).

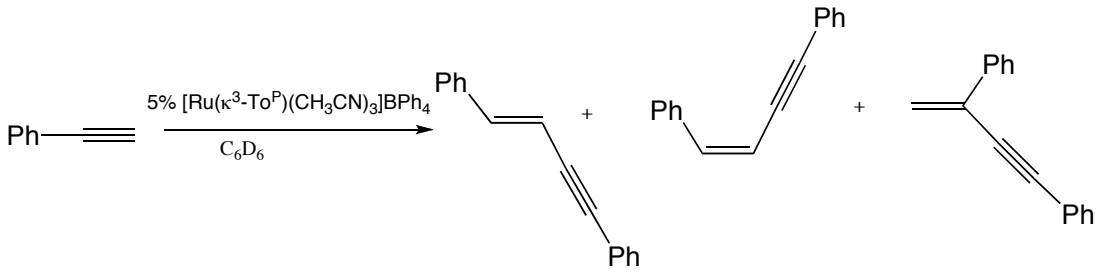

Scheme 10. $[Ru(\kappa^3\text{-}S\text{-To}^P)(NCCH_3)_3]$BPh4 catalyzed dimerization of terminal alkynes

The previous research revealed that terminal alkynes undergo several types of interaction with ruthenium centers to form various products (Scheme 11**).** [37] The first type is

the formation of ruthenium vinylidene species, while a second type of activation provids alkynyl ruthenium complexes via oxidative addition. When these two types of coordination take place at the same metal centre, the migration of the alkynyl ligand onto the C*a* atom of the vinylidene may occur to form enynyl intermediates, which upon protonation by the terminal alkyne led to the formation of enynes corresponding to alkyne dimerization (Scheme 12, cycle A).[37] In special cases, the rearrangement of the enynyl ligand to an allenylidenyl ligand may occur and the formation of the butatriene dimer is observed (Scheme 12, cycle B).[37]

$Ru^{IV}(Cp^*)(L)H_3$, (L=PPh_3, PCy_3, PMe_3)[36] and $Ru^{II}(\kappa^3\text{-Tp})(PPh_3)LCl$ (L=PPh_3, Py)[38] were found to catalyze the dimerization reaction of terminal alkynes RCCH (R=Ph, *t*-Bu, $SiMe_3$, n-Bu) mainly through catalytic circle A. Product from cycle B was observed on rare occasions. For example, a rare form of butatriene dimer, cumulene $PhCH_2CH{=}C{=}C{=}CHCH_2Ph$, was cleanly obtained from the dimerization of HC$\equiv$CCH_2Ph when $Ru(Cp^*)(PCy_3)H_3$ is used as the catalyst.[36] The conversion and selectivity of the reaction strongly depended on both the catalyst environment and the alkyne substrates.

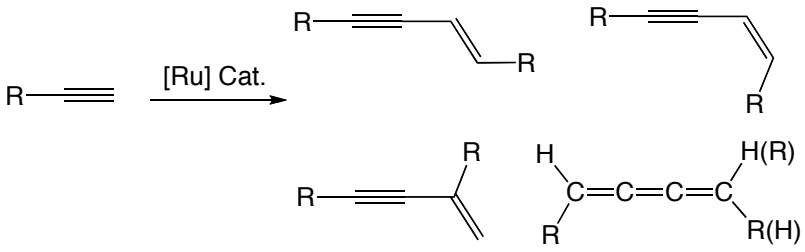

Scheme 11. Ruthenium catalyzed dimerization of terminal alkynes

It is hypothesized that the new catalyst $[Ru^{II}(\kappa^3\text{-To}^P)(NCCH_3)_3][BPh_4]$ proceeds through mechanism route A to achieve the final products base on the product distribution, where the catalytic precursor is the neutral vinylidene complex $L_nRu{=}C{=}CHR$. Detailed study is needed for this reaction to understand selectivity by varying the substrates and using

different L-ligands for the catalyst $[Ru^{II}(\kappa^3\text{-}To^P)(CH_3CN)_2L]^+$. It would also be necessary to isolate and characterize the intermediate vinylidene complex in order to confirm our hypothesis about the mechanism.

It should be noted that there is no change in the oxidation state of $Ru^{IV}(Cp^*)(L)H_3$[36] complex through the catalytic circle, however, both $[Ru^{II}(\kappa^3\text{-}To^P)(NCCH_3)_3][BPh_4]$ and $Ru^{II}(\kappa^3\text{-}Tp)(PPh_3)LCl$ (L=PPh_3, Py)[38] need to go through oxidative addition in order to achieve the catalytic cycle. It would be very interesting to isolate the intermediate of this reaction, because $[Ru^{II}(\kappa^3\text{-}To^P)(NCCH_3)_3][BPh_4]$ is inert towards oxidative addition in other experiments of the later part of discussion.

Ruthenium vinylidene complexes are very active intermediates, which will surely open doors to many catalytic reactions. Three main chemical processes leading to catalytic reactions are as follow: (1) Addition of nucleophiles at C*a*. (2) Carbometallation followed by migration of an alkynyl group to C*a*. (3) [2+2] cycloaddition and formation of ruthenacyclobutane intermediates.[37]

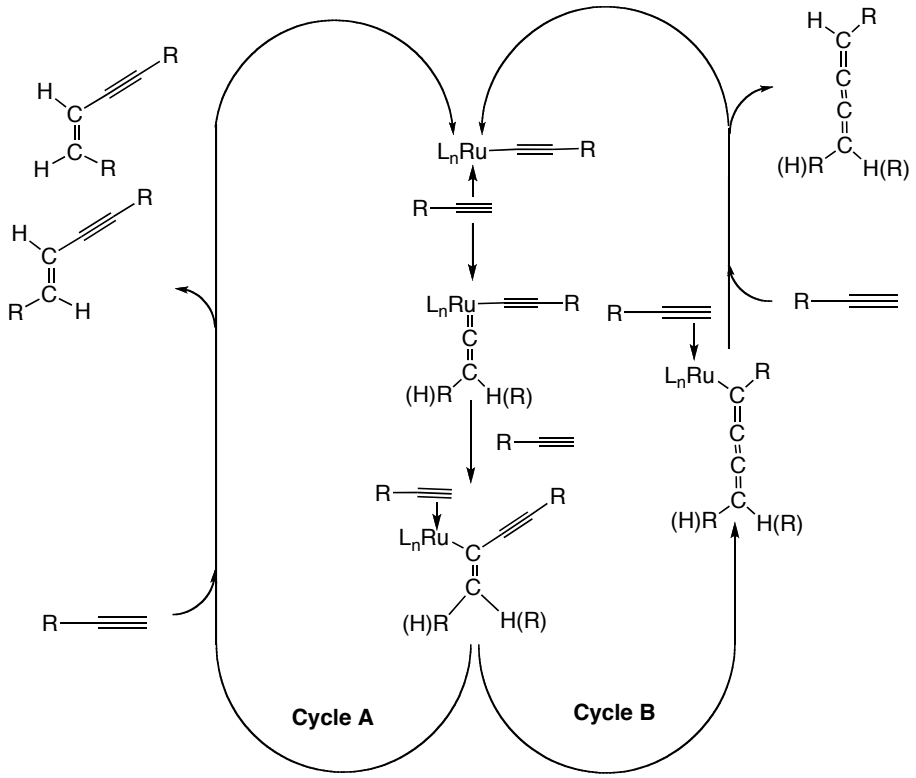

Scheme 12. Catalytic cycle of the ruthenium catalyzed dimerization of terminal alkynes

Catalyst $[Ru(\kappa^3\text{-}To^P)(NCCH_3)_3][BPh_4]$ failed to catalyze the allylic alkylation with $PhCH{=}CHCH_2X$ (X=halogen or carbonate) with morpholine as a nucleophile in various solvents. In CD_3CN, the only noticeable change was the replacement of CH_3CN ligand in the catalyst by its deuterium form. In C_6D_6 and CD_2Cl_2, the solution changed from slight yellow to bright yellow, but no obvious change for the allylic substrates and catalyst in the ^1H NMR (Scheme 13A). It should be noted that all the ^1H NMR peaks of morpholine shifted when heating the catalyst in methylene chloride-d_2, although the reason is still unknown (Scheme 13B).

Based on the established mechanism of $Ru(Cp^*)^+$ catalyzed allylic alkylation,[11] the oxidative addition of allylic substrates to the ruthenium(ii) centre would be a key step for related catalytic processes (Scheme 14). However, attempt of obtaining the alkyl coordinate ruthenium intermediate by mixing $PhCH{=}CHCH_2X$ (X=halogen or carbonate) and $[Ru(\kappa^3\text{-}$

$To^P)(NCCH_3)_3][BPh_4]$ in methylene chloride-d_2 did not lead to any noticeable change in the ^1H NMR of the substrate and the catalyst under either UV light or heat (Scheme 13C). To further explore the oxidative addition potential of $[Ru(\kappa^3\text{-}To^P)(NCCH_3)_3][BPh_4]$, 2.0 equivalents of MeI was added to the methylene chloride solution of catalyst $[Ru(\kappa^3\text{-}To^P)(NCCH_3)_3][BPh_4]$, and no reaction was observed at either room temperature or high temperature. In contrast, $[Ru(\kappa^3\text{-}To^P)(NCCH_3)_3][BPh_4]$ was able to catalyze the dimerization of terminal alkynes, which indicated the oxidative addition of terminal alkyne on the ruthenium metal.

A

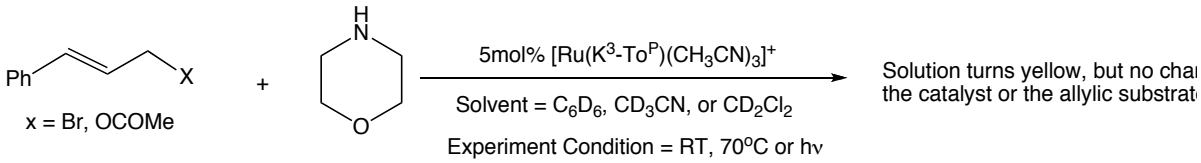

B

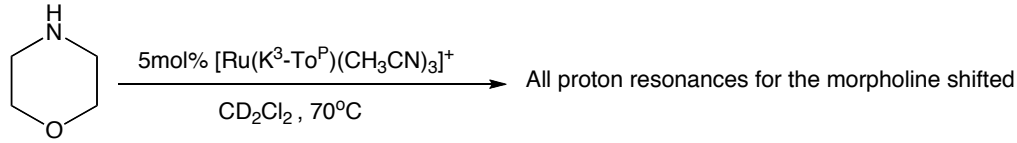

C

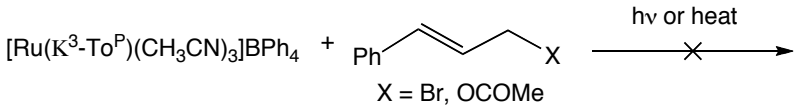

Scheme 13. (A) $[Ru(\kappa^3\text{-}To^P)(NCCH_3)_3][BPh_4]$ catalyzed allylic alkylation in various solvents. (B) Independent study of morpholine reacting with $[Ru(\kappa^3\text{-}To^P)(NCCH_3)_3][BPh_4]$. (C) Independent study of phenyl allyl substrates reacting with $[Ru(\kappa^3\text{-}To^P)(NCCH_3)_3][BPh_4]$.

The available experiment data indicate the chiral ligand $[To^P]^-$ has a very weak electron donating ability; when it comes to oxidative addition, only alkyne with the sp hybridization orbital is electronegative enough to stabilize the oxidative addition product $Ru[To^P]^{IV}$, while methyl iodide and phenylallyl bromide are not such strong oxidizing reagent to form the stabilized product. One possibility to solve this problem is to introduce strong electron donating ligands such as PPh_3 or pyridine to stabilize the oxidative addition product $Ru[To^P]^{IV}$. Future work could be directed towards testing these hypotheses.

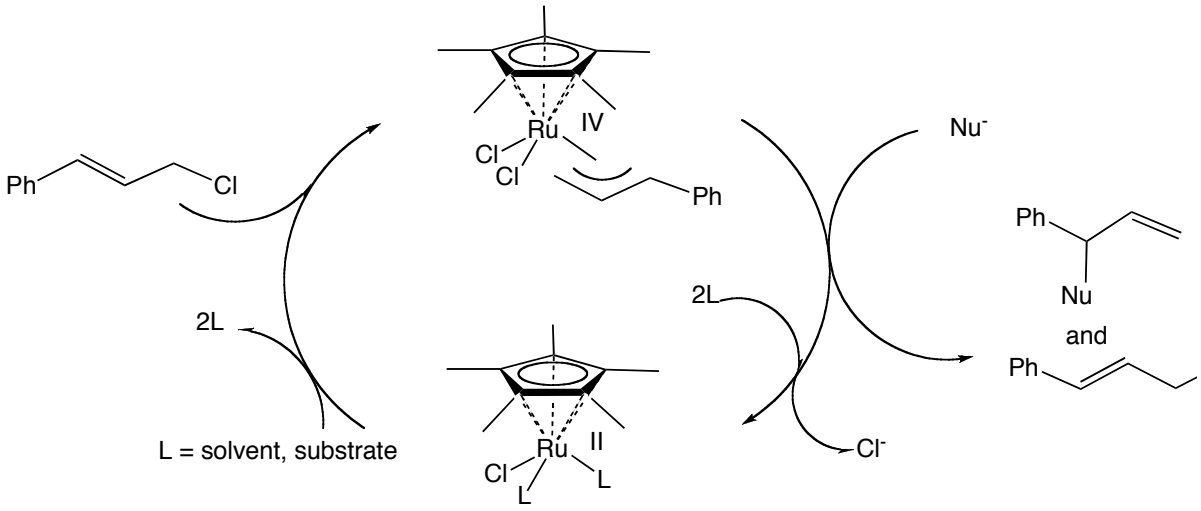

Scheme 14. Proposed mechanism for the $Ru(\kappa^3\text{-}Cp^*)L_2Cl$ catalyzed allylic alkylation

$[Ru(\kappa^3\text{-}To^P)(NCCH_3)_3][BPh_4]$ was also employed as a catalyst in the hydroamination reaction, and it was found the catalyst (5 mol%) was not active in catalyzing the reaction of styrene with morpholine in THF-d_8. Even substrates that coordinate more easily (such as methylacrylonitrile), failed to react with morpholine in THF-d_8. (Scheme 18) As a result, there could be other reasons for the inactivity towards hydroamination besides the difficulty in the formation of the (η^6 - styrene) ruthenium complex.

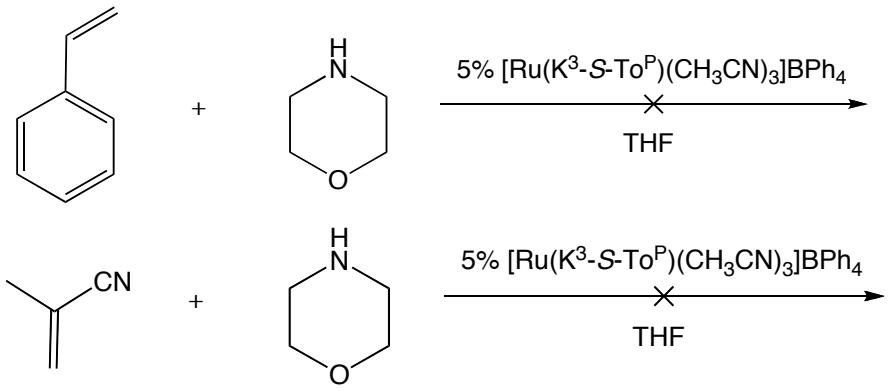

Scheme 15. $[Ru(\kappa^3\text{-}S\text{-}To^P)(NCCH_3)_3]BPh_4$ catalyzed hydroamination

An alternative route was then attempted to access the (η^6 - styrene) ruthenium (II) complex (Scheme 16). A mixture of $[RuCl_2(p\text{-cymene})]_2$ and Li[*S*-To^P] was heated in benzene-d_6 at 120 °C under argon in a Teflon-sealed NMR tube for 5 days, and a blue solution formed. After pumping away the solvent, the product was dissolved in methylene chloride, and hexane was layered on top of the solution to precipitate a blue solid. The ^{1}H NMR of the blue solids showed that both of the *p*-cymene and To^P are in the product and the isopropyl groups were equivalent despite the orientation of the *p*-cymene ligand, which was caused by the rotation of the *p*-cymene ligand around the ruthenium center according to previous study.[39] Further evidence is needed to confirm the products structure. Future work could involve the replacement of the *p*-cymene with another aromatic ligand.

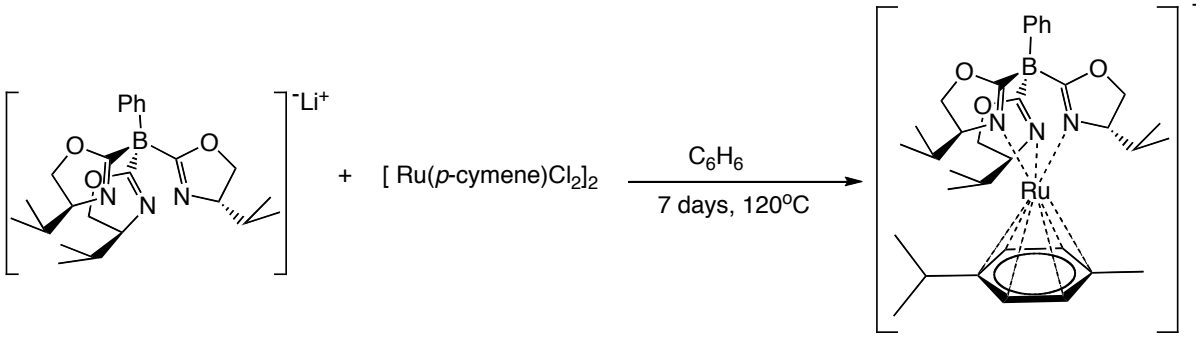

Scheme 16. Synthesis of $[Ru(\kappa^3\text{-}S\text{-}To^P)(p\text{-cymene})]^+$

Both of the compounds, $[Ru(\kappa^3\text{-}To^P)(NCCH_3)_3][BPh_4]$ and $[Ru(\kappa^3\text{-}To^P)(p\text{-cymene})]Cl$ contain no anionic ligand other than $[To^P]^-$. Research involving incorporation of other anionic ligands into the $Ru(\kappa^3\text{-}To^P)^+$ coordination sphere to form a metal–ligand σ-bond was inspired by Gunnoe's work.[28,29] Gunnoe demonstrated that $Ru^{II}(Tp)$ system with highly nucleophilic/basic heteroatom-based ligands including amido and alk-/aryl-/hydroxo ligands provides opportunities for the coordination and activation of external organic substrates towards controlled bond-breaking and bond-forming reactions.[28] Would $Ru^{II}(To^P)$ system have the same prospective when metal–ligand σ-bond is contained in the catalyst? To answer this question, the targeted compound $Ru(\kappa^3\text{-}To^P)(COD)Cl$ was designed as the analog of $Ru(\kappa^3\text{-}Tp)(COD)Cl$[40] and $Ru(Cp)(COD)Cl$ [48]. Four different routes were designed to reach the target the molecule. The first attempt to synthesize this compound was conducted by heating a mixture of $[Ru(COD)Cl_2]_n$ and $LiTo^P$ in THF, however, the poor solubility of $[Ru(COD)Cl_2]_n$ in THF hindered the reaction. Ethanol was then explored as a solvent. $[Ru(COD)Cl_2]_n$ did dissolve as the reaction proceeded, but the reaction did not yield the desired product. According to literature,[48] $[Ru(COD)Cl_2]_n$ could be converted to a more soluble ruthenium complex $Ru(COD)(CH_3CN)_2Cl_2$ to react with $Li[To^P]$ in CH_2Cl_2, which could generated the target molecule. The reactants were sealed in a Teflon-sealed NMR tube and heated at 70°C for 2 days, and the solution turned from yellow to brown with white solids at bottom. ^1H NMR revealed the formation of the desired product with some impurities. However, the conversion yield of $Ru(COD)(CH_3CN)_2Cl_2$ from heating $[Ru(COD)Cl_2]_n$ in CH_3CN was as low as 33%, which can not be considered as a scale up route when considering the cost of $[Ru(COD)Cl_2]_n$. A more practical procedure was obtained by refluxing $[Ru(COD)(NH_2NMe_2)_3H]BPh_4$ and $Li[To^P]$ in dry acetone for 2 hours; the product $Ru(\kappa^3\text{-}To^P)(COD)H$ was obtained after removal of the salt (Scheme 17). In the ^1H NMR, a peak at -5 ppm corresponded to the hydride in the complexes,[41] and there are six doublets found near 2 ppm that represent the methyl groups after breaking the structure's symmetry. It is very remarkable to have a ruthenium hydride bond in this complex, since this compound can promote new types of reactions.[42] For example, $Ru(\kappa^3\text{-}To^P)(COD)L$ (L=Cl, Br) would form after heating $Ru(\kappa^3\text{-}To^P)(COD)H$ in $CHCl_3$ or $CHBr_3$. Ru-halogen bond could be converted to Ru-alkyl bond when reacting with alkyl lithiums.[40] Detailed research is still

needed to optimize the reaction conditions and purification process.

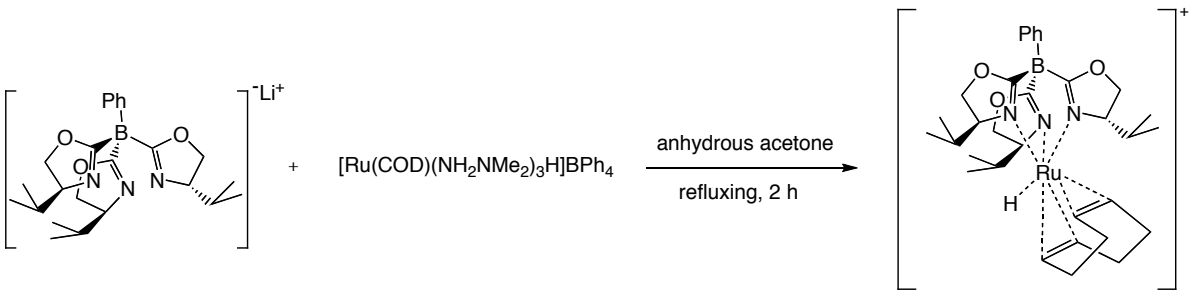

Scheme 17. Synthesis of Ru(κ^3-*S*-To^P)(COD)Cl

4. Conclusions

In summary, we contributed to the preparation of a new class of oxazoline-based scorpionate ligands: the achiral ligand *tris*(4,4-dimethyl-2-oxazolinyl)phenylborate [To^M]$^-$ and the chiral version *tris*((4*S*)-4-isopropyl-2-oxazolinyl)phenylborate [To^P]$^-$. A series of ruthenium complexes containing the chiral ligand [To^P]$^-$ were designed and synthesized and all required further characterization. The crystal structure of [Ru(κ^3-To^P)(NCCH$_3$)$_3$][BPh$_4$] was characterized and the structure strongly resembled its scorpionate analog [Ru(κ^3-Tp)(NCCH$_3$)$_3$]$^+$. However, since the pyrozolyl groups in the original scorpionates are replaced with oxazolynyl groups, different reactivities are shown for the new ruthenium complexes. The structure analysis and catalysis study revealed the *tris*((4*S*)-4-isopropyl-2-oxazolinyl)phenylborate (κ^3-Tp)$^-$ creates a unique chiral pocket around the ruthenium center with a cone angle larger than 200°. This steric environment hindered substitution and reactions involving bulky substrates. A systematic study of oxidative addition also shows that *tris*(4-*S*-isopropyl-2-oxazolinyl)phenylborate (κ^3-Tp)$^-$ is a poorer electron donor compared with cyclopropene and trispyrozolylborate. The combined features will lead to completely different catalysis for the new scorpionate ligands. Future study will focus on application of the chiral scorpionate ligand (κ^3-Tp)$^-$ towards asymmetric catalysis.

5. Acknowledgments

Is given to Prof. Dr. Aaron Sadow for the guidance and help. The author would also like to give special thanks to Benjamin Baird, Dr. Andrew Pawlikowski, Dr. Jerzy W. Wiench and Dr. Marek Pruski for the synthesis and characterization of compound lithium *tris*(4*S*-isopropyl-2-oxazolyn-2-yl)phenyl borate Li[To^{P}], to James Dunne for the synthesis and characterization of lithium *tris*(4,4-dimethyl-2-oxazolynyl)phenyl borate Li[To^{M}], and to Dr. Arkady Ellern and the Molecular Structure Laboratory of Iowa State University for X-ray crystallography analysis.

6. Experimental

6. 1 General Procedures

All manipulations were performed under a dry argon atmosphere using standard Schlenk techniques, or under a nitrogen atmosphere in a glovebox unless otherwise indicated. Dry, oxygen-free solvents were used throughout. Benzene, toluene, hexane, pentane, diethyl ether, methylene chloride and tetrahydrofuran were degassed by sparging with nitrogen, filtered through activated alumina columns, and stored under N2. Benzene-*d*6 and toluene-*d*8 were vacuum transferred from Na/K alloy and stored under N2 in the glovebox. Dichlorophenylborane was purchased from Aldrich and distilled prior to use. The starting materials 4*S*-4-isopropyl-2-oxazoline,[43] [Ru(η^4-COD)Cl_2]n,[44] [Ru(*p*-cymene)Cl_2]$_2$,[45] Ru(COD)(CH_3CN)$_2Cl_2$[46] and [Ru(COD)(NH_2NMe_2)$_3$H]BPh_4[47] were synthesized as previously reported. All other reagents were purchased from Aldrich and used as received.

^{1}H, ^{11}B, ^{13}C{^{1}H} and ^{15}N{^{1}H} solution NMR spectra were collected on Bruker DRX-400, AV-600 or Avance II 700 spectrometers. ^{15}N chemical shifts were determined by ^{1}H-^{15}N HMBC experiments on a Bruker Avance II 700 spectrometer with a Bruker Z-gradient inverse TXI ^{1}H/^{13}C/^{15}N 5mm cryoprobe. ^{15}N chemical shifts were originally recorded with respect to liquid NH3 (machine calibration) and recalculated to the CH3NO2 chemical shift scale by adding -381.9 ppm.

$^{13}C\{^{1}H\}$ and $^{15}N\{^{1}H\}$ solid-state NMR data were acquired on 600 Varian NMR System spectrometer equipped with 1.6 mm T3 narrow bore magic angle spinning (MAS) probe. The samples were loaded in MAS zirconia rotors and tightly capped to minimize the possibility of oxygen/moisture contamination. 1D $X\{^{1}H\}$ cross-polarization (CP) MAS experiments (where X is ^{13}C or ^{15}N) were performed using 1 s relaxation delay, 2.5 μs long ^{1}H preparation pulse, and a tangent spin-lock pulse with the RF magnetic field of around 60 kHz. The other parameters were as follows: $^{13}C\{^{1}H\}$ CPMAS: 1 ms CP contact time, 100 kHz RF field during ^{13}C CP pulse, ^{1}H SPINAL decoupling at 10.5 kHz RF field, 40 kHz MAS rate, 10000 to 12000 scans; $^{15}N\{^{1}H\}$ CPMAS: 8 ms CP contact time, 50 kHz RF field during ^{15}N CP pulse, ^{1}H SPINAL decoupling at 65 kHz RF field, 10 kHz MAS rate, 100 kHz RF field during Carr-Purcell-Meiboom-Gill (CPMG) acquisition, 8 ms delay between CPMG pulses, 5 CPMG echoes, 48000 to 64000 scans. The chemical shifts were referred to TMS (^{13}C) and neat CH3NO2 (^{15}N) using glycine resonances at 43.7 (*C*H2) and -347 (*N*H2) ppm.

Elemental analysis was performed using a Perkin-Elmer 2400 Series II CHN/S by the Iowa State Chemical Instrumentation Facility.

X-ray diffraction data was collected on a Bruker-AXS SMART 1000 CCD diffractometer using Bruker-AXS SHELXTL software.

6.2. Synthesis of Compounds

The preparation procedures of lithium *tris*(4,4-dimetheyl-2-oxazolin-2-yl)phenylborate $Li[To^{M}]$, hydrogen *tris*(4,4-dimethyl-2-oxazolin-2-yl)phenylborate $H[To^{M}]$, 2-lithio-4*S*-isopropyl oxazolide ($Li[Oxa^{iPr}]$), and Lithium *tris*(*4S*-4-isopropyl-2-oxazolinyl)phenyl borate ($Li[To^{P}]$) were published and the following data and figures pertain only to the papers in which they are included.

6.2.1. Hydrogen *tris*(4,4-dimethyl-2-oxazolin-2-yl)phenylborate $H[To^{M}]$.

In air Li[To^{M}] (2.00 g, 5.14mmol) is dissolved in methylene chloride and filtered through a short silica gel plug in a solvent mixture of hexane : isopropanol : triethylamine (15:1:1). A single fraction is collected. The solvent is evaporated under reduced pressure yielding the off-white product in 50% yield (0.985 g, 2.57 mmol). The product is subsequently dried by stirring in neat chlorotrimethylsilane for 3 h, and then isolated by removal of the chlorotrimethylsilane *in vacuo* and stored under N_2. ^{1}H NMR (benzene-d_6, 400 MHz, δ): 7.77 (br s, 2 H, *ortho*-C_6H_5), 7.38 (m, 2 H, *meta*-C6H5), 7.22 (m, 1 H, *para*-C_6H_5), 3.83 (s, 6 H, $\overline{\mathrm{CNCMe_2}\mathit{CH_2}\mathrm{O}}$), 1.14 (s, 18 H, $\overline{\mathrm{CNC}\mathit{Me_2}\mathrm{CH_2O}}$). ^{13}C{^{1}H} NMR (benzene-d_6, 400 MHz, δ): 187.1 (br s, $\overline{\mathrm{CNCMe_2CH_2O}}$ 142.6 (br s, *ipso*-C_6H_5), 134.0 (s, *ortho*-C_6H_5), *meta*-C_6H_5 obscured by benzene-d_6, 127.3 (s, *para*-C6H5), 81.48 (s, $\overline{\mathrm{CNCMe_2}\mathit{CH_2}\mathrm{O}}$), 64.22 (s, $\overline{\mathrm{CNC}\mathit{Me_2}\mathrm{CH_2O}}$), 27.50 (s, $\overline{\mathrm{CNC}\mathit{Me_2}\mathrm{CH_2O}}$). ^{11}B NMR (acetonitrile-*d*3, 400 MHz, δ): -17.82. IR (KBr, cm^{-1}): 3067 m, 3049 m, 2966 br s, 2929 s, 2886 br s, 1669 w, 1627 s, 1594 s, 1461 s, 1425 s, 1387 m, 1361 m, 1317 s, 1189 s, 1149 m, 1114 m, 971 s, 930 m, 750 m, 709 s. Anal. Calcd for C21H32BO4N3: C, 62.9; H, 7.98; N, 10.48. Found: C, 62.9; H, 7.90; N, 10.12. m.p. 104-106 ºC.

6.2.2. 2-Lithio-4-*S*-isopropyl oxazolide (Li[Oxa$^{i\mathrm{Pr}}$]).

An oven-dried 50 mL round bottom Schlenk flask containing a magnetic stir bar is charged with hexamethyldisilazane (3.0 mL, 15 mmol) and 20 mL THF. The flask is cooled with a dry ice-acetone bath to -78 °C, and 2.5 M *n*-butyllithium (6.2 mL, 15 mmol) solution in pentane is added via syringe over 10 min. The resulting solution of lithium hexamethyldisilazide is stirred for 15 min at -78 °C, and then allowed to warm to ambient temperature for another 15 min. This solution is added dropwise via cannula transfer to a 100 mL Schlenk flask which is charged with (4*S*)-4-isopropyl-2-oxazoline (2.0 mL, 14 mmol) and 30 mL of THF. The reaction mixture is then stirred at -78 °C for 1 h and at room temperature for another 1 h. The volatile materials were removed in vacuo, and the resulting white solids were washed with 30 mL of diethyl ether and dried under vacuum, affording 2-lithio-(4*S*)-4-isopropyl oxazolide quantitatively. Solution NMR. ^{1}H NMR (tetrahydrofuran-

*d*8, 400 MHz, δ): 3.85 (m, 2 H, $\overline{CNC(CHMe_2)HCH_2O}$), 3.30 (br m, 1 H, $\overline{CNC(CHMe_2)HCH_2O}$), 1.94 (br m, 1 H, $\overline{CNC(CHMe_2)HCH_2O}$1.01 (d, 3 H, ^3JHH = 7 Hz, $\overline{CNC(CHMe_2)HCH_2O}$), 0.93 (d, 3 H, ^3JHH = 7 Hz, $\overline{CNC(CHMe_2)HCH_2O}$). $^{13}C\{^1H\}$ NMR (THF-*d*8, 100 MHz, δ): 157.86 ($\overline{CNC(CHMe_2)HCH_2O}$), 68.81 ($\overline{CNC(CHMe_2)HCH_2O}$), obscured by solvent ($\overline{CNC(CHMe_2)HCH_2O}$), 28.88 ($\overline{CNC(CHMe_2)HCH_2O}$21.19 ($\overline{CNC(CHMe_2)HCH_2O}$), 16.96 ($\overline{CNC(CHMe_2)HCH_2O}$^{5}N NMR(tetrahydrofuran-*d*8, 71 MHz, δ): -206.9 (coupled to C*H*Me2 and C*H*-*i*-Pr). IR (KBr, cm^{-1}): 3691 (m), 3676 (s), 3411(br m), 2959 (s), 2875 (m), 2138 (w), 1653 (m), 1558 (w), 1466 (m), 1366 (w), 1319 (w), 1249 (s), 1021 (s), 985 (s), 853 (m), 792 (m), 758 (w), 670 (w). Anal. Calcd for C6H10NOLi: C, 60.50; H, 8.48; N, 11.76. Found; C, 60.34; H, 8.42; N, 12.01. m.p. 208-212 °C.

6.2.3. Lithium *tris*(*4S*-isopropyl-2-oxazolinyl)phenyl borate (Li[To^P]).

An oven-dried 50 mL round bottom Schlenk flask with a magnetic stir bar is charged with 2-lithio-4-(*S*)-isopropyl oxazolide (4.00 g, 3.36 mmol) and 150 mL THF. The flask is cooled with a dry ice/acetone bath to -78 °C, and PhBCl2 (1.32 ml, 4.20 mmol) is added dropwise via syringe over 10 min at -78 °C. The mixture is allowed to warm to room temperature and is stirred for 26 h. The volatile materials are removed in vacuo, and the solids are extracted with diethyl ether (3 × 30 mL), the filtrates are combined, and dried in vacuo. Yield: (3.5 mg, 8.1 mmol). 92%. Solution NMR. ^{1}H NMR (methanol-*d*4, 700 MHz, δ): 7.39 (d, 2 H, ^3JHH = 7.7 Hz, *ortho*-C6H5), 7.04 (t, 2 H, ^3JHH = 7.7 Hz, *meta*-C6H5), 6.97 (t, 1 H, ^3JHH = 7.7 Hz, *para*-C6H5), 3.98 (dd, 3 H, ^2JHH = 8.6 Hz, ^3JHH = 10.1 Hz, $\overline{CNC(CHMe_2)HCH_2O}$), 3.90 (ddd, 3 H, ^3JHH = 5.1 Hz, ^3JHH = 7.1 Hz, ^3JHH = 10.1 Hz, $\overline{CNC(CHMe_2)HCH_2O}$), 3.83 (dd, 3 H, ^2JHH = 8.6 Hz, ^3JHH = 7.1 Hz, $\overline{CNC(CHMe_2)HCH_2O}$, 1.81 (m, 3 H, $\overline{CNC(CHMe_2)HCH_2O}$), 0.91 (d, 9 H, ^3JHH = 7.0 Hz, $\overline{CNC(CHMe_2)HCH_2O}$), 0.82 (d, 9 H, ^3JHH = 7.0 Hz, $\overline{CNC(CHMe_2)HCH_2O}$).

$^{13}C\{^{1}H\}$ NMR (methanol-*d*4, 175 MHz, δ): 135.21 (*ortho*-C6H5), 127.54 (*meta*-C6H5), 125.66 (*para*-C6H5), 71.98 ($\overline{CNC(CHMe_2)HCH_2O}$, 68.39 ($\overline{CNC(CHMe_2)HCH_2O}$, 33.29 ($\overline{CNC(CHMe_2)HCH_2O}$), 19.54 ($\overline{CNC(CHMe_2)HCH_2O}$), 17.56 ($\overline{CNC(CHMe_2)HCH_2O}$. ^{11}B NMR (methanol-*d*4, 400 MHz, δ): -16.8. ^{15}N NMR (methanol-*d*4, 71 MHz, δ): -166.3. Solid-state NMR $^{13}C\{^{1}H\}$ CPMAS (150.8 MHz, δ): 187.2 ($\overline{CNC(CHMe_2)HCH_2O}$-NCO-), 183.5, 152.5 (*i*-C6H5), 149.7, 132.8 (*o*-C6H5), 125.5 (*m*-C6H5, *p*-C6H5), 73.2 ($\overline{CNC(CHMe_2)HCH_2O}$), 70.8, 67.9 ($\overline{CNC(CHMe_2)HCH_2O}$), 64.6, 31.0 ($\overline{CNC(CHMe_2)HCH_2O}$ 19.5 ($\overline{CNC(CHMe_2)HCH_2O}$, 17.7, 14.5. $^{15}N\{^{1}H\}$ CPMAS (60.8 MHz, δ): -171 (2 N), -161 (1 N). IR (KBr, cm^{-1}): 3396 w, 3068 w, 3045 w, 2951 s, 2895 s, 1589 s, 1480 m, 1465 m, 1431 w, 1388 w, 1370 w, 1340 w, 1266 w, 1173 m, 1111 m, 1034 w, 971 s, 926 m, 830 w, 793 w, 734 m, 703 m. Anal. Calcd for C24H35N3O3BLi: C, 66.8; H, 8.18; N, 9.74. Found: C, 66.4; H, 8.45; N, 9.52. m.p. 218-220 °C.

6.2.5.Hydrogen *tris*(*4S*-4-isopropyl-2-oxazolinyl)phenyl borate (H[To^{P}])

An oven dried 50 mL Schlenk flask containing a magnetic stir bar is charged with Li[*S*-To^{P}] (1.08 g, 2.50 mmol), [NEt_3H]Cl (0.35 g, 3.46 mmol), and 30 mL THF. The mixture is stirred for 6 hours and then the solvent is removed under reduced pressure. The solid residue is extracted with diethyl ether (2 × 50 mL), and 0.66 g of crude product is obtained. To further purify the compound, a solution of H[*S*-To^{P}] in toluene is filtered through Grade III neutral alumina, and the filtrate is evaporated in vacuo yielding 0.36 g (0.85 mmol, 34 %).^{1}H NMR (benzene-d_6, 400 MHz, δ): 8.14 (d, 2 H, $^{3}J_{HH}$ = 6.8 Hz, *ortho*-C_6H_5), 7.47 (m, 2 H, *meta*-C_6H_5), 7.27 (t, 1 H, $^{3}J_{HH}$ = 7.6 Hz, *para*-C_6H_5), 3.84 (m, 3 H, $\overline{CNC(CHMe_2)HCH_2O}$), 3.61 (m, 3 H, $\overline{CNC(CHMe_2)HCH_2O}$), 3.42 (m, 3 H, $\overline{CNC(CHMe_2)HCH_2O}$), 1.42 (m, 3 H, $\overline{CNC(CHMe_2)HCH_2O}$), 0.88 (d, 9 H, $^{3}J_{HH}$ = 6.8 Hz, $\overline{CNC(CHMe_2)HCH_2O}$), 0.68 (d, 9 H, $^{3}J_{HH}$ = 6.8 Hz, $\overline{CNC(CHMe_2)HCH_2O}$). $^{13}C\{^{1}H\}$ NMR (CD_2Cl_2, 100 MHz, δ): 134.11 (*meta*-C_6H_5), 127.59 (*ortho*-C_6H_5), 126.03 (*para*-C_6H_5), 71.12 ($\overline{CNC(CHMe_2)HCH_2O}$), 69.76 ($\overline{CNC(CHMe_2)HCH_2O}$), 33.29 ($\overline{CNC(CHMe_2)HCH_2O}$),

19.05 ($\overline{\text{CNC(CH}Me_2\text{)HCH}_2\text{O}}$), 18.73 ($\overline{\text{CNC(CH}Me_2\text{)HCH}_2\text{O}}$). IR (KBr, cm^{-1}): 3069 m, 3044 m, 2959 s, 2874 s, 2348 w, 2299 w, 2137 w, 1594 s (C=N), 1479 m, 1431 w, 1388 w, 1389 w, 1339 w, 1262 m, 1173 m, 1111 m, 1032 m, 989 m, 970 m, 925 w, 980 w, 798 m, 736 m, 702 m.

6.2.5. Ruthenium *tris*(κ^3-*4S*-4-isopropyl-2-oxazolinyl)phenylborate*tris*(acetonitrile) tetraphenylborate [Ru(κ^3-*S*-To^P)(NCCH$_3$)$_3$]BPh$_4$

An oven-dried 100 mL Schlenk tube is charged with a mixture of lithium *tris*(*4S*-4-isopropyl-2-oxazolinyl)phenyl borate Li[To^P] (0.210 g, 0.487 mmole) , ruthenium (η^4-cycloocta-1,5-diene) dichloride $[Ru(COD)Cl_2]_n$ (0.140 g, 0.500 mmole) and sodium tetraphenylborate $NaBPh_4$ (0.366 g, 1.06 mmole) in the glovebox. The solids are suspended in acetonitrile (20 mL), and the mixture is stirred and heated to 60-70^{o}C for 24 hours until the solids dissolve completely and form a bright yellow solution with some white crystals precipitate at the bottom. The solvent is evaporated under reduced pressure yielding a crude pale yellow solid. The solid is extracted with methylene chloride (1 × 10 mL) to form a yellow solution with undissolved white crystals of LiCl at the bottom. The solution is filtered, and the filtrate is layered with 100 mL methylene chloride on the top. The product precipitates out of the solution as yellow needle-like crystals at -40^{o}C (0.158 g, 32.6 %). ^{1}H NMR (CD_3CN, 400 MHz, δ): 7.64 (d, 2 H, $^3J_{HH}$ = 6.8 Hz, *ortho*-C_6H_5-[*S*-To^P]), 7.3 (br, 8 H, *ortho*-$B(C_6H_5)_4$) 7.20 (t, 2 H, $^3J_{HH}$ = 7.6 Hz, *meta*-C_6H_5-[*S*-To^P]), 7.17 (t, 1 H, $^3J_{HH}$ = 7.6 Hz, *para*-C_6H_5-[*S*-To^P]), 7.02 (t, 8 H, $^3J_{HH}$ = 7.2 Hz, *meta*-$B(C_6H_5)_4$), 6.87 (t, 4 H, $^3J_{HH}$ = 7.2 Hz, *para*-$B(C_6H_5)_4$), 4.24 (m, 6 H, $\overline{\text{CNC(CHMe}_2\text{)HC}H_2\text{O}}$), 4.11 (m, 3 H, $^3J_{HH}$ = 3.6Hz, $\overline{\text{CNC(CHMe}_2\text{)}H\text{CH}_2\text{O}}$), 2.44 (s, 9 H, CH_3CN), 2.33 (m, 3 H, $^3J_{HH}$ = 3.6 Hz, $\overline{\text{CNC(C}H\text{Me}_2\text{)HCH}_2\text{O}}$), 0.89 (d, 9 H, $^3J_{HH}$ = 6.8 Hz, $\overline{\text{CNC(CH}Me_2\text{)HCH}_2\text{O}}$), 0.60 (d, 9 H, $^3J_{HH}$ = 6.8 Hz, $\overline{\text{CNC(CH}Me_2\text{)HCH}_2\text{O}}$).^{11}B NMR (acetonitrile-d_3, 400 MHz, δ): -6.53 ($B(C_6H_5)_4$), -19.30 (*S*-To^P). IR (KBr, cm^{-1}): 3054 m, 2998 m, 2964 m, 2920 w, 2873 w, 2268 m (CH_3CN), 1593 m (oxazoline C=N), 1581 m (oxazoline C=N), 1479 m,

1464 w, 1427 w, 1391 w, 1364 w, 1321 w, 1265 w, 1220 m, 1183 w, 1146 w, 1116 w, 1067 w, 1032 w, 1013 w, 969 m, 870 w, 846 w, 800 w, 732 m, 704 s.

6.2.6. Ruthenium *tris*(κ^3-*4S*-4-isopropyl-2-oxazolinyl)phenylborate (η^6-*p*-cymeme) chloride Ru(κ^3-*S*-To^P)(η^6-*p*-cymeme)Cl

An oven dried, Teflon sealed 50 mL Schlenk tube is charged with the dimer of ruthenium (η^6-*p*-cymeme) dichloride (0.103 g, 0.168 mmole) lithium *tris*(*4S*-4-isopropyl-2-oxazolinyl)phenylborate (0.123 g, 0.285 mmole) and a stir bar. The solids are suspended in anhydrous benzene (20 mL), and the flask is heated to 120 ^{o}C for 5 days. The solids dissolved and formed a deep blue solution. The solvents are removed under reduced pressure yielding a crude blue solid. The solids are extracted with methylene chloride (1 × 15 mL) to form a brown solution with undissolved white crystals of LiCl at the bottom. The solution is filtered, and the filtrate is layered with hexane. Blue solid product precipitates out of the solution at a 50% yield. (0.0986 g, 0.142 mmole) ^{1}H NMR (C_6D_6, 400 MHz, δ): 8.45 (d, $^3J_{HH}$ = 3.6 Hz, 2H, *ortho*-C_6H_5-[*S*-To^P]), 7.53 (t, $^3J_{HH}$ = 7.2 Hz, 2H, *meta*-C_6H_5-[*S*-To^P]), 7.32 (m, 1H, *para*-C_6H_5-[*S*-To^P]), 4.88 (t, $^3J_{HH}$ = 5.6 Hz, 2H, $(CH_3)_2CH(CC_2H_2C_2H_2C)CH_3$), 4.53 (d, $^3J_{HH}$ = 6.4 Hz, 2H, $(CH_3)_2CH(CC_2H_2CH_2C)CH_3$), 4.23 (m, 3H, $\overline{CNC(CHMe_2)HCH_2O}$), 3.99 (m, 6H, $\overline{CNC(CHMe_2)HCH_2O}$), 2.97 (m, 3H, $\overline{CNC(CHMe_2)HCH_2O}$), 2.75 (m, 3H, $(CH_3)_2CH(CC_2H_2CH_2C)CH_3$), 1.79 (s, 3H, $(CH_3)_2CH(CC_2H_2CH_2C)CH_3$), 1.09 (m, 6H, $(CH_3)_2CH(CC_2H_2CH_2C)CH_3$), 0.72 (dd, $^3J_{HH}$ = 4.0 Hz, $\overline{CNC(CHMe_2)HCH_2O}$). ^{13}B NMR ($C_6D_6$, 400 MHz, δ): -19.24.

6.2.7. Ruthenium *tris*(κ^3-*4S*-isopropyl-2-oxazolinyl)phenylborate (η^4-cycloocta-1,5-diene) hydride [Ru(κ^3-*S*-To^P)(η^4-COD)H]

An oven dried 50 mL Schlenk flask is charged with ruthenium (η^4-cycloocta-1,5-diene) *tris*(dimethylhydrazine)hydride *tetra*phenylborate (0.0722 g, 0.101 mmole), lithium *tris*(*4S*-4-isopropyl-2-oxazolinyl)phenylborate (0.0440 g, 0.102 mmole) and a stir bar. The

solids are suspended in anhydrous ethanol (10 mL), and the flask is charged with a cold finger. The mixture is heated to reflux, and the solution immediately turns brown. The solution keeps refluxing for 2 hours, and the solvent is evaporated under reduced pressure yielding a crude brown solid. The solid is extracted with methylene chloride (1 × 10 mL) to form a brown solution with undissolved white crystals of $LiBPh_4$ at the bottom. The solution is filtered, and the filtrate is evaporated under reduced pressure yielding a brown solid product. (0.0232 g, 36.6%) ^{1}H NMR (CD_3CN, 400 MHz, δ): (Figure S1) 7.57 (d, *ortho*-C_6H_5--[*S*-To^P]), 7.28 (br, *ortho*-$(C_6H_5)_4B^-$), 7.19 (m, *meta*-C_6H_5-[*S*-To^P]), 7.12(m, *para*-C_6H_5-[*S*-To^P]), 7.00 (t, *meta*-$(C_6H_5)_4B^-$), 6.85 (t, *para*-$(C_6H_5)_4B^-$), 4.80 (m, COD), 4.39(m, COD), 4.16 (m, COD), 4.03(m, COD), 3.94 (m, COD), 3.76 (m, COD), 1.13-0.37 (a series of doublets, [To^P]), -5.11(s, Ru-H).

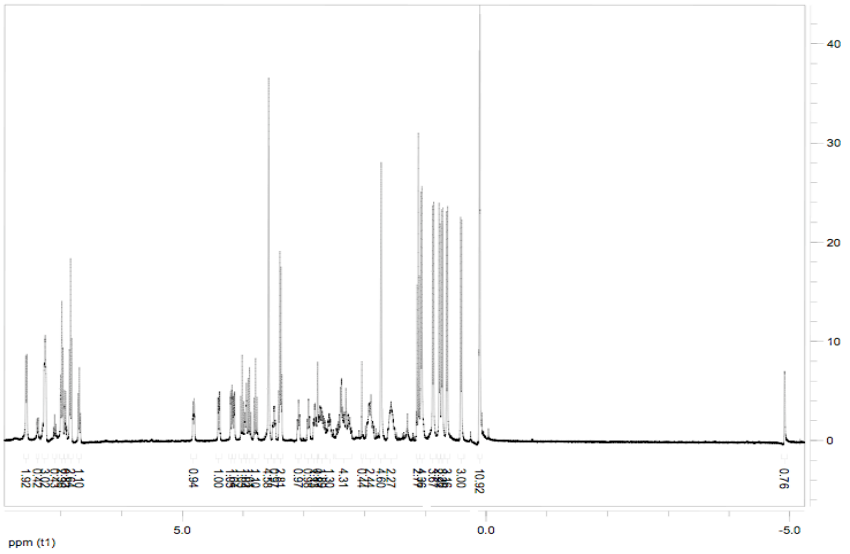

Figure S1 ^{1}H NMR of [Ru(κ^3-*S*-To^P)(η^4-COD)H] in acetonitrile-d_4

6.3. X-ray Crystallographic Data for Compounds

6.3.1. Hydrogen *tris*(4,4-dimethyl-2-oxazolin-2-yl)phenylborate (H[To^M]).

The structure of hydrogen *tris*(4,4-dimethyl-2-oxazolin-2-yl)phenylborate (H[To^{M}]) was previously reported by the group, and the following data and figures pertain only to the papers in which they are included.

Formula: C21H29.50BN3O3.25 (C21H28BN3O3.(H2O)1/4)

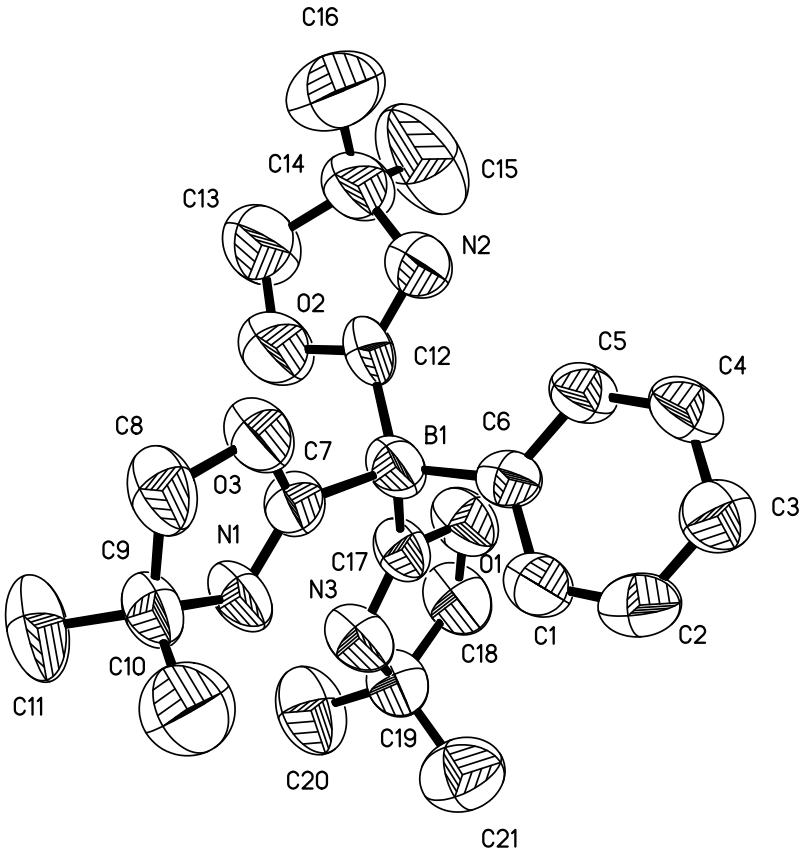

Figure S2. ORTEP plot of one of the [To^{M}]$^{-}$ molecules in the unit cell. Ellipsoids are plotted at 50% probability level. Hydrogen atoms, the second [To^{M}]$^{-}$unit, and a water molecule modeled at 50% occupancy are omitted for clarity.

Experimental for H[To^{M}].

Data Collection

A colorless small crystal was selected under ambient conditions. The crystal was

mounted and centered in the X-ray beam by using a video camera. The crystal evaluation and data collection were performed at 293 K on a Bruker CCD-1000 diffractometer with Mo Kα (λ = 0.71073 Å) radiation and the detector to crystal distance of 5.03 cm. Room temperature data collection was necessary because the crystal broke when cooled.

The initial cell constants were obtained from three series of ω scans at different starting angles. Each series consisted of 30 frames collected at intervals of 0.3º in a 10º range about ω with the exposure time of 30 seconds per frame. The obtained reflections were successfully indexed by an automated indexing routine built in the SMART program. The final cell constants were calculated from a set of strong reflections from the actual data collection. The data were collected using the full sphere routine by collecting four sets of frames with 0.3º scans in ω with an exposure time 30 sec per frame. This dataset was corrected for Lorentz and polarization effects. The absorption correction was based on fitting a function to the empirical transmission surface as sampled by multiple equivalent measurements[1] using SADABS software[2].

Structure Solution and Refinement

Although a full sphere of data was collected, the resolution of data was as low as 1.1 Å. The systematic absences in the diffraction data were consistent with the space group *P*21/n [2], yielding chemically reasonable and computationally stable results of refinement. The positions of almost all nonhydrogen atoms were found by direct methods. The remaining atoms were located in an alternating series of least-squares cycles and difference Fourier maps. All non-hydrogen atoms were refined in full-matrix anisotropic approximation except of C39 which was NPD and refined isotropically. All hydrogen atoms were placed in the structure factor calculation at idealized positions and were allowed to ride on the neighboring atoms with relative isotropic displacement coefficients.

The ORTEP diagram for one of two crystallographically independent molecules was drawn at 50% probability level. The second molecule is shown in ball-and-stick

representation. H-atoms were omitted for clarity. One significant peak of positive electron density was found in the voids between molecules in a crystal packing mode. This peak was assigned as O-atom of a solvent water molecule, and its occupancy factor was refined. The obtained value was found close to 0.5, therefore, it was stated that there is half of a water molecule per each 2 organic molecules.

Table S1. Crystal data and structure refinement for C21H29.50BN3O3.25 (H[To^{M}]).

Identification code	sad01	
Empirical formula	C21 H29.50 B N3 O3.25	
Formula weight	386.79	
Temperature	298(2) K	
Wavelength	0.71073 Å	
Crystal system	Monoclinic	
Space group	P2(1)/n	
Unit cell dimensions	a = 17.756(2) Å	α= 90°.
	b = 14.0182(17) Å	β= 108.613(2)°.
	c = 19.789(2) Å	γ = 90°.
Volume	4667.9(10) Å^3	
Z	8	
Density (calculated)	1.101 Mg/m^3	
Absorption coefficient	0.074 mm^{-1}	
F(000)	1660	
Crystal size	0.50 x 0.40 x 0.35 mm^3	
Theta range for data collection	1.34 to 20.82°.	
Index ranges	-17<=h<=17, -14<=k<=14, -19<=l<=19	
Reflections collected	23736	
Independent reflections	4881 [R(int) = 0.0641]	
Completeness to theta = 20.82°	100.0 %	
Absorption correction	Semi-empirical from equivalents	
Max. and min. transmission	1 and 0.74	
Refinement method	Full-matrix least-squares on F^2	
Data / restraints / parameters	4881 / 3 / 521	
Goodness-of-fit on F^2	1.063	
Final R indices [I>2sigma(I)]	R1 = 0.0808, wR2 = 0.2211	
R indices (all data)	R1 = 0.1303, wR2 = 0.2618	
Largest diff. peak and hole	0.660 and -0.501 e.Å^{-3}	

Table S2. Atomic coordinates (x 10^4) and equivalent isotropic displacement parameters ($Å^2$ x 10^3) for C21H29.50BN3O3.25 (H[To^M]). U(eq) is defined as one third of the trace of the orthogonalized U^{ij} tensor.

	x	y	z	U(eq)
B(1)	6942(4)	8789(5)	1861(4)	65(2)
B(2)	1902(4)	9019(4)	2585(3)	48(2)
C(1)	7980(4)	8842(4)	3133(4)	69(2)
C(2)	8227(4)	8852(5)	3869(4)	77(2)
C(3)	7690(4)	8838(5)	4235(4)	75(2)
C(4)	6906(4)	8796(5)	3850(4)	74(2)
C(5)	6648(4)	8781(4)	3108(4)	64(2)
C(6)	7179(3)	8808(4)	2728(3)	56(2)
C(7)	7359(4)	7849(4)	1668(3)	61(2)
C(8)	7557(5)	6275(5)	1557(4)	86(2)
C(9)	8241(4)	6805(4)	1422(4)	69(2)
C(10)	9008(5)	6612(6)	2007(5)	122(3)
C(11)	8289(6)	6623(6)	683(4)	111(3)
C(12)	6016(4)	8737(5)	1423(4)	73(2)
C(13)	5011(5)	8606(9)	358(5)	148(4)
C(14)	4679(5)	8705(9)	967(4)	117(3)
C(15)	4198(7)	9629(11)	922(6)	188(6)
C(16)	4210(8)	7886(11)	1033(6)	203(7)
C(17)	7335(4)	9706(4)	1618(3)	61(2)
C(18)	7403(5)	11282(5)	1397(4)	86(2)
C(19)	8137(4)	10781(4)	1343(4)	70(2)
C(20)	8239(6)	10912(6)	618(4)	113(3)
C(21)	8868(5)	11082(6)	1927(5)	115(3)
C(22)	3385(3)	9023(4)	2602(3)	56(2)
C(23)	4201(3)	9058(4)	2919(4)	67(2)
C(24)	4507(4)	9095(5)	3643(4)	75(2)
C(25)	4008(4)	9116(5)	4047(4)	71(2)

Table S2. (continued)

	x	y	z	U(eq)
C(26)	3195(3)	9089(4)	3721(3)	54(2)
C(27)	2857(3)	9044(3)	2989(3)	41(1)
C(28)	1352(3)	8988(4)	3075(3)	51(2)
C(29)	130(5)	9004(7)	3206(5)	112(3)
C(30)	737(5)	8796(9)	3881(4)	125(4)
C(31)	610(8)	7736(15)	4034(10)	291(12)
C(32)	755(7)	9322(16)	4483(8)	322(14)
C(33)	1692(3)	9969(4)	2086(3)	47(2)
C(34)	1450(4)	11524(4)	1823(3)	75(2)
C(35)	1481(4)	11028(4)	1155(3)	63(2)
C(36)	2219(5)	11306(6)	959(5)	112(3)
C(37)	738(5)	11139(5)	535(4)	119(3)
C(38)	1686(3)	8116(4)	2045(3)	45(1)
C(39)	1643(2)	7263(3)	2337(2)	12(1)
C(40)	1467(3)	7096(4)	1118(3)	48(2)
C(41)	2196(4)	6795(5)	943(4)	76(2)
C(42)	738(4)	6995(5)	479(4)	89(2)
N(1)	7989(3)	7795(3)	1483(3)	71(2)
N(2)	5412(4)	8755(5)	1611(3)	97(2)
N(3)	7962(3)	9768(3)	1445(3)	74(2)
N(4)	1492(3)	8828(5)	3720(3)	104(2)
N(5)	1578(3)	10022(3)	1409(3)	58(1)
N(6)	1576(3)	8104(3)	1378(3)	53(1)
O(1)	6968(3)	10559(3)	1636(2)	79(1)
O(2)	5859(3)	8678(5)	690(3)	129(2)
O(3)	7066(3)	6995(3)	1733(2)	79(1)
O(4)	554(2)	9052(4)	2694(2)	89(2)
O(5)	1659(2)	10809(3)	2385(2)	65(1)
O(6)	1390(4)	6559(4)	1775(3)	125(2)
O(8)	518(6)	1184(7)	8708(5)	106(3)

Table S3. Bond lengths [Å] and angles [°] for Sad01.

B(1)-C(12)	1.598(10)	C(11)-H(11C)	0.9600
B(1)-C(17)	1.608(10)	C(12)-N(2)	1.241(8)
B(1)-C(7)	1.615(9)	C(12)-O(2)	1.389(8)
B(1)-C(6)	1.631(10)	C(13)-O(2)	1.441(9)
B(2)-C(28)	1.581(9)	C(13)-C(14)	1.507(11)
B(2)-C(38)	1.621(9)	C(13)-H(13A)	0.9700
B(2)-C(33)	1.628(9)	C(13)-H(13B)	0.9700
B(2)-C(27)	1.629(8)	C(14)-C(16)	1.448(14)
C(1)-C(2)	1.381(9)	C(14)-N(2)	1.505(10)
C(1)-C(6)	1.392(8)	C(14)-C(15)	1.538(14)
C(1)-H(1)	0.9300	C(15)-H(15A)	0.9600
C(2)-C(3)	1.369(9)	C(15)-H(15B)	0.9600
C(2)-H(2)	0.9300	C(15)-H(15C)	0.9600
C(3)-C(4)	1.358(9)	C(16)-H(16A)	0.9600
C(3)-H(3)	0.9300	C(16)-H(16B)	0.9600
C(4)-C(5)	1.391(9)	C(16)-H(16C)	0.9600
C(4)-H(4)	0.9300	C(17)-N(3)	1.268(7)
C(5)-C(6)	1.382(8)	C(17)-O(1)	1.368(7)
C(5)-H(5)	0.9300	C(18)-O(1)	1.441(7)
C(7)-N(1)	1.286(7)	C(18)-C(19)	1.515(9)
C(7)-O(3)	1.329(7)	C(18)-H(18A)	0.9700
C(8)-O(3)	1.447(7)	C(18)-H(18B)	0.9700
C(8)-C(9)	1.518(9)	C(19)-N(3)	1.482(8)
C(8)-H(8A)	0.9700	C(19)-C(21)	1.497(10)
C(8)-H(8B)	0.9700	C(19)-C(20)	1.513(9)
C(9)-N(1)	1.474(8)	C(20)-H(20A)	0.9600
C(9)-C(10)	1.504(10)	C(20)-H(20B)	0.9600
C(9)-C(11)	1.514(9)	C(20)-H(20C)	0.9600
C(10)-H(10A)	0.9600	C(21)-H(21A)	0.9600
C(10)-H(10B)	0.9600	C(21)-H(21B)	0.9600
C(10)-H(10C)	0.9600	C(21)-H(21C)	0.9600
C(11)-H(11A)	0.9600	C(22)-C(23)	1.385(8)
C(11)-H(11B)	0.9600	C(22)-C(27)	1.386(7)

Table S3. (continued)

C(22)-H(22)	0.9300	C(34)-C(35)	1.511(9)
C(23)-C(24)	1.360(9)	C(34)-H(34A)	0.9700
C(23)-H(23)	0.9300	C(34)-H(34B)	0.9700
C(24)-C(25)	1.370(9)	C(35)-N(5)	1.488(7)
C(24)-H(24)	0.9300	C(35)-C(37)	1.496(9)
C(25)-C(26)	1.382(8)	C(35)-C(36)	1.532(10)
C(25)-H(25)	0.9300	C(36)-H(36A)	0.9600
C(26)-C(27)	1.381(7)	C(36)-H(36B)	0.9600
C(26)-H(26)	0.9300	C(36)-H(36C)	0.9600
C(28)-N(4)	1.242(7)	C(37)-H(37A)	0.9600
C(28)-O(4)	1.379(6)	C(37)-H(37B)	0.9600
C(29)-O(4)	1.444(8)	C(37)-H(37C)	0.9600
C(29)-C(30)	1.453(11)	C(38)-N(6)	1.271(6)
C(29)-H(29A)	0.9700	C(38)-C(39)	1.341(6)
C(29)-H(29B)	0.9700	C(39)-O(6)	1.447(7)
C(30)-C(32)	1.392(13)	C(39)-H(39A)	0.9700
C(30)-N(4)	1.473(9)	C(39)-H(39B)	0.9700
C(30)-C(31)	1.547(19)	C(40)-N(6)	1.494(7)
C(31)-H(31A)	0.9600	C(40)-C(42)	1.500(8)
C(31)-H(31B)	0.9600	C(40)-C(41)	1.504(8)
C(31)-H(31C)	0.9600	C(40)-O(6)	1.546(8)
C(32)-H(32A)	0.9600	C(41)-H(41A)	0.9600
C(32)-H(32B)	0.9600	C(41)-H(41B)	0.9600
C(32)-H(32C)	0.9600	C(41)-H(41C)	0.9600
C(33)-N(5)	1.292(7)	C(42)-H(42A)	0.9600
C(33)-O(5)	1.328(6)	C(42)-H(42B)	0.9600
C(34)-O(5)	1.454(7)	C(42)-H(42C)	0.9600
C(12)-B(1)-C(17)	110.1(6)	C(28)-B(2)-C(38)	108.7(5)
C(12)-B(1)-C(7)	107.7(6)	C(28)-B(2)-C(33)	109.1(5)
C(17)-B(1)-C(7)	107.8(5)	C(38)-B(2)-C(33)	106.2(5)
C(12)-B(1)-C(6)	116.5(5)	C(28)-B(2)-C(27)	116.7(5)
C(17)-B(1)-C(6)	108.1(5)	C(38)-B(2)-C(27)	109.3(5)
C(7)-B(1)-C(6)	106.1(5)	C(33)-B(2)-C(27)	106.4(4)

Table S3. (continued)

C(2)-C(1)-C(6)	122.0(6)	C(9)-C(10)-H(10A)	109.5
C(2)-C(1)-H(1)	119.0	C(9)-C(10)-H(10B)	109.5
C(6)-C(1)-H(1)	119.0	H(10A)-C(10)-H(10B)	109.5
C(3)-C(2)-C(1)	121.1(7)	C(9)-C(10)-H(10C)	109.5
C(3)-C(2)-H(2)	119.4	H(10A)-C(10)-H(10C)	109.5
C(1)-C(2)-H(2)	119.4	H(10B)-C(10)-H(10C)	109.5
C(4)-C(3)-C(2)	117.9(7)	C(9)-C(11)-H(11A)	109.5
C(4)-C(3)-H(3)	121.1	C(9)-C(11)-H(11B)	109.5
C(2)-C(3)-H(3)	121.1	H(11A)-C(11)-H(11B)	109.5
C(3)-C(4)-C(5)	121.6(6)	C(9)-C(11)-H(11C)	109.5
C(3)-C(4)-H(4)	119.2	H(11A)-C(11)-H(11C)	109.5
C(5)-C(4)-H(4)	119.2	H(11B)-C(11)-H(11C)	109.5
C(6)-C(5)-C(4)	121.6(6)	N(2)-C(12)-O(2)	114.1(6)
C(6)-C(5)-H(5)	119.2	N(2)-C(12)-B(1)	132.4(6)
C(4)-C(5)-H(5)	119.2	O(2)-C(12)-B(1)	113.4(6)
C(5)-C(6)-C(1)	115.8(6)	O(2)-C(13)-C(14)	104.4(7)
C(5)-C(6)-B(1)	125.5(6)	O(2)-C(13)-H(13A)	110.9
C(1)-C(6)-B(1)	118.6(6)	C(14)-C(13)-H(13A)	110.9
N(1)-C(7)-O(3)	112.2(5)	O(2)-C(13)-H(13B)	110.9
N(1)-C(7)-B(1)	128.4(6)	C(14)-C(13)-H(13B)	110.9
O(3)-C(7)-B(1)	119.3(6)	H(13A)-C(13)-H(13B)	108.9
O(3)-C(8)-C(9)	106.2(5)	C(16)-C(14)-N(2)	109.1(9)
O(3)-C(8)-H(8A)	110.5	C(16)-C(14)-C(13)	112.4(10)
C(9)-C(8)-H(8A)	110.5	N(2)-C(14)-C(13)	103.1(7)
O(3)-C(8)-H(8B)	110.5	C(16)-C(14)-C(15)	110.3(10)
C(9)-C(8)-H(8B)	110.5	N(2)-C(14)-C(15)	108.9(8)
H(8A)-C(8)-H(8B)	108.7	C(13)-C(14)-C(15)	112.6(9)
N(1)-C(9)-C(10)	109.3(6)	C(14)-C(15)-H(15A)	109.5
N(1)-C(9)-C(11)	110.4(6)	C(14)-C(15)-H(15B)	109.5
C(10)-C(9)-C(11)	113.3(7)	H(15A)-C(15)-H(15B)	109.5
N(1)-C(9)-C(8)	99.6(5)	C(14)-C(15)-H(15C)	109.5
C(10)-C(9)-C(8)	110.9(6)	H(15A)-C(15)-H(15C)	109.5
C(11)-C(9)-C(8)	112.4(6)	H(15B)-C(15)-H(15C)	109.5

Table S3. (continued)

C(14)-C(16)-H(16A)	109.5	C(23)-C(22)-C(27)	122.9(6)
C(14)-C(16)-H(16B)	109.5	C(23)-C(22)-H(22)	118.6
H(16A)-C(16)-H(16B)	109.5	C(27)-C(22)-H(22)	118.6
C(14)-C(16)-H(16C)	109.5	C(24)-C(23)-C(22)	119.1(6)
H(16A)-C(16)-H(16C)	109.5	C(24)-C(23)-H(23)	120.5
H(16B)-C(16)-H(16C)	109.5	C(22)-C(23)-H(23)	120.5
N(3)-C(17)-O(1)	114.5(6)	C(23)-C(24)-C(25)	120.1(6)
N(3)-C(17)-B(1)	129.6(6)	C(23)-C(24)-H(24)	120.0
O(1)-C(17)-B(1)	115.8(6)	C(25)-C(24)-H(24)	120.0
O(1)-C(18)-C(19)	105.1(5)	C(24)-C(25)-C(26)	120.0(6)
O(1)-C(18)-H(18A)	110.7	C(24)-C(25)-H(25)	120.0
C(19)-C(18)-H(18A)	110.7	C(26)-C(25)-H(25)	120.0
O(1)-C(18)-H(18B)	110.7	C(27)-C(26)-C(25)	122.0(6)
C(19)-C(18)-H(18B)	110.7	C(27)-C(26)-H(26)	119.0
H(18A)-C(18)-H(18B)	108.8	C(25)-C(26)-H(26)	119.0
N(3)-C(19)-C(21)	109.4(6)	C(26)-C(27)-C(22)	115.9(5)
N(3)-C(19)-C(20)	109.8(6)	C(26)-C(27)-B(2)	123.5(5)
C(21)-C(19)-C(20)	111.2(7)	C(22)-C(27)-B(2)	120.6(5)
N(3)-C(19)-C(18)	102.2(5)	N(4)-C(28)-O(4)	114.0(5)
C(21)-C(19)-C(18)	111.6(6)	N(4)-C(28)-B(2)	132.5(5)
C(20)-C(19)-C(18)	112.2(6)	O(4)-C(28)-B(2)	113.1(5)
C(19)-C(20)-H(20A)	109.5	O(4)-C(29)-C(30)	104.7(6)
C(19)-C(20)-H(20B)	109.5	O(4)-C(29)-H(29A)	110.8
H(20A)-C(20)-H(20B)	109.5	C(30)-C(29)-H(29A)	110.8
C(19)-C(20)-H(20C)	109.5	O(4)-C(29)-H(29B)	110.8
H(20A)-C(20)-H(20C)	109.5	C(30)-C(29)-H(29B)	110.8
H(20B)-C(20)-H(20C)	109.5	H(29A)-C(29)-H(29B)	108.9
C(19)-C(21)-H(21A)	109.5	C(32)-C(30)-C(29)	119.2(12)
C(19)-C(21)-H(21B)	109.5	C(32)-C(30)-N(4)	113.3(9)
H(21A)-C(21)-H(21B)	109.5	C(29)-C(30)-N(4)	104.7(6)
C(19)-C(21)-H(21C)	109.5	C(32)-C(30)-C(31)	107.8(13)
H(21A)-C(21)-H(21C)	109.5	C(29)-C(30)-C(31)	105.1(10)
H(21B)-C(21)-H(21C)	109.5	N(4)-C(30)-C(31)	105.7(10)

Table S3. (continued)

C(30)-C(31)-H(31A)	109.5	C(35)-C(37)-H(37A)	109.5
C(30)-C(31)-H(31B)	109.5	C(35)-C(37)-H(37B)	109.5
H(31A)-C(31)-H(31B)	109.5	H(37A)-C(37)-H(37B)	109.5
C(30)-C(31)-H(31C)	109.5	C(35)-C(37)-H(37C)	109.5
H(31A)-C(31)-H(31C)	109.5	H(37A)-C(37)-H(37C)	109.5
H(31B)-C(31)-H(31C)	109.5	H(37B)-C(37)-H(37C)	109.5
C(30)-C(32)-H(32A)	109.5	N(6)-C(38)-C(39)	115.1(5)
C(30)-C(32)-H(32B)	109.5	N(6)-C(38)-B(2)	128.4(5)
H(32A)-C(32)-H(32B)	109.5	C(39)-C(38)-B(2)	116.5(5)
C(30)-C(32)-H(32C)	109.5	C(38)-C(39)-O(6)	108.9(4)
H(32A)-C(32)-H(32C)	109.5	C(38)-C(39)-H(39A)	109.9
H(32B)-C(32)-H(32C)	109.5	O(6)-C(39)-H(39A)	109.9
N(5)-C(33)-O(5)	113.3(5)	C(38)-C(39)-H(39B)	109.9
N(5)-C(33)-B(2)	127.3(5)	O(6)-C(39)-H(39B)	109.9
O(5)-C(33)-B(2)	119.4(5)	H(39A)-C(39)-H(39B)	108.3
O(5)-C(34)-C(35)	106.2(5)	N(6)-C(40)-C(42)	111.2(5)
O(5)-C(34)-H(34A)	110.5	N(6)-C(40)-C(41)	108.5(5)
C(35)-C(34)-H(34A)	110.5	C(42)-C(40)-C(41)	110.7(5)
O(5)-C(34)-H(34B)	110.5	N(6)-C(40)-O(6)	102.0(4)
C(35)-C(34)-H(34B)	110.5	C(42)-C(40)-O(6)	112.3(5)
H(34A)-C(34)-H(34B)	108.7	C(41)-C(40)-O(6)	111.8(5)
N(5)-C(35)-C(37)	110.6(5)	C(40)-C(41)-H(41A)	109.5
N(5)-C(35)-C(34)	100.0(5)	C(40)-C(41)-H(41B)	109.5
C(37)-C(35)-C(34)	113.6(6)	H(41A)-C(41)-H(41B)	109.5
N(5)-C(35)-C(36)	108.1(5)	C(40)-C(41)-H(41C)	109.5
C(37)-C(35)-C(36)	111.6(7)	H(41A)-C(41)-H(41C)	109.5
C(34)-C(35)-C(36)	112.2(6)	H(41B)-C(41)-H(41C)	109.5
C(35)-C(36)-H(36A)	109.5	C(40)-C(42)-H(42A)	109.5
C(35)-C(36)-H(36B)	109.5	C(40)-C(42)-H(42B)	109.5
H(36A)-C(36)-H(36B)	109.5	H(42A)-C(42)-H(42B)	109.5
C(35)-C(36)-H(36C)	109.5	C(40)-C(42)-H(42C)	109.5
H(36A)-C(36)-H(36C)	109.5	H(42A)-C(42)-H(42C)	109.5
H(36B)-C(36)-H(36C)	109.5	H(42B)-C(42)-H(42C)	109.5

Table S3. (continued)

C(7)-N(1)-C(9)	113.1(5)
C(12)-N(2)-C(14)	110.0(6)
C(17)-N(3)-C(19)	110.0(5)
C(28)-N(4)-C(30)	109.3(6)
C(33)-N(5)-C(35)	111.6(5)
C(38)-N(6)-C(40)	109.3(4)
C(17)-O(1)-C(18)	107.3(5)
C(12)-O(2)-C(13)	108.2(6)
C(7)-O(3)-C(8)	108.7(5)
C(28)-O(4)-C(29)	106.8(5)
C(33)-O(5)-C(34)	107.9(5)
C(39)-O(6)-C(40)	103.0(4)

Table 4. Anisotropic displacement parameters ($Å^2 x\ 10^3$) for Sad01. The anisotropic displacement factor exponent takes the form: $-2p^2[\ h^2\ a^{*2}U^{11} + ... + 2\ h\ k\ a^*\ b^*\ U^{12}\ ]$

	U^{11}	U^{22}	U^{33}	U^{23}	U^{13}	U^{12}
B(1)	67(5)	62(5)	76(6)	-7(4)	37(4)	2(4)
B(2)	48(4)	47(4)	44(4)	1(3)	8(3)	-5(3)
C(1)	64(5)	71(5)	81(5)	-2(4)	33(4)	0(3)
C(2)	60(4)	71(5)	99(6)	1(4)	22(5)	-8(3)
C(3)	76(5)	79(5)	71(5)	8(4)	24(4)	-5(4)
C(4)	67(5)	89(5)	75(5)	12(4)	38(4)	0(4)
C(5)	58(4)	76(5)	63(5)	9(3)	25(4)	-2(3)
C(6)	54(4)	39(4)	79(5)	0(3)	26(4)	-2(3)
C(7)	73(4)	47(4)	70(4)	-6(3)	33(4)	-11(3)
C(8)	122(6)	49(4)	108(6)	-6(4)	65(5)	3(4)
C(9)	86(5)	53(4)	81(5)	-5(3)	47(4)	5(4)
C(10)	109(7)	100(7)	149(9)	-9(6)	32(7)	17(5)
C(11)	181(9)	87(6)	97(6)	-11(5)	90(6)	2(5)
C(12)	83(5)	94(5)	53(5)	-10(4)	39(4)	-1(4)
C(13)	94(7)	260(14)	87(7)	-36(7)	25(6)	-3(7)
C(14)	79(6)	201(11)	75(6)	-21(6)	31(5)	-17(7)
C(15)	149(10)	295(18)	127(9)	26(10)	52(8)	102(11)
C(16)	176(12)	285(18)	159(11)	-69(11)	70(9)	-128(13)
C(17)	70(4)	49(4)	70(4)	0(3)	34(4)	10(3)
C(18)	110(6)	55(4)	111(6)	8(4)	59(5)	0(4)
C(19)	89(5)	52(4)	78(5)	7(3)	39(4)	-2(4)
C(20)	161(8)	98(6)	106(7)	14(5)	80(6)	1(5)
C(21)	101(6)	98(7)	135(8)	-1(6)	24(6)	-3(5)
C(22)	59(4)	53(4)	58(4)	3(3)	22(3)	5(3)
C(23)	42(4)	79(5)	81(5)	5(4)	22(4)	5(3)
C(24)	45(4)	85(5)	81(6)	11(4)	3(4)	4(3)
C(25)	54(4)	94(5)	55(4)	16(4)	2(4)	4(4)
C(26)	50(4)	51(4)	56(4)	7(3)	11(3)	0(3)
	U^{11}	U^{22}	U^{33}	U^{23}	U^{13}	U^{12}

Table 4. (continued)

C(27)	50(3)	29(3)	41(4)	4(2)	10(3)	0(2)
C(28)	39(4)	58(4)	49(4)	-3(3)	4(3)	-3(3)
C(29)	70(5)	172(9)	104(7)	-4(6)	41(5)	-2(5)
C(30)	62(5)	261(13)	61(5)	5(7)	32(4)	-16(6)
C(31)	181(14)	390(30)	350(20)	240(20)	157(16)	36(15)
C(32)	123(10)	650(40)	228(15)	-300(20)	101(10)	-96(15)
C(33)	42(3)	32(4)	62(4)	-8(3)	8(3)	4(2)
C(34)	92(5)	40(4)	78(5)	5(4)	6(4)	10(3)
C(35)	82(5)	38(4)	56(4)	5(3)	2(4)	1(3)
C(36)	145(8)	77(6)	129(8)	12(5)	63(6)	-20(5)
C(37)	132(7)	84(6)	96(6)	8(5)	-30(5)	26(5)
C(38)	44(3)	51(4)	39(4)	2(3)	9(3)	0(3)
C(40)	58(4)	34(3)	45(4)	4(3)	5(3)	0(3)
C(41)	92(5)	64(4)	81(5)	-2(4)	41(4)	1(4)
C(42)	91(5)	78(5)	72(5)	-4(4)	-10(4)	-10(4)
N(1)	83(4)	52(3)	99(4)	-4(3)	59(4)	7(3)
N(2)	68(4)	148(6)	77(4)	-23(4)	26(4)	-8(4)
N(3)	88(4)	48(3)	103(4)	9(3)	56(4)	1(3)
N(4)	61(4)	195(8)	58(4)	3(4)	22(3)	-9(4)
N(5)	77(4)	45(3)	43(3)	13(2)	7(3)	1(2)
N(6)	74(3)	33(3)	46(3)	-1(2)	12(3)	-2(2)
O(1)	90(3)	55(3)	107(4)	3(3)	52(3)	10(3)
O(2)	88(4)	210(7)	93(5)	-30(4)	36(3)	-9(4)
O(3)	99(3)	50(3)	112(4)	-9(2)	65(3)	-10(3)
O(4)	53(3)	147(5)	67(3)	-1(3)	17(3)	6(3)
O(5)	84(3)	42(3)	60(3)	-5(2)	12(2)	6(2)
O(6)	139(5)	115(5)	118(5)	12(4)	39(4)	-10(4)
O(8)	115(8)	103(8)	79(7)	-1(6)	3(6)	-7(6)

Table 5. Hydrogen coordinates (x 10^4) and isotropic displacement parameters (Å^{2}x 10^3) for Sad01.

	x	y	z	U(eq)
H(1)	8360	8860	2900	83
H(2)	8768	8868	4121	93
H(3)	7857	8857	4730	90
H(4)	6531	8776	4089	88
H(5)	6107	8752	2863	77
H(8A)	7254	5925	1134	104
H(8B)	7754	5828	1947	104
H(10A)	9434	6942	1906	183
H(10B)	9114	5939	2035	183
H(10C)	8967	6832	2453	183
H(11A)	7772	6701	337	166
H(11B)	8474	5985	658	166
H(11C)	8652	7069	586	166
H(13A)	4868	7994	123	178
H(13B)	4816	9110	11	178
H(15A)	3723	9598	518	282
H(15B)	4512	10165	871	282
H(15C)	4058	9701	1350	282
H(16A)	4462	7313	949	304
H(16B)	3688	7934	689	304
H(16C)	4167	7869	1504	304
H(18A)	7548	11802	1737	104
H(18B)	7088	11534	938	104
H(20A)	8669	10520	585	170
H(20B)	8355	11569	556	170
H(20C)	7757	10731	253	170
H(21A)	8795	10970	2381	172
H(21B)	8963	11748	1878	172
H(21C)	9315	10720	1897	172

Table 5. (continued)

	x	y	z	U(eq)
H(22)	3181	8983	2108	67
H(23)	4536	9057	2642	80
H(24)	5054	9106	3863	90
H(25)	4217	9149	4542	85
H(26)	2864	9101	4003	65
H(29A)	-268	8503	3082	135
H(29B)	-130	9606	3230	135
H(31A)	1090	7484	4363	436
H(31B)	474	7381	3596	436
H(31C)	188	7686	4236	436
H(32A)	710	9989	4367	484
H(32B)	1247	9206	4855	484
H(32C)	319	9132	4642	484
H(34A)	1824	12050	1943	90
H(34B)	921	11771	1756	90
H(36A)	2686	11210	1363	168
H(36B)	2183	11965	820	168
H(36C)	2251	10917	569	168
H(37A)	791	10795	133	179
H(37B)	651	11802	415	179
H(37C)	295	10890	658	179
H(39A)	1266	7290	2600	14
H(39B)	2159	7090	2667	14
H(41A)	2275	7216	589	114
H(41B)	2128	6155	763	114
H(41C)	2650	6823	1366	114
H(42A)	281	7204	598	133
H(42B)	672	6339	333	133
H(42C)	795	7378	96	133

6.3.2. Experimental for $[Ru(NCCH_3)_5Cl]Cl.(CH_2Cl_2)$

Formula $C_{11}\ H_{17}\ Cl_4\ N_5\ Ru$

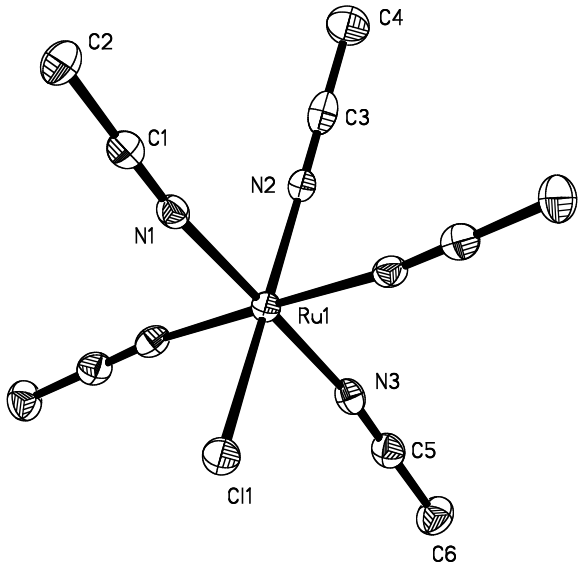

Figure S3 The ORTEP diagram was drawn at 50% probability level. H-atoms were omitted for clarity.

Data Collection

A colorless prismatic crystal was selected under ambient conditions under the layer of solvent. The crystal was covered with epoxy glue, mounted and centered in the X-ray beam by using a video camera.

The crystal evaluation and data collection were performed at 173 K on a Bruker CCD-1000 diffractometer with Mo K_α (λ = 0.71073 Å) radiation and the detector to crystal distance of 5.03 cm.

The initial cell constants were obtained from three series of ω scans at different starting angles. Each series consisted of 30 frames collected at intervals of 0.3º in a 10º range about ω with the exposure time of 10 seconds per frame. The obtained reflections were successfully indexed by an automated indexing routine built in the SMART program. The

final cell constants were calculated from a set of strong reflections from the actual data collection.

The data were collected using the full sphere routine by collecting four sets of frames with 0.3º scans in ω with an exposure time 10 sec per frame. This dataset was corrected for Lorentz and polarization effects. The absorption correction was based on fitting a function to the empirical transmission surface as sampled by multiple equivalent measurements[1] using SADABS software[2].

Structure Solution and Refinement

Observed data had a high internal R-factor as crystal was of a bad quality and unstable. All peaks were very wide and ESD for cell parameters were very high, therefore standard routine lead to unreasonable lattice. The structure was solved as a triclinic and it was found the result is very different from proposed formula. Analysis of atomic coordination proves that the right system is orthorhombic. The systematic absences in the diffraction data were close for the space groups $Pca2_1$ and *Pbcm*[2] and the last one yielded chemically reasonable and computationally stable results of refinement. The position of Ru and almost all non-hydrogen atoms were found by direct methods. The remaining atoms were located in an alternating series of least-squares cycles and difference Fourier maps. All non-hydrogen atoms including CH_2Cl_2 solvent were refined in full-matrix anisotropic approximation. All hydrogen atoms were placed in the structure factor calculation at idealized positions and were allowed to ride on the neighboring atoms with relative isotropic displacement coefficients. The cation: Cl^-: solvent ratio is 1:1:1.

Table S5. Crystal data and structure refinement for Sad04.

Identification code	sad04
Empirical formula	C11 H17 Cl4 N5 Ru
Formula weight	462.17
Temperature	173(2) K
Wavelength	0.71073 Å

Table S5. (continued)

Crystal system	Orthorhombic	
Space group	Pbcm	
Unit cell dimensions	a = 12.08(3) Å	a= 90°.
	b = 11.85(2) Å	b= 90°.
	c = 12.63(3) Å	g = 90°.
Volume	1809(6) $Å^3$	
Z	4	
Density (calculated)	1.697 Mg/m^3	
Absorption coefficient	1.457 mm^{-1}	
F(000)	920	
Crystal size	0.30 x 0.15 x 0.10 mm^3	
Theta range for data collection	2.41 to 28.77°.	
Index ranges	-15<=h<=15, -15<=k<=13, -16<=l<=16	
Reflections collected	12754	
Independent reflections	2320 [R(int) = 0.2117]	
Completeness to theta = 25.00°	98.6 %	
Absorption correction	Semi-empirical from equivalents	
Max. and min. transmission	1 and 0.62	
Refinement method	Full-matrix least-squares on F^2	
Data / restraints / parameters	2320 / 0 / 111	
Goodness-of-fit on F^2	1.007	
Final R indices [I>2sigma(I)]	R1 = 0.0666, wR2 = 0.1445	
R indices (all data)	R1 = 0.0998, wR2 = 0.1679	
Largest diff. peak and hole	2.254 and -3.501 $e.Å^{-3}$	

$R1 = \Sigma \, | \, |F_o| - |F_c| \, | \, / \, \Sigma \, |F_o|$ and $wR2 = \{ \, \Sigma \, [\, w(F_o^2 - F_c^2)^2 \,] \, / \, \Sigma \, [\, w(F_o^2)^2 \,] \, \}^{1/2}$

Table S6. Atomic coordinates (x 10^4) and equivalent isotropic displacement parameters ($Å^2$x 10^3) for Sad04. U(eq) is defined as one third of the trace of the orthogonalized U^{ij} tensor.

	x	y	z	U(eq)
Ru(1)	3660(1)	2470(1)	7500	16(1)
C(1)	5321(4)	1472(4)	5834(4)	21(1)
C(2)	6093(4)	933(6)	5116(3)	26(1)
C(3)	2710(6)	-6(7)	7500	25(2)
C(4)	2430(7)	-1166(7)	7500	34(2)
C(5)	2064(4)	3552(4)	9186(4)	23(1)
C(6)	1334(4)	4120(6)	9925(4)	30(2)
C(7)	933(7)	6297(7)	7500	37(2)
Cl(1)	4618(1)	4209(2)	7500	22(1)
Cl(2)	38(2)	5124(2)	7500	53(1)
Cl(3)	8743(2)	2500	0	35(1)
Cl(4)	2313(2)	5859(2)	7500	38(1)
N(1)	4706(3)	1874(3)	6388(3)	19(1)
N(2)	2916(5)	926(5)	7500	23(1)
N(3)	2634(3)	3101(3)	8609(3)	19(1)

Table S7. Bond lengths [Å] and angles [°] for Sad04.

Ru(1)-N(3)	2.014(5)	N(1)-Ru(1)-Cl(1)	89.91(15)
Ru(1)-N(1)	2.017(5)	N(2)-Ru(1)-Cl(1)	176.81(17)
Ru(1)-N(2)	2.039(7)	N(1)-C(1)-C(2)	178.6(5)
Ru(1)-Cl(1)	2.364(4)	C(1)-C(2)-H(2A)	109.5
C(1)-N(1)	1.127(6)	C(1)-C(2)-H(2B)	109.5
C(1)-C(2)	1.449(7)	H(2A)-C(2)-H(2B)	109.5
C(2)-H(2A)	0.9800	C(1)-C(2)-H(2C)	109.5
C(2)-H(2B)	0.9800	H(2A)-C(2)-H(2C)	109.5
C(2)-H(2C)	0.9800	H(2B)-C(2)-H(2C)	109.5
C(3)-N(2)	1.132(9)	N(2)-C(3)-C(4)	178.8(8)
C(3)-C(4)	1.415(12)	C(3)-C(4)-H(4A)	109.5
C(4)-H(4A)	0.9800	C(3)-C(4)-H(4B)	109.5
C(4)-H(4B)	0.9800	H(4A)-C(4)-H(4B)	109.5
C(4)-H(4C)	0.9800	C(3)-C(4)-H(4C)	109.5
C(5)-N(3)	1.136(6)	H(4A)-C(4)-H(4C)	109.5
C(5)-C(6)	1.451(7)	H(4B)-C(4)-H(4C)	109.5
C(6)-H(6A)	0.9800	N(3)-C(5)-C(6)	179.6(6)
C(6)-H(6B)	0.9800	C(5)-C(6)-H(6A)	109.5
C(6)-H(6C)	0.9800	C(5)-C(6)-H(6B)	109.5
C(7)-Cl(4)	1.747(9)	H(6A)-C(6)-H(6B)	109.5
C(7)-Cl(2)	1.762(9)	C(5)-C(6)-H(6C)	109.5
C(7)-H(7A)	0.9900	H(6A)-C(6)-H(6C)	109.5
C(7)-H(7B)	0.9900	H(6B)-C(6)-H(6C)	109.5
N(3)#1-Ru(1)-N(3)	88.2(3)	Cl(4)-C(7)-Cl(2)	110.6(5)
N(3)#1-Ru(1)-N(1)#1	178.65(15)	Cl(4)-C(7)-H(7A)	109.5
N(3)-Ru(1)-N(1)#1	91.8(2)	Cl(2)-C(7)-H(7A)	109.5
N(3)-Ru(1)-N(1)	178.65(15)	Cl(4)-C(7)-H(7B)	109.5
N(1)#1-Ru(1)-N(1)	88.3(3)	Cl(2)-C(7)-H(7B)	109.5
N(3)#1-Ru(1)-N(2)	93.55(19)	H(7A)-C(7)-H(7B)	108.1
N(3)-Ru(1)-N(2)	93.54(19)	C(1)-N(1)-Ru(1)	173.7(4)
N(1)-Ru(1)-N(2)	87.80(19)	C(3)-N(2)-Ru(1)	166.5(6)
N(3)#1-Ru(1)-Cl(1)	88.74(15)	C(5)-N(3)-Ru(1)	173.5(4)
N(3)-Ru(1)-Cl(1)	88.74(16)		

Symmetry transformations used to generate equivalent atoms:
#1 x,y,-z+3/2

Table S8. Anisotropic displacement parameters ($Å^2 x\ 10^3$) for Sad04. The anisotropic displacement factor exponent takes the form: $-2p^2[\ h^2\ a^{*2}U^{11} + ... + 2\ h\ k\ a^*\ b^*\ U^{12}\ ]$

	U^{11}	U^{22}	U^{33}	U^{23}	U^{13}	U^{12}
Ru(1)	17(1)	17(1)	15(1)	0	0	0(1)
C(1)	21(3)	21(3)	23(2)	1(2)	-2(2)	-1(2)
C(2)	24(3)	32(4)	23(2)	-3(2)	5(2)	1(3)
C(3)	20(4)	39(5)	16(3)	0	0	-2(4)
C(4)	34(5)	30(5)	38(4)	0	0	-2(4)
C(5)	22(3)	23(3)	24(2)	3(2)	2(2)	-7(2)
C(6)	30(3)	34(4)	26(3)	-4(2)	3(2)	5(3)
C(7)	35(5)	41(6)	34(4)	0	0	9(4)
Cl(1)	22(1)	22(1)	23(1)	0	0	-5(1)
Cl(2)	36(1)	73(2)	50(1)	0	0	-11(1)
Cl(3)	26(1)	47(2)	31(1)	-3(1)	0	0
Cl(4)	32(1)	43(2)	39(1)	0	0	0(1)
N(1)	22(2)	16(2)	19(2)	2(2)	-2(2)	-3(2)
N(2)	34(4)	22(4)	14(2)	0	0	4(3)
N(3)	16(2)	22(2)	20(2)	5(2)	0(2)	-3(2)

Table S9 Hydrogen coordinates (x 10^4) and isotropic displacement parameters (Å^{2}x 10^3) for Sad04.

	x	y	z	U(eq)
H(2A)	6220	153	5344	39
H(2B)	6796	1346	5122	39
H(2C)	5786	935	4399	39
H(4A)	1905	-1318	8074	51
H(4B)	3100	-1618	7606	51
H(4C)	2091	-1365	6820	51
H(6A)	1607	4011	10649	45
H(6B)	587	3805	9865	45
H(6C)	1314	4928	9763	45
H(7A)	789	6765	6866	44
H(7B)	789	6765	8134	44

6.3.3. Ruthenium *tris*(4*S*-4-isopropyl-2-oxazolin-2-yl)phenylborate *tris*acetonitrile *tetra*phenylborate [Ru(κ^3-*S*-To^P)(NCCH$_3$)$_3$]BPh$_4$

Formula: C54 H64 B2 N6 O3 Ru

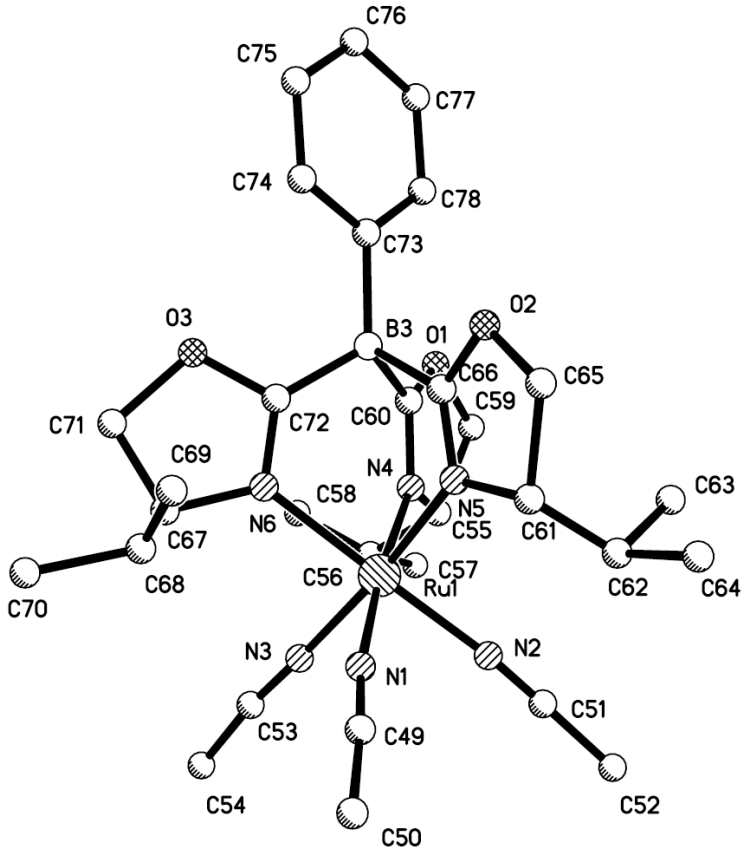

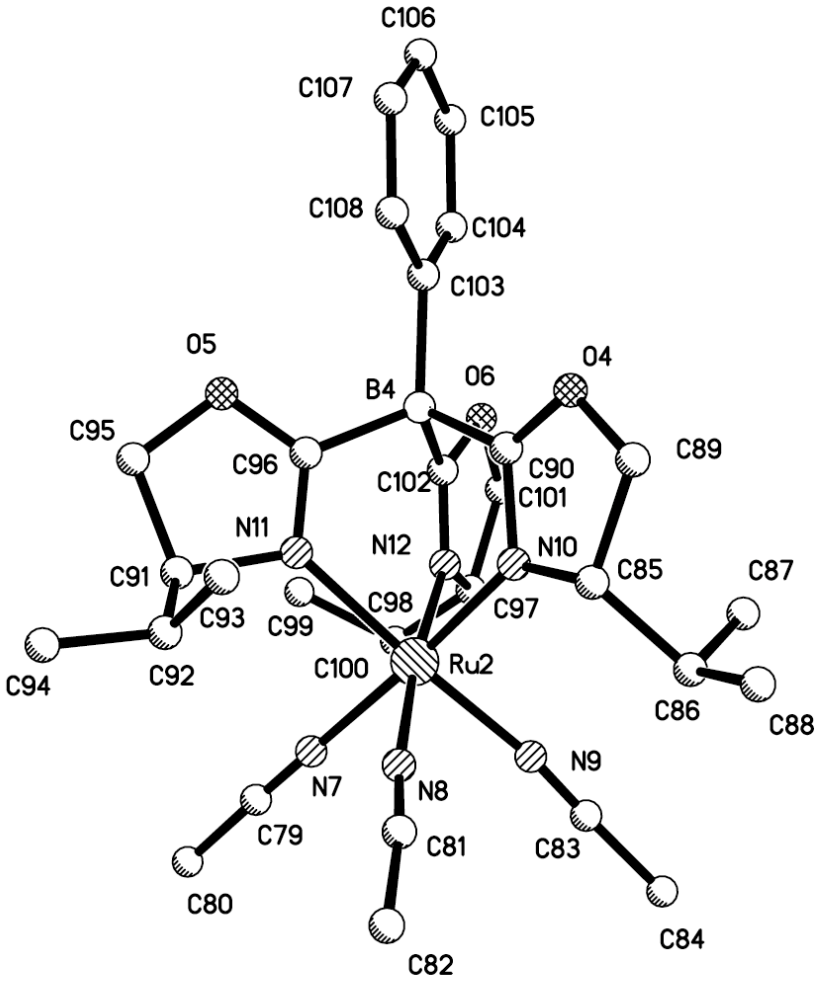

Figure S4. ORTEP plot of $[Ru(k^3\text{-}S\text{-}To^P)(NCCH_3)_3]^+$ molecules in the unit cell. Hydrogen atoms, the second $[Ru(k^3\text{-}S\text{-}To^P)(NCCH_3)_3]^+$ unit at 50% occupancy are omitted for clarity.

Experimental for $[Ru(\kappa^3\text{-}S\text{-}To^P)(NCCH_3)_3]BPh_4$

Data Collection

A yellow crystal was selected under ambient conditions. The crystal was mounted and centered in the X-ray beam by using a video camera.

The crystal evaluation and data collection were performed room temperature on a Bruker CCD-1000 diffractometer with Mo K_α (λ = 0.71073 Å) radiation and the detector to crystal distance of 5.03 cm. Crystal diffracted X-ray very weakly and it was clear from the very beginning that data will be of a very poor quality, however, the results of X-ray structure analysis proof the reaction path. Structure was refined in isotropic approximation for all atoms except of Ru and lead to reasonable molecular geometry and crystal packing mode. Structure might be published as it is, but collecting the low temperature data for the fresh crystal is strongly recommended. All geometrical parameters are for reference because of high values of ESD.

The initial cell constants were obtained from three series of w scans at different starting angles. Each series consisted of 30 frames collected at intervals of 0.3º in a 10º range about w with the exposure time of 60 seconds per frame. The obtained reflections were successfully indexed by an automated indexing routine built in the SMART program. The final cell constants were calculated from a set of strong reflections from the actual data collection.

The data were collected using the full sphere routine by collecting four sets of frames with 0.3º scans in w with an exposure time 60 sec per frame. This dataset was corrected for Lorentz and polarization effects. The absorption correction was based on fitting a function to the empirical transmission surface as sampled by multiple equivalent measurements[1] using SADABS software[2].

Structure Solution and Refinement

The systematic absences in the diffraction data were consistent for the space groups $P2_1$[2] yielded chemically reasonable and computationally stable results of refinement. The positions of almost all non-hydrogen atoms were found by direct methods (ESEL 1.45). The remaining atoms were located in an alternating series of least-squares cycles and difference

Fourier maps. All non-hydrogen atoms were refined in isotropic approximation. All Ph rings were constrained with AFIX 66 to increasy data-to-parameter ratio. H-atoms were included to calculation at idealized positions and were allowed to ride on the neighboring atoms with relative isotropic displacement coefficients.

The diagrams with atomic numbers show two structurally independent Ru clusters. H-atoms and counterions were omitted for clarity. The resulting CIF file has been tested with PLATON[3] software. The results and comments have been included to output package (Platon_Lar15.doc.). The X-Ray structure determination description from this report may be also added to correspondent fields of CIF file.

The crystal diffracted X-ray very weakly and it was clear from the very beginning that data will be of a very poor quality, however, the results of X-ray structure analysis proof the reaction path. Structure was refined in isotropic approximation for all atoms except of Ru and lead to reasonable molecular geometry and crystal packing mode. All geometrical parameters are for reference because of high values of ESD. Crystal data: $C_{54}H_{64}B_2N_6O_3Ru$, fw = 967.80g, monoclinic, space group *P*2(1) (no. 4), *a* = 17.295(3) Å, b = 12.632(2) Å, *c* = 26.098(5) Å, *V* = 5696.8(19) Å^3, *Z* = 4, *Dx* = 1.128 Mg/m^3, *m* = 0.67 mm^{-1}, *T* = 298(2) K. The crystal evaluation and data collection were performed room temperature on a Bruker CCD-1000 diffractometer with Mo K_α (λ = 0.71073 Å) radiation and the detector to crystal distance of 5.03 cm, with 0.3°*w* scan frames covering the entire reciprocal space up to q_{max}=10°, 22912 reflections collected, 8969 independent. This dataset was corrected for Lorentz and polarization effects. The absorption correction was based on fitting a function to the empirical transmission surface as sampled by multiple equivalent measurements using SADABS software.

Table S10. Crystal data and structure refinement for Sad05**.**

Identification code	sad05	
Empirical formula	C54 H64 B2 N6 O3 Ru	
Formula weight	967.80	
Temperature	298(2) K	
Wavelength	0.71073 Å	
Crystal system	Monoclinic	
Space group	P2(1)	
Unit cell dimensions	a = 17.295(3) Å	a= 90°.
	b = 12.632(2) Å	b= 92.312(4)°.
	c = 26.098(5) Å	g = 90°.
Volume	5696.8(19) $Å^3$	
Z	4	
Density (calculated)	1.128 Mg/m^3	
Absorption coefficient	0.318 mm^{-1}	
F(000)	2032	
Crystal size	0.45 x 0.23 x 0.16 mm^3	
Theta range for data collection	1.18 to 18.85°.	
Index ranges	-15<=h<=15, -11<=k<=11, -23<=l<=23	
Reflections collected	22912	
Independent reflections	8969 [R(int) = 0.1227]	
Completeness to theta = 18.85°	99.9 %	
Absorption correction	Semi-empirical from equivalents	
Max. and min. transmission	1 and 0.6	
Refinement method	Full-matrix least-squares on F^2	
Data / restraints / parameters	8969 / 1 / 378	
Goodness-of-fit on F^2	1.064	
Final R indices [I>2sigma(I)]	R1 = 0.1171, wR2 = 0.2954	
R indices (all data)	R1 = 0.1795, wR2 = 0.3462	
Absolute structure parameter	0.07(11)	
Largest diff. peak and hole	1.040 and -0.991 $e.Å^{-3}$	

---

*R*1 = S\SONDZEICHEN SYMBOL \f "Symbol" | $|F_o| - |F_c|$ | / S\SONDZEICHEN SYMBOL \f "Symbol" $|F_o|$ and w*R2* = { S\SONDZEICHEN SYMBOL \f "Symbol" [$w(F_o^2 - F_c^2)^2$] / S\SONDZEICHEN SYMBOL \f "Symbol" [$w(F_o^2)^2$] }$^{1/2}$

Table S11. Atomic coordinates (x 10^4) and equivalent isotropic displacement parameters ($Å^2$x 10^3) for $[Ru(\kappa^3\text{-}S\text{-}To^P)(NCCH_3)_3]^+$. U(eq) is defined as one third of the trace of the orthogonalized U^{ij} tensor.

	x	y	z	U(eq)
Ru(1)	2953(1)	3743(2)	8762(1)	46(1)
Ru(2)	7183(1)	2463(2)	6316(1)	47(1)
B(1)	97(15)	6520(20)	6205(10)	37(8)
B(2)	188(16)	9550(20)	8848(11)	43(8)
B(3)	4771(16)	4400(20)	8962(11)	44(8)
B(4)	5350(20)	2040(30)	6319(13)	68(10)
C(1)	-634(3)	6944(4)	6543(2)	28(6)
C(2)	-1406(3)	6880(5)	6377(2)	66(8)
C(3)	-1982(3)	7240(6)	6690(2)	75(9)
C(4)	-1785(2)	7664(5)	7169(2)	105(11)
C(5)	-1013(2)	7728(4)	7336(2)	58(7)
C(6)	-437(2)	7368(4)	7022(2)	52(7)
C(7)	882(3)	7236(5)	6240(2)	68(8)
C(8)	830(3)	8320(5)	6324(2)	51(7)
C(9)	1494(3)	8941(5)	6333(2)	88(9)
C(10)	2209(3)	8478(6)	6257(2)	79(9)
C(11)	2261(3)	7394(6)	6173(2)	97(10)
C(12)	1597(3)	6773(5)	6164(2)	62(8)
C(13)	234(3)	5280(4)	6423(2)	53(7)
C(14)	823(4)	5036(4)	6782(2)	53(7)
C(15)	891(4)	4014(4)	6975(2)	80(9)
C(16)	369(5)	3236(4)	6811(3)	80(9)
C(17)	-220(5)	3480(4)	6452(2)	68(8)
C(18)	-287(4)	4503(4)	6258(2)	55(7)
C(19)	-116(3)	6463(5)	5555(2)	58(8)
C(20)	199(4)	5655(5)	5269(2)	74(9)
C(21)	70(4)	5630(6)	4740(2)	108(12)
C(22)	-375(5)	6414(6)	4497(2)	98(11)
C(23)	-690(4)	7223(6)	4784(2)	92(10)

Table S11. (continued)

	x	y	z	U(eq)
C(24)	-560(4)	7247(6)	5313(2)	70(8)
C(25)	74(3)	10753(4)	8578(2)	34(6)
C(26)	-402(3)	10911(4)	8143(2)	42(6)
C(27)	-440(4)	11902(4)	7911(2)	56(7)
C(28)	-2(5)	12735(4)	8116(2)	66(8)
C(29)	474(5)	12577(5)	8551(2)	54(7)
C(30)	512(4)	11586(5)	8782(2)	51(7)
C(31)	272(4)	9637(5)	9482(2)	48(7)
C(32)	-117(4)	10405(6)	9753(2)	68(8)
C(33)	-111(4)	10365(6)	10286(2)	90(10)
C(34)	284(5)	9559(7)	10547(2)	121(13)
C(35)	673(5)	8791(6)	10276(2)	80(9)
C(36)	667(4)	8830(6)	9743(2)	83(9)
C(37)	931(3)	9021(5)	8546(2)	53(7)
C(38)	1675(3)	9036(6)	8768(2)	78(9)
C(39)	2299(3)	8727(6)	8484(2)	138(14)
C(40)	2179(2)	8403(6)	7978(2)	107(12)
C(41)	1435(2)	8388(5)	7756(2)	70(8)
C(42)	811(2)	8697(4)	8040(2)	38(6)
C(43)	-615(3)	8743(5)	8749(2)	53(7)
C(44)	-1356(3)	9158(5)	8680(2)	59(8)
C(45)	-1983(3)	8485(6)	8594(2)	79(9)
C(46)	-1870(3)	7396(6)	8577(2)	83(9)
C(47)	-1129(3)	6981(5)	8646(2)	69(8)
C(48)	-501(3)	7654(5)	8732(2)	60(7)
C(49)	2189(13)	1942(19)	8080(9)	37(6)
C(50)	1783(17)	1160(30)	7783(11)	83(10)
C(51)	1586(15)	5140(20)	8313(10)	55(8)
C(52)	918(16)	5700(20)	8102(11)	76(9)
C(53)	1840(16)	3070(20)	9633(11)	62(8)
C(54)	1280(16)	2810(30)	10009(11)	84(10)

Table S11. (continued)

	x	y	z	U(eq)
C(55)	3000(17)	5920(20)	9364(12)	79(9)
C(56)	2620(20)	5630(30)	9847(15)	117(13)
C(57)	2270(20)	6700(30)	10034(15)	141(16)
C(58)	3062(19)	5210(30)	10225(13)	114(12)
C(59)	3610(17)	6830(30)	9447(12)	87(10)
C(60)	4145(15)	5260(20)	9143(10)	58(8)
C(61)	3668(12)	3900(20)	7627(8)	44(6)
C(62)	3111(16)	4610(20)	7386(10)	64(8)
C(63)	3301(17)	5780(20)	7486(12)	88(10)
C(64)	3164(17)	4530(30)	6808(11)	90(10)
C(65)	4567(14)	4000(20)	7494(10)	75(9)
C(66)	4452(16)	4240(20)	8344(10)	60(8)
C(67)	3815(18)	1920(20)	9413(11)	77(9)
C(68)	3735(18)	950(20)	9039(11)	75(9)
C(69)	4240(30)	900(40)	8671(19)	190(20)
C(70)	3740(20)	-140(30)	9330(15)	136(15)
C(71)	4539(19)	1850(30)	9716(13)	111(12)
C(72)	4515(16)	3290(20)	9157(11)	67(8)
C(73)	5672(10)	4750(20)	9039(8)	83(10)
C(74)	6233(15)	3962(16)	9073(9)	163(17)
C(75)	7006(13)	4230(20)	9163(9)	114(13)
C(76)	7218(10)	5290(20)	9219(8)	102(11)
C(77)	6657(15)	6075(16)	9184(9)	144(15)
C(78)	5884(13)	5806(19)	9094(8)	115(13)
C(79)	8097(14)	4060(20)	7023(9)	48(7)
C(80)	8533(14)	4790(20)	7358(9)	62(8)
C(81)	8227(15)	3160(20)	5433(10)	51(7)
C(82)	8743(17)	3530(30)	5010(11)	94(10)
C(83)	8526(17)	850(20)	6570(11)	66(9)
C(84)	9203(15)	110(20)	6703(11)	76(9)
C(85)	6740(13)	1040(20)	5343(9)	48(7)

Table S11. (continued)

	x	y	z	U(eq)
C(86)	7435(18)	200(30)	5387(12)	89(10)
C(87)	7150(20)	-630(40)	5788(16)	164(18)
C(88)	7530(20)	-70(40)	4798(15)	151(16)
C(89)	5947(16)	600(30)	5114(11)	85(10)
C(90)	5743(16)	1430(20)	5869(11)	71(9)
C(91)	6295(13)	4712(19)	6143(9)	43(7)
C(92)	6675(16)	5000(20)	5662(10)	68(8)
C(93)	6340(18)	4510(30)	5183(12)	97(11)
C(94)	6630(20)	6150(30)	5551(15)	139(15)
C(95)	5452(15)	4970(20)	6170(11)	67(9)
C(96)	5574(13)	3266(18)	6235(8)	36(6)
C(97)	6786(18)	1350(30)	7407(11)	86(10)
C(98)	7121(16)	2130(20)	7735(10)	71(9)
C(99)	6630(30)	3080(40)	7802(18)	173(19)
C(100)	7430(20)	1710(30)	8270(13)	118(13)
C(101)	6040(20)	820(30)	7533(14)	116(13)
C(102)	5830(20)	1710(30)	6800(12)	91(11)
C(103)	4399(8)	1832(16)	6250(8)	68(8)
C(104)	4023(12)	1309(17)	6636(7)	89(10)
C(105)	3225(12)	1174(18)	6599(8)	136(14)
C(106)	2803(8)	1563(18)	6175(9)	104(11)
C(107)	3180(11)	2086(17)	5789(7)	88(10)
C(108)	3978(11)	2220(16)	5826(7)	94(10)
N(1)	2510(9)	2551(16)	8353(6)	34(5)
N(2)	2111(11)	4617(16)	8435(7)	37(5)
N(3)	2242(12)	3360(17)	9314(8)	58(6)
N(4)	3407(12)	5103(18)	9138(8)	61(7)
N(5)	3754(10)	4018(15)	8219(6)	45(5)
N(6)	3844(12)	2898(16)	9135(7)	52(6)
N(7)	7772(11)	3486(16)	6792(7)	46(6)
N(8)	7826(10)	2966(14)	5743(7)	28(5)

Table S11. (continued)

	x	y	z	U(eq)
N(9)	8014(12)	1376(18)	6465(8)	58(6)
N(10)	6561(11)	1536(17)	5832(8)	51(6)
N(11)	6274(9)	3509(14)	6216(6)	35(5)
N(12)	6540(12)	1798(17)	6876(8)	58(6)
O(1)	4300(10)	6181(16)	9357(7)	74(6)
O(2)	4974(10)	4268(15)	7974(7)	78(6)
O(3)	4966(12)	2840(17)	9544(8)	96(7)
O(4)	5411(10)	914(14)	5455(7)	63(5)
O(5)	5070(10)	4014(14)	6215(6)	67(5)
O(6)	5466(14)	1050(20)	7191(9)	116(8)

Table S12. Bond lengths [Å] and angles [°] for $[Ru(\kappa^3\text{-}S\text{-}To^P)(NCCH_3)_3]^+$.

Ru(1)-N(1)	1.982(19)	C(5)-C(6)	1.3900
Ru(1)-N(3)	1.99(2)	C(7)-C(8)	1.3900
Ru(1)-N(2)	1.992(19)	C(7)-C(12)	1.3900
Ru(1)-N(5)	2.050(18)	C(8)-C(9)	1.3900
Ru(1)-N(6)	2.08(2)	C(9)-C(10)	1.3900
Ru(1)-N(4)	2.11(2)	C(10)-C(11)	1.3900
Ru(2)-N(8)	2.002(19)	C(11)-C(12)	1.3900
Ru(2)-N(10)	2.00(2)	C(13)-C(14)	1.3900
Ru(2)-N(9)	2.01(2)	C(13)-C(18)	1.3900
Ru(2)-N(7)	2.04(2)	C(14)-C(15)	1.3900
Ru(2)-N(12)	2.05(2)	C(15)-C(16)	1.3900
Ru(2)-N(11)	2.062(17)	C(16)-C(17)	1.3900
B(1)-C(7)	1.63(3)	C(17)-C(18)	1.3900
B(1)-C(1)	1.66(3)	C(19)-C(20)	1.3900
B(1)-C(13)	1.69(3)	C(19)-C(24)	1.3900
B(1)-C(19)	1.72(3)	C(20)-C(21)	1.3900
B(2)-C(31)	1.66(3)	C(21)-C(22)	1.3900
B(2)-C(37)	1.67(3)	C(22)-C(23)	1.3900
B(2)-C(25)	1.69(3)	C(23)-C(24)	1.3900
B(2)-C(43)	1.73(3)	C(25)-C(26)	1.3900
B(3)-C(72)	1.57(4)	C(25)-C(30)	1.3900
B(3)-C(60)	1.61(4)	C(26)-C(27)	1.3900
B(3)-C(73)	1.62(3)	C(27)-C(28)	1.3900
B(3)-C(66)	1.70(4)	C(28)-C(29)	1.3900
B(4)-C(102)	1.53(4)	C(29)-C(30)	1.3900
B(4)-C(90)	1.58(4)	C(31)-C(32)	1.3900
B(4)-C(96)	1.61(4)	C(31)-C(36)	1.3900
B(4)-C(103)	1.67(4)	C(32)-C(33)	1.3900
C(1)-C(2)	1.3900	C(33)-C(34)	1.3900
C(1)-C(6)	1.3900	C(34)-C(35)	1.3900
C(2)-C(3)	1.3900	C(35)-C(36)	1.3900
C(3)-C(4)	1.3900	C(37)-C(38)	1.3900
C(4)-C(5)	1.3900	C(37)-C(42)	1.3900

Table S12. (continued)

C(38)-C(39)	1.3900	C(96)-N(11)	1.25(2)
C(39)-C(40)	1.3900	C(96)-O(5)	1.29(2)
C(98)-C(99)	1.48(5)	C(97)-C(98)	1.42(4)
C(68)-C(70)	1.57(5)	C(97)-C(101)	1.51(4)
C(71)-O(3)	1.53(4)	C(97)-N(12)	1.54(3)
C(72)-N(6)	1.26(3)	C(98)-C(100)	1.57(4)
C(72)-O(3)	1.37(3)	C(101)-O(6)	1.34(4)
C(73)-C(74)	1.3900	C(102)-N(12)	1.24(3)
C(73)-C(78)	1.3900	C(102)-O(6)	1.48(4)
C(74)-C(75)	1.3900	C(103)-C(104)	1.3900
C(75)-C(76)	1.3900	C(103)-C(108)	1.3900
C(76)-C(77)	1.3900	C(104)-C(105)	1.3900
C(77)-C(78)	1.3900	C(105)-C(106)	1.3900
C(79)-N(7)	1.09(3)	C(106)-C(107)	1.3900
C(79)-C(80)	1.46(3)	C(107)-C(108)	1.3900
C(81)-N(8)	1.11(3)	N(1)-Ru(1)-N(3)	88.1(8)
C(81)-C(82)	1.52(4)	N(1)-Ru(1)-N(2)	86.0(7)
C(83)-N(9)	1.13(3)	N(3)-Ru(1)-N(2)	89.0(8)
C(83)-C(84)	1.52(4)	N(1)-Ru(1)-N(5)	90.8(7)
C(85)-N(10)	1.47(3)	N(3)-Ru(1)-N(5)	174.4(8)
C(85)-C(89)	1.57(3)	N(2)-Ru(1)-N(5)	96.4(7)
C(85)-C(86)	1.60(4)	N(1)-Ru(1)-N(6)	97.2(8)
C(86)-C(87)	1.58(5)	N(3)-Ru(1)-N(6)	90.3(8)
C(86)-C(88)	1.59(4)	N(2)-Ru(1)-N(6)	176.8(8)
C(89)-O(4)	1.37(3)	N(5)-Ru(1)-N(6)	84.4(7)
C(90)-O(4)	1.36(3)	N(1)-Ru(1)-N(4)	174.7(8)
C(90)-N(10)	1.43(3)	N(3)-Ru(1)-N(4)	95.2(8)
C(91)-C(92)	1.49(3)	N(2)-Ru(1)-N(4)	90.0(8)
C(91)-C(95)	1.50(3)	N(5)-Ru(1)-N(4)	86.3(8)
C(91)-N(11)	1.53(3)	N(6)-Ru(1)-N(4)	86.9(9)
C(92)-C(94)	1.48(4)	N(8)-Ru(2)-N(10)	90.8(7)
C(92)-C(93)	1.49(4)	N(8)-Ru(2)-N(9)	87.0(8)
C(95)-O(5)	1.39(3)	N(10)-Ru(2)-N(9)	94.8(9)

Table S12. (continued)

N(8)-Ru(2)-N(7)	88.6(7)	C(26)-C(25)-C(30)	120.0
N(10)-Ru(2)-N(7)	176.3(8)	C(26)-C(25)-B(2)	121.8(10)
N(9)-Ru(2)-N(7)	88.8(8)	C(30)-C(25)-B(2)	118.1(10)
N(8)-Ru(2)-N(12)	174.3(8)	C(27)-C(26)-C(25)	120.0
N(10)-Ru(2)-N(12)	85.2(8)	C(26)-C(27)-C(28)	120.0
N(9)-Ru(2)-N(12)	89.2(9)	C(29)-C(28)-C(27)	120.0
C(3)-C(4)-C(5)	120.0	C(28)-C(29)-C(30)	120.0
C(6)-C(5)-C(4)	120.0	C(29)-C(30)-C(25)	120.0
C(5)-C(6)-C(1)	120.0	C(89)-C(85)-C(86)	116(2)
C(8)-C(7)-C(12)	120.0	C(87)-C(86)-C(88)	123(3)
C(8)-C(7)-B(1)	119.6(10)	C(87)-C(86)-C(85)	103(3)
C(12)-C(7)-B(1)	120.3(10)	C(88)-C(86)-C(85)	100(3)
C(9)-C(8)-C(7)	120.0	O(4)-C(89)-C(85)	105(2)
C(8)-C(9)-C(10)	120.0	O(4)-C(90)-N(10)	112(2)
C(11)-C(10)-C(9)	120.0	O(4)-C(90)-B(4)	130(3)
C(10)-C(11)-C(12)	120.0	N(10)-C(90)-B(4)	117(2)
C(11)-C(12)-C(7)	120.0	C(92)-C(91)-C(95)	117(2)
C(14)-C(13)-C(18)	120.0	C(92)-C(91)-N(11)	111(2)
C(14)-C(13)-B(1)	121.6(9)	C(95)-C(91)-N(11)	100.6(19)
C(18)-C(13)-B(1)	118.3(9)	C(94)-C(92)-C(91)	113(3)
C(13)-C(14)-C(15)	120.0	C(94)-C(92)-C(93)	103(3)
C(16)-C(15)-C(14)	120.0	C(91)-C(92)-C(93)	116(2)
C(17)-C(16)-C(15)	120.0	C(32)-C(31)-C(36)	120.0
C(16)-C(17)-C(18)	120.0	C(32)-C(31)-B(2)	122.1(10)
C(17)-C(18)-C(13)	120.0	C(36)-C(31)-B(2)	117.4(11)
C(20)-C(19)-C(24)	120.0	C(33)-C(32)-C(31)	120.0
C(20)-C(19)-B(1)	119.3(9)	C(32)-C(33)-C(34)	120.0
C(24)-C(19)-B(1)	120.6(9)	C(33)-C(34)-C(35)	120.0
C(21)-C(20)-C(19)	120.0	C(36)-C(35)-C(34)	120.0
C(20)-C(21)-C(22)	120.0	C(35)-C(36)-C(31)	120.0
C(21)-C(22)-C(23)	120.0	C(38)-C(37)-C(42)	120.0
C(24)-C(23)-C(22)	120.0	C(38)-C(37)-B(2)	121.0(10)
C(23)-C(24)-C(19)	120.0	C(42)-C(37)-B(2)	118.5(10)

Table S12. (continued)

C(39)-C(38)-C(37)	120.0	C(103)-C(104)-C(105)	120.0
C(38)-C(39)-C(40)	120.0	C(106)-C(105)-C(104)	120.0
C(41)-C(40)-C(39)	120.0	C(105)-C(106)-C(107)	120.0
C(42)-C(41)-C(40)	120.0	C(108)-C(107)-C(106)	120.0
C(41)-C(42)-C(37)	120.0	C(107)-C(108)-C(103)	120.0
C(44)-C(43)-C(48)	120.0	C(49)-N(1)-Ru(1)	171.4(18)
C(44)-C(43)-B(2)	121.9(10)	C(51)-N(2)-Ru(1)	170.6(19)
C(48)-C(43)-B(2)	118.1(10)	C(53)-N(3)-Ru(1)	176(2)
C(43)-C(44)-C(45)	120.0	C(60)-N(4)-C(55)	113(2)
C(46)-C(45)-C(44)	120.0	C(60)-N(4)-Ru(1)	119(2)
C(45)-C(46)-C(47)	120.0	C(55)-N(4)-Ru(1)	127.9(19)
C(48)-C(47)-C(46)	120.0	C(66)-N(5)-C(61)	109.1(19)
C(47)-C(48)-C(43)	120.0	C(66)-N(5)-Ru(1)	121.5(16)
N(1)-C(49)-C(50)	176(3)	C(102)-B(4)-C(90)	104(3)
N(2)-C(51)-C(52)	173(3)	C(102)-B(4)-C(96)	104(3)
N(3)-C(53)-C(54)	173(3)	C(90)-B(4)-C(96)	105(2)
N(4)-C(55)-C(56)	115(3)	C(102)-B(4)-(103)	123(3)
N(4)-C(55)-C(59)	105(2)	C(90)-B(4)-C(103)	107(2)
C(56)-C(55)-C(59)	112(3)	C(96)-B(4)-C(103)	112(2)
C(58)-C(56)-C(55)	118(3)	C(2)-C(1)-C(6)	120.0
C(58)-C(56)-C(57)	109(3)	C(2)-C(1)-B(1)	124.0(9)
C(55)-C(56)-C(57)	104(3)	C(6)-C(1)-B(1)	116.0(9)
O(1)-C(59)-C(55)	97(2)	C(1)-C(2)-C(3)	120.0
N(4)-C(60)-O(1)	109(2)	C(4)-C(3)-C(2)	120.0
C(97)-C(98)-C(100)	114(3)	N(4)-C(60)-B(3)	124(3)
C(99)-C(98)-C(100)	110(3)	O(1)-C(60)-B(3)	126(2)
O(6)-C(101)-C(97)	112(3)	C(62)-C(61)-N(5)	114.2(19)
N(12)-C(102)-O(6)	113(3)	C(62)-C(61)-C(65)	119(2)
N(12)-C(102)-B(4)	127(3)	N(5)-C(61)-C(65)	98.7(16)
O(6)-C(102)-B(4)	119(3)	C(61)-C(62)-C(64)	109(2)
C(104)-C(103)-C(108)	120.0	C(61)-C(62)-C(63)	113(2)
C(104)-C(103)-B(4)	119.0(17)	C(64)-C(62)-C(63)	102(2)
C(108)-C(103)-B(4)	120.9(17)	O(2)-C(65)-C(61)	105.7(19)

Table S12. (continued)

N(5)-C(66)-O(2)	119(2)	C(90)-N(10)-C(85)	105(2)
N(5)-C(66)-B(3)	123(2)	C(90)-N(10)-Ru(2)	121.6(18)
O(2)-C(66)-B(3)	119(2)	C(85)-N(10)-Ru(2)	132.3(15)
N(6)-C(67)-C(71)	107(3)	C(96)-N(11)-C(91)	106.0(18)
N(6)-C(67)-C(68)	111(2)	C(96)-N(11)-Ru(2)	124.9(16)
C(71)-C(67)-C(68)	110(3)	C(91)-N(11)-Ru(2)	129.0(13)
C(69)-C(68)-C(67)	116(4)	C(102)-N(12)-C(97)	110(2)
C(69)-C(68)-C(70)	108(4)	C(102)-N(12)-Ru(2)	119(2)
C(67)-C(68)-C(70)	113(3)	C(97)-N(12)-Ru(2)	130.8(18)
C(67)-C(71)-O(3)	102(3)	C(60)-O(1)-C(59)	114(2)
N(6)-C(72)-O(3)	111(2)	O(5)-C(95)-C(91)	106(2)
N(6)-C(72)-B(3)	128(3)	N(11)-C(96)-O(5)	118(2)
O(3)-C(72)-B(3)	117(2)	N(11)-C(96)-B(4)	119(2)
C(74)-C(73)-C(78)	120.0	O(5)-C(96)-B(4)	123(2)
C(74)-C(73)-B(3)	119(2)	C(98)-C(97)-C(101)	121(3)
C(78)-C(73)-B(3)	121(2)	C(98)-C(97)-N(12)	112(3)
C(75)-C(74)-C(73)	120.0	C(101)-C(97)-N(12)	99(2)
C(74)-C(75)-C(76)	120.0	C(97)-C(98)-C(99)	114(3)
C(77)-C(76)-C(75)	120.0	C(40)-C(41)	1.3900
C(78)-C(77)-C(76)	120.0	C(41)-C(42)	1.3900
C(77)-C(78)-C(73)	120.0	C(43)-C(44)	1.3900
N(7)-C(79)-C(80)	177(3)	C(43)-C(48)	1.3900
N(8)-C(81)-C(82)	174(3)	C(44)-C(45)	1.3900
N(9)-C(83)-C(84)	178(3)	C(45)-C(46)	1.3900
N(10)-C(85)-C(89)	105.7(19)	C(46)-C(47)	1.3900
N(10)-C(85)-C(86)	114(2)	C(47)-C(48)	1.3900
C(61)-N(5)-Ru(1)	129.1(13)	C(49)-N(1)	1.17(2)
C(72)-N(6)-C(67)	111(2)	C(49)-C(50)	1.42(3)
C(72)-N(6)-Ru(1)	118.8(19)	C(51)-N(2)	1.16(3)
C(67)-N(6)-Ru(1)	129.6(19)	C(51)-C(52)	1.45(4)
C(79)-N(7)-Ru(2)	176(2)	C(53)-N(3)	1.17(3)
C(81)-N(8)-Ru(2)	173(2)	C(53)-C(54)	1.44(4)
C(83)-N(9)-Ru(2)	173(2)	C(55)-N(4)	1.39(3)

Table S12. (continued)

C(55)-C(56)	1.49(4)	N(12)-Ru(2)-N(11)	85.4(8)
C(55)-C(59)	1.57(4)	C(7)-B(1)-C(1)	116.5(17)
C(56)-C(58)	1.33(4)	C(7)-B(1)-C(13)	112.9(16)
C(56)-C(57)	1.57(5)	C(1)-B(1)-C(13)	102.6(15)
C(59)-O(1)	1.47(3)	C(7)-B(1)-C(19)	103.0(15)
C(60)-N(4)	1.29(3)	C(1)-B(1)-C(19)	113.7(15)
C(60)-O(1)	1.31(3)	C(13)-B(1)-C(19)	108.2(15)
C(61)-C(62)	1.44(3)	C(31)-B(2)-C(37)	117.4(17)
C(61)-N(5)	1.55(3)	C(31)-B(2)-C(25)	110.9(17)
C(61)-C(65)	1.61(3)	C(37)-B(2)-C(25)	103.9(16)
C(62)-C(64)	1.52(3)	C(31)-B(2)-C(43)	103.2(15)
C(62)-C(63)	1.53(4)	C(37)-B(2)-C(43)	109.0(17)
C(65)-O(2)	1.45(3)	C(25)-B(2)-C(43)	112.8(16)
C(66)-N(5)	1.27(3)	C(72)-B(3)-C(60)	108(2)
C(66)-O(2)	1.35(3)	C(72)-B(3)-C(73)	119(2)
C(67)-N(6)	1.43(3)	C(60)-B(3)-C(73)	116(2)
C(67)-C(71)	1.46(4)	C(72)-B(3)-C(66)	97(2)
C(67)-C(68)	1.57(4)	C(60)-B(3)-C(66)	99(2)
C(68)-C(69)	1.33(5)	C(73)-B(3)-C(66)	115(2)
N(7)-Ru(2)-N(12)	95.6(8)	C(66)-O(2)-C(65)	107(2)
N(8)-Ru(2)-N(11)	98.4(7)	C(72)-O(3)-C(71)	107(2)
N(10)-Ru(2)-N(11)	84.7(7)	C(90)-O(4)-C(89)	112(2)
N(9)-Ru(2)-N(11)	174.6(8)	C(96)-O(5)-C(95)	108.7(19)
N(7)-Ru(2)-N(11)	91.8(7)	C(101)-O(6)-C(102)	105(3)

Table S13. Anisotropic displacement parameters ($Å^2 x\ 10^3$) for $[Ru(\kappa^3\text{-}S\text{-}To^P)(NCCH_3)_3]^+$. The anisotropic displacement factor exponent takes the form: $-2p^2[\ h^2\ a^{*2}U^{11} + \ldots + 2\ h\ k\ a^*\ b^*\ U^{12}\ ]$

	U^{11}	U^{22}	U^{33}	U^{23}	U^{13}	U^{12}
Ru(1)	46(1)	52(2)	39(1)	2(1)	-8(1)	-15(1)
Ru(2)	43(1)	47(2)	53(1)	6(1)	7(1)	-1(1)

[1] Blessing, R.H. *Acta Cryst*. **1995**, *A51*, 33-38.

[2] All software and sources of the scattering factors are contained in the SHELXTL (version 5.1) program library (G. Sheldrick, Bruker Analytical X-Ray Systems, Madison, WI).

[3] A.L.Spek, J.Appl.Cryst. *36*, 7-13.

7. References

1. (a) Trofimenko, S. *J. Am. Chem. Soc.* **1966**, *88,* 1842-1844. (b) Trofimenko, S. *J. Am. Chem. Soc.* **1967**, *89*, 3170-3177. (c) Trofimenko, S. *J. Am. Chem. Soc.* **1967**, *89*, 6288-6294.
2. For reviews in the field of scorpionates, see: (a) Trofimenko, S. *Scorpionates: The Coordination Chemistry of Polypyrazolylborate Ligands*, University College Press, London, **1999**. (b) Trofimenko, S. *Chem. Rev.* **1993,** *93*, 943–980 (c) Trofimenko, S. *Polyhedron*, **2004**, *23*, 197–203 (d) Pettinari, C. *Scorpionates II: Chelating Borate Ligands*, Imperial College Press, **2008**.
3. Dunne, J. F.; Su, J.; Ellern, A.; Sadow, A. D. *Organometallics* **2008,** *27,* 2399–2401.
4. Sorrell, T. N.; Pigge, F.C.; White, P. S. *Inorg. Chim. Acta.* **1993**, *210*, 87-90.
5. Kawasaki, K.; Tsumura, S.; Katsuki, T. *Synlett,* **1995**, 1245-1247.
6. Kohmura, Y.; Katsuki, T.; *Tetrahedron Lett.* **2000**, *41*, 3941-3945.
7. Bellemin-Laponnaz, S.; Gade, L. H. *Angew. Chem. Int. Ed.* **2002**, *41*, 3473-3475.
8. Chuang, T.-H.; Fang, J.-M.; Bolm, C. *Synth. Commun.* **2000**, *30*, 1627-1641.

9. (a) Kim, S.-G.; Ahn, K. H. *Chem. Eur. J.* **2000**, *6*, 3399-3403. (b) Kim, H.-J.; Kim, Y.-H.; Hong, J.-I. *Tetrahedron Lett.* **2001**, *42*, 5049-5052.
10. Rocchetti, M. T.; Fino, V.; Capriati, V.; Florio, S.; Luisi, R., *J. Org. Chem.* **2003**, *68*, 1394-1400.
11. Kawasaki, K; Katsuki, T. *Tetrahedron* **1997**, *53*, 6337-6350.
12. Kohmura, Y.; Kawasaki, K.; Katsuki, T. *Synlett*, **1997**, 1456-1458.
13. Chan, T. H.; Zheng, G. Z.; *Can. J. Chem.*, **1997**, *75*, 629.
14. (a) Zhou J.; Tang, Y.; *J. Am. Chem. Soc.* **2002**, *124*, 9030-9031. (b) Zhuang, W.; Hansen, T.; Jørgensen, K. A.; *Chem. Commun.* **2001**, 347-348. (c) Zhou, J.; Ye, M.-C.; Huang, Z.-Z.; Tang, Y.; *J. Org. Chem.* **2004**, *69*, 1309-1320. (d) Zhou, J.; Tang, Y.; *Chem. Commun.* **2004**, 432-433.
15. Kim, S.-G.; Ahn, K. H. ; *Tetrahedron Lett*. **2001**, *42*, 4175-4177.
16. Zhou, J.; Tang, Y.; *Org. Biomol. Chem.* **2004**, *2*, 429-433.
17. Huang, Z.-Z.; Kang, Y.-B.; Zhou, J.; Tang, Y.; *Org. Lett.* **2004**, *6*, 1677-1679.
18. Zhou, J.; Tang, Y. *Chem. Soc. Rev.* **2005**, *34*, 664–676.
19. Köhler, V.; Mazet, C.; Toussaint, A.; Kulicke, K.; Häussinger, D.; Neuburger, M.; Schaffner, S.; Kaiser, S.; Pfaltz, A.; *Chem. Eur. J.* **2008**, *14*, 28, 8530 – 8539.
20. Baird, B; Pawlikowski, A. V.; Su, J.; Wiench, J. W.; Pruski, M.; Sadow, A. D. *Inorg. Chem.*, **2008**, *47*, 10208-10210.
21. For reviews in ruthenium catalyzed reactions, see: (a) Naota, T.; Takaya, H.; Murahashi, S.-I. *Chem. Rev.* **1998**, *98*, 2599. (b) Grubbs, R. H.; Chang, S. *Tetrahedron* **1998**, *39*, 2805. (c) *Alkene Metathesis in Organic Synthesis*; Fürstner, A, Ed.; New York: Springer, 1998. (d) Noyori, R.; Yamakawa, M; Hashiguchi, S. *J. Org. Chem.*, **2001**, *66*, 7931-7944. (e) Trost, B. M.; Toste, F. D.; Pinkerton, A. B.; *Chem. Rev.* **2001,** *101,* 2067-2096. (f) Fan, Q.-H.; Li, Y.M.; Chan, A. S. C. *Chem. Rev.* **2002,** *102,* 3385-3466.
22. Trost, B. M.; Fraisse, P. L.; Ball, Z. T. *Angew. Chem. Int. Ed.* **2002**, 41, 1059-1061.
23. For a review of Bruneau's research, see: Bruneau, C.; Renaud, J. -L.; Demerseman, B. *Chem. Eur. J.* **2006**, *12*, 5178 –5187.
24. K. Onitsuka, Y. Matsushima, S. Takahashi, *Organometallics*, **2005**, *24*, 6472 –6474.

25. M. D. Mbaye, J.-L. Renaud, B. Demerseman, C. Bruneau, *Chem. Commun*. **2004**, 1870 –1871.

26. Utsunomiya, M. and Hartwig, J. F.; *J. Am. Chem. Soc.* **2005**, *126*, 2702-2703.

27. Takaya, J.; Hartwig, J. F.; *J. Am. Chem. Soc.* **2005**, *127*, 5756-5757.

28. Gunnoe, T. B. *Eur. J. Inorg. Chem.* **2007**, 1185–1203.

29. Lail, M.; Arrowood, B. N.; Gunnoe, T. B.; *J. Am. Chem. Soc*. **2003**, *125*, 7506-7507.

30. Peng, J.; Barr, M. E.; Ashburn, D. A.; Odom, J. D.; Dunlap, R. B.; Silks, L. A.; *J. org. Chem.* **1994,** *59*, 4977-4987.

31. Meyers, A. I.; Collington, E. W. *J. Am. Chem. Soc.* **1970***, 92,* 6676-6678.

32. Kidd, R.G. *NMR of Newly Accessible Nuclei*; Laszlo, P., Ed.; Academic Press: New York, **1983**; *2*, 49 – 77.

33. (a) Jansen, A.; Gorls, H.; and Pitter, S.; Organometallics, **2000**, *19*, 135-138. (b) Dehand, J.; Rose, J. *J. Chem. Res.* **1979**, 2167. (c) Tuttle, T.; Wang, D.; Thiel, W.; Köhler, J.; Hofmann, M.; Weis, J. *J. Organomet. Chem.* **2007**, *692*, 2282-2290.

34. Rüba, E.; Simanko, W.; Mereiter, K.; Schmid R.; Kirchner, K.; *Inorg. Chem.* **2000,** *39*, 382-384.

35. Luginbühl, W.; Zbinden, P. A.; Armbruster, T.; Bürgi, H.-B.; Merbach, A.E.; Ludi. A. *Inorg .Chem.* **1991***, 30*, 2350- 2355.

36. Yi, C. S.; Liu, N. *Organometallics* **1996,** *15,* 3968-3971.

37. Bruneau, C. *Topics Organomet Chem*, **2004**, *11*, 125–153.

38. Slugovc, C.; Mereiter, Kurt; Zobetz, E.; Schmid, R.; Kirchner, K. *Organometallics* **1996,** *15,* 5275-5277.

39. Jensen, S.B.; Rodger, S. J.; Spicer, M.D.; *J. Organomet. Chem.* **1998**, *556*, 151-158.

40. Gemel, C.; Trimmel, G.; Slugovc, C.; Kremel, S.; Mereiter, K.; Schmid, R.; Kirchner, K. *Organometallics,* **1996**, *15*, 3998.

41. Witanowski, M.; Stefaniak, L.; Webb, G.A. in: Webb, G.A., Ed.; *Ann. Rep. NMR Spectrosc. 25*, Academic Press, London, **1993**.

42. (a) Lau, C. P,; Nga, S. M.; Jia, G.; Lin, Z. Y. *Coord. Chem. Rev*. **2007**, *251*, 2223–2237. (b) Krompiec, S.; Kùznik, N.; Krompiec, M.; Penczek, R.; Mrzigod, J.; Tòrz, A. *J. Mole. Cat. A: Chem,* **2006**, *253*, 132–146. (c) Clapham, S. E.; Hadzovic, A.;

Morris, R. H. *Coord. Chem. Rev*, **2004**, *248,* 2201–2237.

43. Leonard, W. R.; Romine, J. L.; Meyers, A. I. *J. Org. Chem.* **1991**, *56*, 1961 – 1963.
44. M.A. Bennett and G. Wilkinson, *Chem. Ind.* **1959**, 1516.
45. Bennett, M. A.; Smith, A. K. *J. Chem. Soc., Dalton Trans.* **1974**, 233.
46. M.O. Albers, T.V. Ashworth, H.E. Oosthuizen and E. Singleton. *Inorg. Synth.* **1989**, *26*, 68.
47. Ashworth, T. V.; Singleton, E.; Hough, J. J. *Dalton Trans.* **1997,** 1809-1815.
48. (a) Albers, M. O.; Robinson, D. J.; Shaver, A.; Singleton, E. *Organometallics,* **1986**, *5*, 2199-2205. (b) Fagan, P. J.; Mahoney, W. S.; Calabrese, J. C.; Williams, I. D. *Organometallics,* **1990**, *9*, 1843-1852. (c) Oshima, N.; Suzuki, H.; Moro-oka, Y. *Chem. Lett*. **1984**, 1161-1164. (d) Tilley, T. D.; Grubbs, R. H.; Bercaw, J. E. *Organometallics* **1984**, *3*, 274-278. (e) Conroy-Lewis, F. M.; Simpson, S. J. *J. Organomet.Chem.* **1987**, *322*, 221-228.

CHAPTER 3. SYNTHESIS OF OLIGOCHOLATE FOLDAMERS WITH VARIOUS SPACERS USING "CLICK" CHEMISTRY

1. Abstract

This chapter describes the design and attempted synthesis of several oligocholate foldamers. Extended oligocholates with various spacers in between the second and third cholate units were to be constructed through click chemistry, and labeled with a naphthyl and a dansyl at the chain ends. The synthesis route has been paved out through the careful synthesis and characterization of different building blocks. Experimental conditions and possible results are discussed. New approaches to monomer synthesis and new ways to construct the oligomers, which are expected to speed up the future research, were established during the exploration.

2. Introduction

Biomolecules, such as proteins, are usually flexible and dynamic. They can change their conformation in response to changes in the environment or other factors, such as a change in temperature, pH, voltage, ion concentration, or the binding of a ligand. A change in conformation produces a change in the shape and distribution of functional groups for the biomolecule and, as a result, its interaction with other biomolecules. Chemists try to study nature's optimal "design" of biomolecules and then imitate these designs and processes to solve important scientific problems. As a result, artificial molecules called foldamers), that mimic the ability of proteins, nucleic acids, and polysaccharides to fold into well-defined conformations, have emerged in recent years.[1]

A foldamer is normally a discrete chain molecule that adopts a specific compact structure (e.g., helices and β sheets) stabilized by noncovalent interactions. Similar to proteins and RNAs, of which the structures are hierarchical, the term "compact" is associated with the tertiary structure. However, synthetic polymers with the tertiary structures have been

rarely reported. The first essential step, hence the current research focus, is the synthesis of the well-defined secondary structures. In proteins, regular secondary structures are defined largely by H-bonding between sites embedded in the polymeric backbone, while in RNA, regular secondary structure is defined in terms of base pairing. This knowledge inspired some researchers to employ the directional noncovalent interactions such as hydrogen bonding to fold the synthetic foldamers. [1]

It should be noted that the information for molecular recognition in the directional noncovalent interactions is encoded in a donor-acceptor motif. For example, a D-D-A hydrogen bonding motif is most suitable to interact with an A-A-D motif. However, these directional forces are not necessarily the only, or even the major, driving forces for the observed secondary structures of proteins; other important factors such as solvophobic and van der Waals interactions can also be utilized for conformation control. In contrast to the directional forces, the complementarity that needed for the selectivity in solvophobic and van der Waals interactions is required for the entire bonding surface instead of a localized pair of interacting functional groups. Hence, complementary solvophobic surfaces are created for molecular recognition as another constructional approach in foldamer chemistry.

Iverson[2] and Moore[3] pioneered work in this area by tethering aromatic units together with spacers to form oligomers stabilized by aromatic interactions. Iverson[2] and coworkers polarized the aromatic systems, making one unit rich in electron density and the other deficient, and used flexible spacers to link them together. With two different kinds of monomer units in an oligomer, different folding motifs may be obtained from the sequence of the monomer units. However, these robust foldamers with the motif of columns of aromatic rings are unlikely to unfold under reasonable conditions (Scheme 1). Moore[3] and coworkers designed *m*-phenylene ethynylene, which utilized semirigid aromatic backbone to constrain the chain in the way to avoid association of neighboring units. With a 120^{o} angle created by the *meta*-connectivity and the linear ethynylene spacer, an *m*PE oligomer was geometrically poised to fold upon itself, forming a conformer resembling macrocycle. A remarkable feature is that the folding in these foldamers is reversible when proper solvent or

other stimulus is applied, which is one step closer to most biofoldamers characterized by the dynamic conformational changes (Scheme 2).

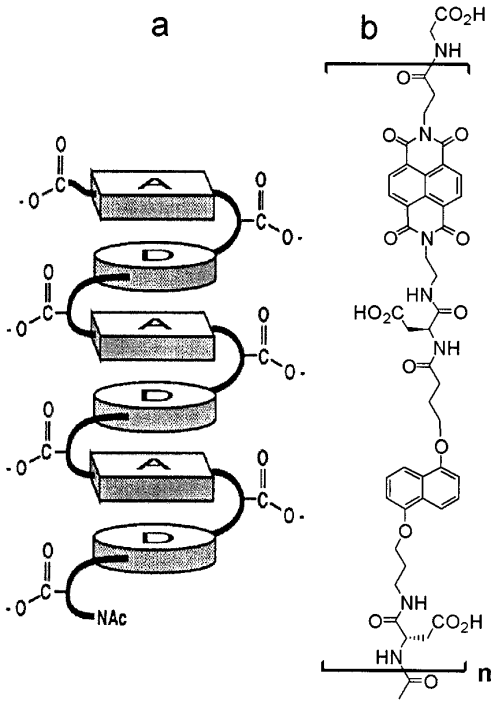

Scheme 1. (a) Schematic representation of folded aedamer structure. (b) Chemical structure of aedamer oligomers. [2]

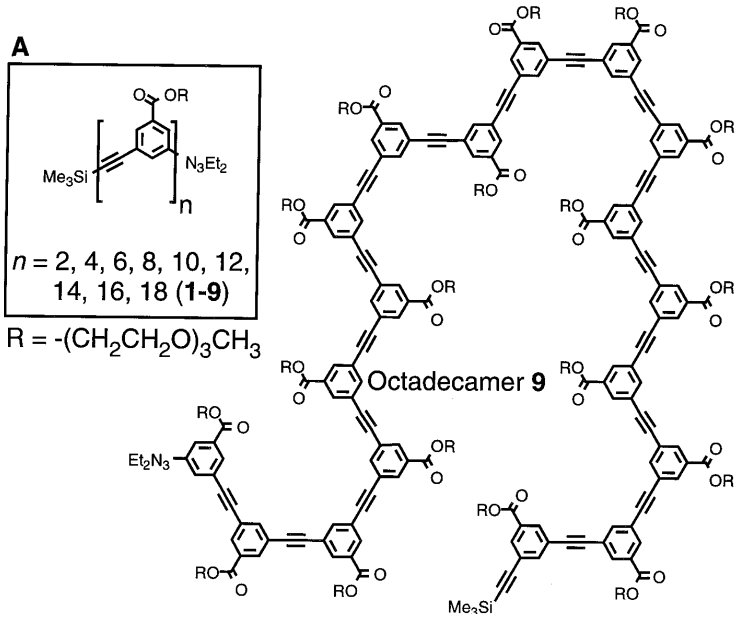

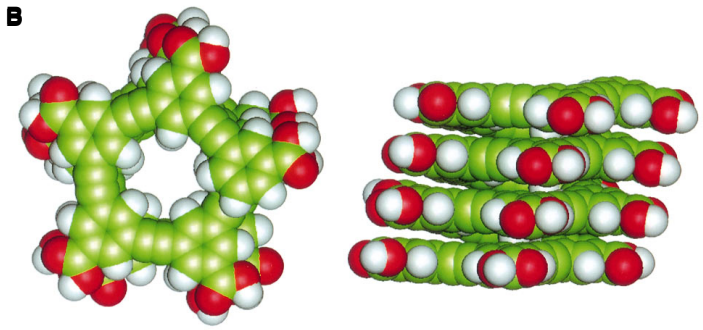

Scheme 2. (**A**) Phenylacetylene oligomers **1** to **9** (inset, upper left). Also shown is octadecamer **9** in a representative random coil conformation. (**B**) Helical con-formation of a *meta*-substituted phenylacetylene octadecamer (*n*=18), where R = H and the end groups have been removed. [3]

Aliphatic hydrocarbons in general are not considered as good building blocks for foldamers since they lack the strong and well-defined interactions as aromatic unites do (π - π interactions), which might make the controllable folding process difficult. The Zhao group[4] recently developed oligomeric cholates derived from facially amphiphilic cholic acid, which demonstrated the successful assembly of foldamer made of aliphatic hydrocarbons.

The term "facial amphiphiles" was originally used for molecules with the hydrophilic and hydrophobic groups located on two opposite faces, rather than at two ends as in the more conventional head/tail amphiphiles. Cholic acid, the facial amphiphile used in our research, has a large, rigid backbone with four fused rings, and a hydroxylated α face and a hydrocarbon containing β face. The amphiphilic oligomers were synthesized through coupling five to seven cholate units together in a head to tail fashion.

A

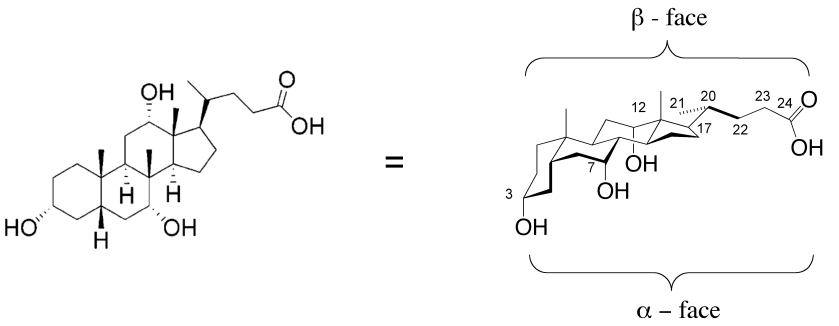

B

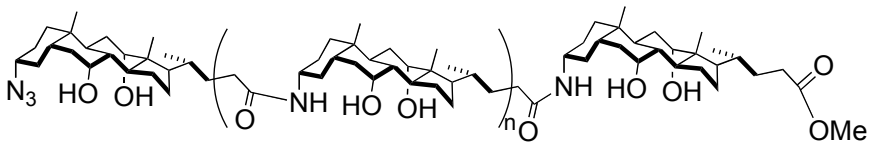

n = 3
n = 4
n = 5

Scheme 3. (A) Cholic acid (B) Cholate oligomers

The chain-like oligomers possessed novel properties that could not be obtained from a monomer. The molecules adopted helical structures with nanometer-sized hydrophilic internal cavities in solvent mixtures consisting of mostly non-polar solvents (such as carbon tetrachloride or ethyl acetate/hexane) and 2-5% of a polar solvent (such as methanol or dimethyl sulfone). Folding was cooperative, as evidenced by the sigmoidal curves in solvent denaturation experiments, and the folding/unfolding equilibrium was highly sensitive toward the amount of polar solvent.

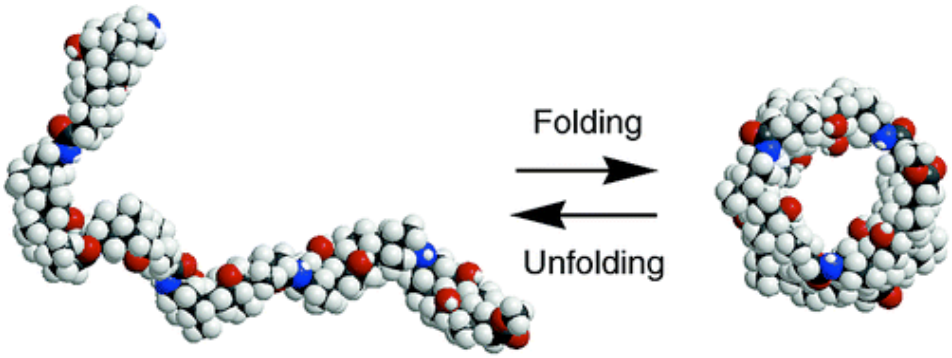

Scheme 4. The equilibrium from folding to unfolding state of hexamer cholate [4]

It was found that the folded conformers became more stable with an increase in the chain length. However, amide coupling employed in the early oligocholate synthesis failed beyond the octamer. As a result, we introduced the click reaction, 1,3-dipolar cycloaddition, between an alkynyl-terminated cholate trimer and an azido-functionalized cholate hexamer to form nonamer and dodecamer, which folded similarly as the parent foldamers.[5]

Inspired by the fact that nature also generates substances (such as proteins or sugars) by joining small modular units, “click” chemistry was first introduced by K. Barry Sharpless in 2001 to describe chemistry tailored to generate substances quickly and reliably by joining small units together.[5] A click reaction ideally is characterized by features such as modular synthesis, high chemical yield, generation of inoffensive byproducts, stereospecificity, simple reaction conditions, readily available starting materials and reagent, no solvent involved or a benign solvent (preferably water), easy product isolation by crystallization or distillation (but not preparative chromatography), physiological stability, large thermodynamic driving force, and high atom economy. The Huisgen 1,3-dipolar cycloaddition, in particular the Cu(I)-catalyzed stepwise variant, fits all the above criteria very well, and is often referred to simply as the "click reaction". As a result of its unique features, it has rapidly established a prominent role in materials science, medicinal, and bioconjugation chemistry.[5] Its applications include the preparative organic synthesis of 1,4-substituted triazoles; modification of peptide function, DNA and nucleotides; synthesis of polymers, dendrimers and carbohydrate clusters, the construction of nanostructure, surface

modification and in vivo labeling.[5]

The introduction of the "click" chemistry to our oligomer synthesis is important for two reasons: first, the azide group is already present at the chain end; the direct usage of azide is a more efficient approach to connect the amphiphilic units to build foldamers, especially longer ones. Second, in contrast to the time-consuming synthesis of functionalized long oligomers through amide coupling, "click" chemistry can direct introduce the functional group to the oligomer through functionalized alkyne or azide building groups. "Click" chemistry is a very useful tool for us to solve other problems in the cholate foldamer system, such as the impact of spacer incorporation to control folding behavior.

As mentioned above, the semi-rigid backbone is quite essential in the construction of foldamer. When amino acids were incorporated in the foldamer as a way to introduce functionality, enhanced folding resulted,[7] which might be due to reduced strain in the folded helix. An independent study of the oligocholate foldamers with 4-aminobutyroyl spacers in between the cholate units confirmed this hypothesis.[8] The flexible 4-aminobutyroyl spacers stabilized the folded confirmation to the extent that the spaced oligocholates required as few as three or four cholates to fold, whereas the parent cholates required at least five. It was hypothesized that the spacers could influence the foldability greatly. Although 4-aminobutyroyl spacer did not alter the folding mechanism in oligocholates, some other spacers might make similar backbones adopt completely different conformations. In the current research, spacers with different chain lengths are introduced through "click" chemistry in between the second and the third cholate to study the influence of spacers on the folding. We also employed a 60^{o} turn in the backbone to investigate the change in the folded state.

3. Results and Discussion

3.1. Molecular Design

A

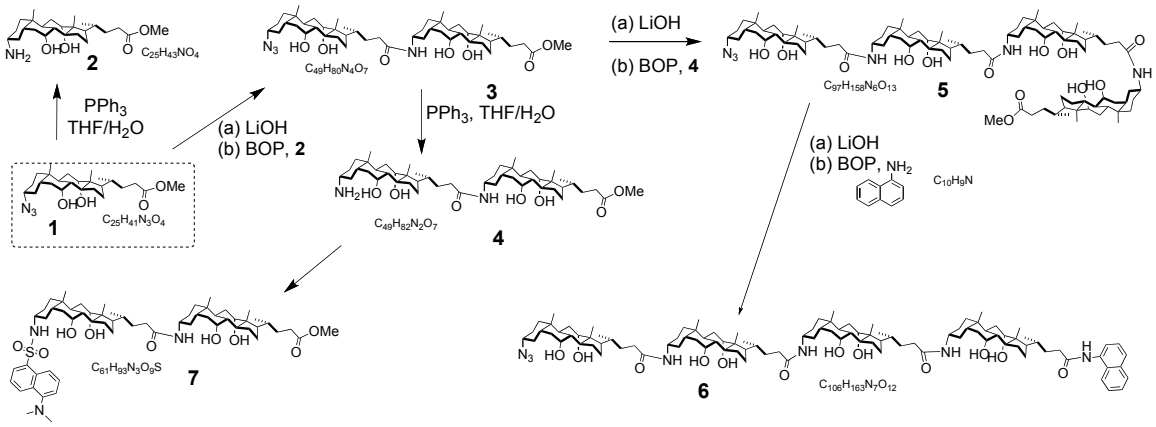

B

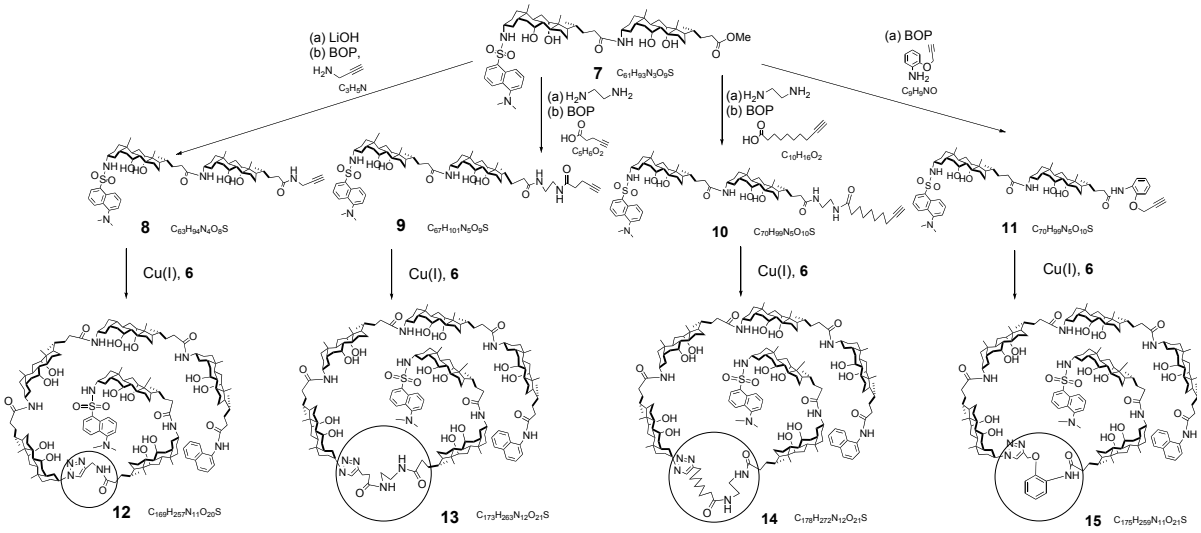

Scheme 5. (A) Synthesis of the building blocks, compound **6** and **7**. (B) Synthesis of the targeted molecules, compound **12**, **13**, **14**, **15**.

Four oligomers were designed with different spacers in between the second and third units. The tetramer **5** and the dimer **4** were prepared and labeled with naphthalene group and dansyl group, respectively. The dansyl dimer **7** was further decorated on the ester end through amide coupling. Compound **7** was hydrolyzed and coupled with propargyl amine to

give **8**. Compound **9** was designed to have five additional rotatable bonds than **8**, and **10** five still more rotational bonds than **9**. Unlike oligomers **8**, **9** and **10** with the flexible aliphatic spacers**,** compound **11** incorporated 2-(prop-2-ynyloxy) aniline, an aromatic spacer with a 60^{o} turn. Compound **11** was designed to be prepared through amide coupling from **7**. The spaced dimer **8, 9, 10** and **11,** with a terminal alkyne, were to be connected with azide group on tetramer through Huisgen 1,3-dipolar cycloaddition to yield the corresponding oligomers **12, 13, 14** and **15.**

3.2.Typical Synthesis of Cholate Oligomers

The tetrameric azide ester **5** was prepared as described in our previous research,[4] (Scheme 1, conversion of **1** to **5**). Azide ester **1** was reduced by triphenylphosphine in aqueous THF to give monomeric amine ester **2**. Standard amide coupling between the monomeric amine ester **2** and monomeric azide carboxylic acid using benzotriazol-1-yloxytris(dimethylamino) phosphonium hexafluorophosphate (BOP) yielded dimeric azide ester **3**. Repetition of the procedures gave the tetrameric azide ester **5**, which was then hydrolyzed and coupled with 1-aminonaphthalene to form the tetrameric naphthalene donor molecule **6**. The dansyl acceptor molecule **7** was prepared through the reaction of dansyl chloride and the dimer amine. The spacer was added on the dansyl acceptor molecule using BOP catalyzed amide coupling with the compound propargl amine. Then the spaced dansyl acceptor molecule **8** could be connected with the naphthalene donor molecule **6** through copper catalyzed 1,3-dipolar cycloaddition to yield oligomer **12**. Other oligomeric cholates **13, 14** and **15**, could be synthesized in similar fashions.

3.3. Improved Synthesis of the Monomeric Azid

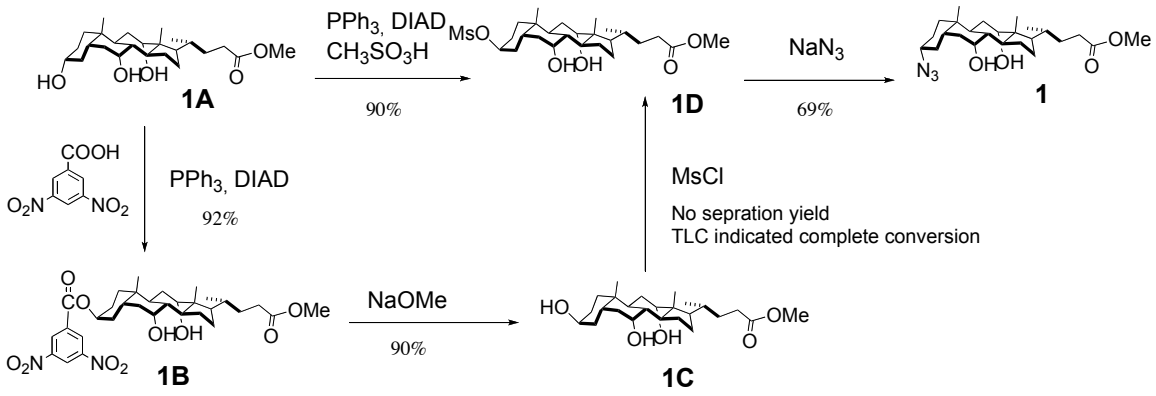

Scheme 6. Synthesis pathways for the monomer

Following a procedure reported by Davis and colleagues,[9] we were able to obtain the *β*-mesylate **1D** from methyl cholate **1A** using triphenylphosphine and diisopropyl azodicarboxylate (DIAD). Then *β*-mesylate **1D** was attacked by sodium azide by an S_N2 reaction to afford monomeric azide ester **1** in a satisfactory yield (Scheme 4). However, the synthetic sequence was problematic on large scale since every step required column chromatography and a large amount of triphenylphospine was used.

Another synthesis route was developed for the azide ester **1** (Scheme 2). In this route, the azide ester **1** was obtained from the α cholate ester **1A** following a 4 steps synthesis. The first three steps gave an over 90% yield and required easy purification. Only the last step requited column chromatography. The reactions could be conducted on up to a 30 g scale.

3.3.1. From 1A to 1B

Cholate acid was first treated with methanol in acidic condition to yield methyl cholate **1A**, and **1A** further reacted with triphenylphosphine, diisopropyl azodicarboxylate (DIAD), and 3, 5-dinitrobenzoic acid in a Mitsunobu reaction to produce **1B**. This Mitsunobu reaction yielded β-ester **1B** at the C-3 position since the most reactive hydroxyl was the one at the C-3 position among all three hydroxyl groups on the cholate unit. It should be noted

that Mitsunobu reaction is quite sensitive to moisture. All the reagents and solvent should be properly dried and the entire process should be handled with care.

3.3.2. From 1B to 1C

The β-ester **1B** was deprotected under basic conditions to yield β–hydroxy cholate ester **1C**. Our recent research demonstrated that sodium methoxide was effective at a catalytic amount and was best to be used as freshly prepared.

3.3.3. From 1C to 1D

β-hydroxy cholate ester **1C** was activated with mesyl chloride and triethylamine in methylene chloride. Our investigation established that the key factor in this step was the choice of the solvent for the reaction. β–Hydroxy cholate ester was not very soluble in most non-polar solvents (such as methylene chloride and acetonitrile); however, it was fairly soluble in the dimethylformamide (6 g/ 12 mL) and tetrahydrofuran (6 g/1000 mL). Our attempts to conduct the mesylate reaction in methylene chloride was not successful because the solubility was so poor that only a tiny amount of the β-hydroxy cholate ester **1C** dissolved. This generally led to mesyl chloride giving over-mesylated product and leaving a large amount of unreacted starting material behind. Dimethylformamide was a good solvent for cholates, and one pot synthesis from **1C** to **1** was attempted. However, the yield of the reaction was very low (around 30%). The main problem with using dimethylformamide as a solvent was its activation of chloride anion from methyl chloride, which would act as a nucleophile to attack the mesylate.

Tetrahydrofuran was chosen as a solvent for the reaction since it has a moderate solubility for the cholates and does not activate chloride anion. Five hundred milliliters of tetrahydrofuran was able to dissolve 3 g of β-hydroxy cholate ester **1C** completely, giving a clear solution. The solution was then treated with 1.2 equivalent triethylamine, and reacted with a quantitative amount of mesylate chloride at 0 ^{o}C. To avoid over-mesylation, the

reaction was stopped after 2 h. Most of the starting material was found to have converted to the mesylate, although some elimination had also occurred. The crude product after extraction was dried without further purification, and applied to the next step.

3.3.4. From 1D to 1

The crude product from previous step was dissolved in DMF and reacted with 6 equivalents of sodium azide to form the desired azide monomer **1**. Column chromatography was applied for the purification. The yield of this step was around 60%.

3.4. Synthesis and Purification of Other Cholate Based Compounds

The reactions in Scheme 4 could be categorized into four types: Staudinger reaction, hydrolysis, amide coupling, and "click" reaction.

3.4.1. Staudinger reaction[11]

The azide group in the molecule was reduced to amine by triphenyl phosphine in methanol, the mechanism is shown in Scheme 2. Triphenylphosphine reacts with the azide to generate a phosphazide, which loses N_2 to form an iminophosphorane. Aqueous work up leads to the amine and very stable triphenylphosphine oxide. Purification of the amine is facilitated by its extremely high polarity on silica gel. During purification, 4:1 methylene chloride / methanol was used to remove triphenylphosphine oxide and some less polar impurities; the amine product was subsequently washed off the column by adding triethylamine to the eluent.

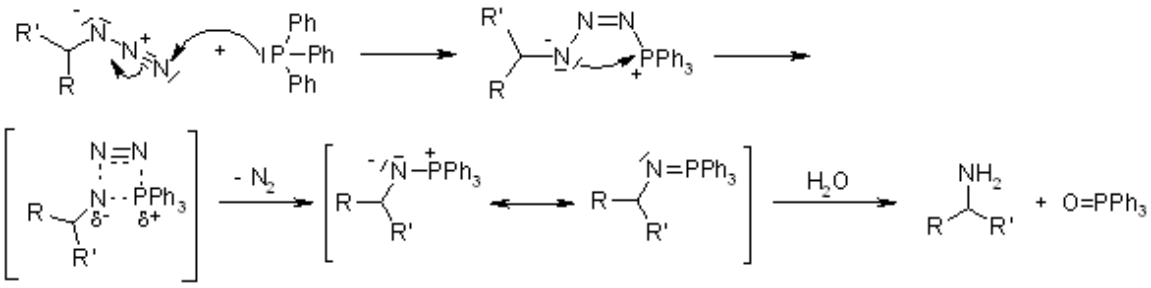

Scheme 7. Mechanism of Staudinger Reaction

3.4.2. Hydrolysis

The ester group was hydrolyzed into the carboxylic acid in methanol. The ester was dissolved in the methanol and treated with 1M LiOH solution. Methanol was then removed under reduced pressure after the reaction is complete (as shown by TLC), and 1M HCl solution was added to precipitate the acid product. It is very important to remove methanol as ester hydrolysis is reversible; if HCl is present, the carboxylic acid may form the ester again. For the same reason, the solid product should be washed with water thoroughly before the next step.

3.4.3. Amide coupling

The cholate groups are mostly joined by amide bonds. Amide coupling between acid and amine is a condensation reaction. Upon mixing an amine with a carboxylic acid, an acid–base reaction occurs first to form a salt.[9] The direct condensation of the salt can be achieved at high temperature (160–180^{o}C), which is not compatible with most other functional groups. (As shown in Scheme 8) Therefore, the carboxylic acid is usually activated before coupling. Activation is usually done through attachment of a good leaving group to the carbonyl of the acid to allow fast attack by the amine.

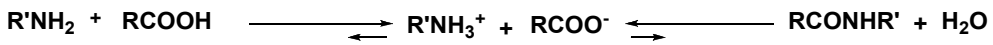

Scheme 8. Amide coupling reaction

One way to activate the carboxylic acid is to form a reactive aromatic ester. Aromatic esters are easily prepared and can react with a wide range of nucleophiles. Hydroxy benzotriazole (HOBt) is a commonly used reagent in peptide synthesis for acid activation. In our case, BOP, a HOBt-based onium salt reagent, served as the coupling agent.[9] (The reaction mechanism is shown in Scheme 9) When the amide coupling is performed in the presence of BOP and triethylamine, the deprotonated acid first reacts with BOP to generate both HOBt and an activated acylphosphonium species. HOBt readily reacts with the activated acid to produce a reactive ester, which finally undergoes aminolysis. The formation of the phosphonium oxide is the major driving force for this phosphonium-based reaction. It was observed that addition of HOBt in the reaction mixture prior to the addition of BOP greatly sped up our reaction, especially in the formation of long chain oligomer, such as the tetramer. When the tetrameric ester was treated with 1-aminnnaphthalene under BOP/HOBt/NEt_3 condition, longer reaction time (6 days) and extra 1-aminnnaphthalene (4 equivalents) were needed in order to obtain the desired product. The slow reaction was presumably caused by the weak nucleophilicity of 1-aminonaphthalene (due to conjugation with the aromatic ring).

The product of amide coupling is purified by established procedures: 1) The product mixture is added to acidic water to remove diisopropylethylamine (DIPEA) and DMF, as most cholate oligomers are not soluble in water. 2) The product is dried under air, and then purified by column chromatography. The solvent mixture for cholate oligomers is usually methylene chloride/ methanol (20:1) or ethyl acetate/ methanol (15:1). The composition of elute may vary slightly due to the different length and functional groups, but usually falls in the above range.

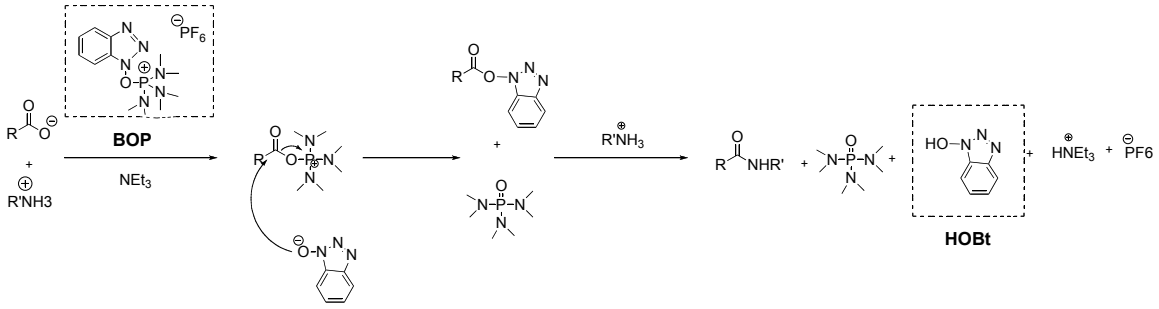

Scheme 9. Mechanism of BOP catalyzed amide coupling

3.4.4. "Click" Reaction

The Huisgen cycloaddition is the reaction of a dipolarophile with a 1,3-dipolar compound that leads to a 5-membered heterocycle.[5] The copper(I)-catalyzed cycloaddition between azide and alkyne proceeds through a stepwise mechanism as shown in Scheme 10. According to Rodionov et al.[12], the mechanism starts by coordination of the alkyne **15** to Cu(I) , displacement of one ligand, and then re-coordination to give copper acetylide **17**. In the next step, azide **18** replaces one of the ligands and the copper complex binds to the nitrogen adjacent to the carbon, forming intermediate **19**. Attack by the terminal nitrogen of **19** on C-2 in the acetylide forms the unusual six-membered Cu(III) intermediate **20**. Rearrangement of **20** gives the five-membered specie **21**, which is transformed to **22** by proteolysis. The copper (I) is generated in situ by using Cu(II)SO_4.5H_2O and sodium ascorbate as reducing agent. Cu(0), derived from copper turnings, has also resulted in regiospecific reactions.[5,12] According to our previous research, "click" chemistry worked very well in oligocholates synthesis. A cholate hexamer with one or two azide groups and a trimer with an alkynyl group were stirred with $CuSO_4 \cdot 5H_2O$ and sodium ascorbate in THF/MeOH/H_2O at 60 °C. The reaction proceeded smoothly and was complete within 2 days. Preparative TLC afforded the final products in 50-70% isolated yield. Similar reaction conditions were expected to succeed for the preparation of compounds **12**, **13**, **14** and **15**. Further investigation is still needed for the application of "click" chemistry to different building blocks.

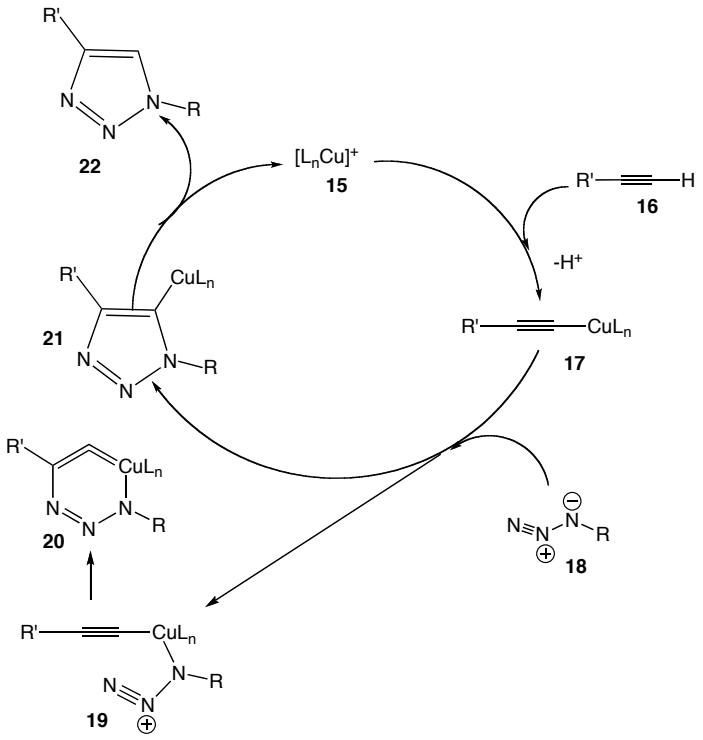

Scheme 10. Mechanism of copper (I) catalyzed Huisgen cycloaddition reaction

3. 5. Conformation Analysis of the Oligomers

The synthesis of the long heterogeneous oligocholates was not completed. The impact of the spacers on the conformation is not clear, but the conformation analysis could be made based on the knowledge from previous research.[4,6,7,8] According to our past learning from the cholate foldamer system, the foldability of the oligomer mainly depends on two factors: the intrinsic folding propensities of the cholate backbone, which comes from the intrinsic curvature and the rigidity of the monomer units, as well as the solvent composition. The nature of the oligomer is a key factor to its foldability. The monomer is composed of four fused rings, which make the parent cholate backbone rather rigid. Conformational freedom only exists near the carboxylic group at the end. As the rotation around C17-C20 is sterically hindered (as shown in Scheme 3), there are only three or four bonds capable of rotation in the entire repeat unit. Therefore, the short, inflexible spacers provide the curvature needed in a folding conformation. Solvent composition also has a profound influence on the folding.

When the solvent mixture has similar preference for the α and the β faces, conformational entropy favors the unfolded, random conformation of a linear molecule over the folded, compact conformation. When the mixture is comprised largely of a nonpolar solvent and a small amount of a polar solvent, which preferentially solvates the hydrophobic β faces, the molecule is expected to bury the α faces. Several possibilities exist to minimize the high energy solvophobic exposure, including precipitation, intermolecular aggregation, self aggregation and folding into a helical structure. If sufficiently low concentration is used, precipitation and intermolecular aggregation are excluded. Previous research[5] also ruled out the possibility of self-aggregation for the parent oligomer, since the tether spacers are short, inflexible and non-hydrogen bonding. When longer and more flexible linkers, such as 4-aminobutyroyl spacers, were introduced in between each unit, the oligomer still favored the helix structure to self-aggregation, which was suggested by the chain-length dependence experiment in our previous research.[8] Most of the spacers employed in our research are aliphatic spacers. What would happen if we incorporate other types of spacers in our research? A recent research revealed the aspartate-triazole linker did not destroy, but rather enhanced the foldability of the compounds despite the introduction of a heterocyclic ring introduced by "click" chemistry. [6]

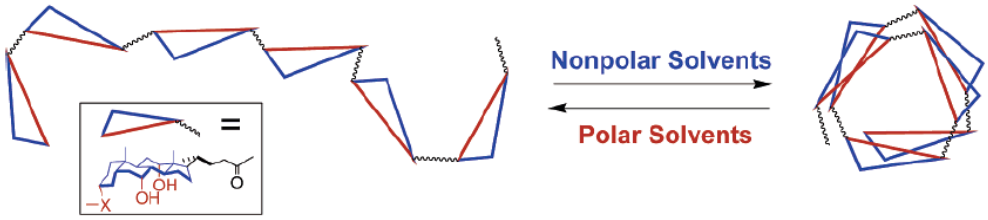

Scheme 11. The proposed folding structure of the parent oligomer.[4]

In our current research, spacers were only introduced between the second and third unit. At a low concentration, complete self-aggregation can be ruled out due to the rigidity of other joints. There are two possibilities for the conformations of foldamer in the non-polar solvent mixture: the hexamer could be stabilized by intra and inter hydrogen bonding to fold

at the joint between the second and third units so that two terminal cholates can hydrogen bond with its immediate neighbor, or curl into a helical structure, in which a few polar solvent molecules are concentrated from the bulk and preferentially solvate the introverted polar groups of the oligocholates (Scheme 8). The foldability of oligomers **12**, **13**, **14** and **15** are still unclear. Compound **12** has two additional rotatable bonds to the parent oligomer, compound **13** five more, and compound **14** ten more. It is hypothesized that compound **12** and **13** are likely to fold just as the parent foldamers. The foldability of **14** is difficult to predict (Scheme 12). Incorporation of a rigid aromatic spacer was also planned for oligomer **14.** The aggregation dimer form, which is discussed for the oligomers **12, 13** and **14** is not attainable since the aromatic joint is rigid with a 60^{o} angle. It is possible the oligomer **15** could adopt a distorted helix as shown in Scheme 13.

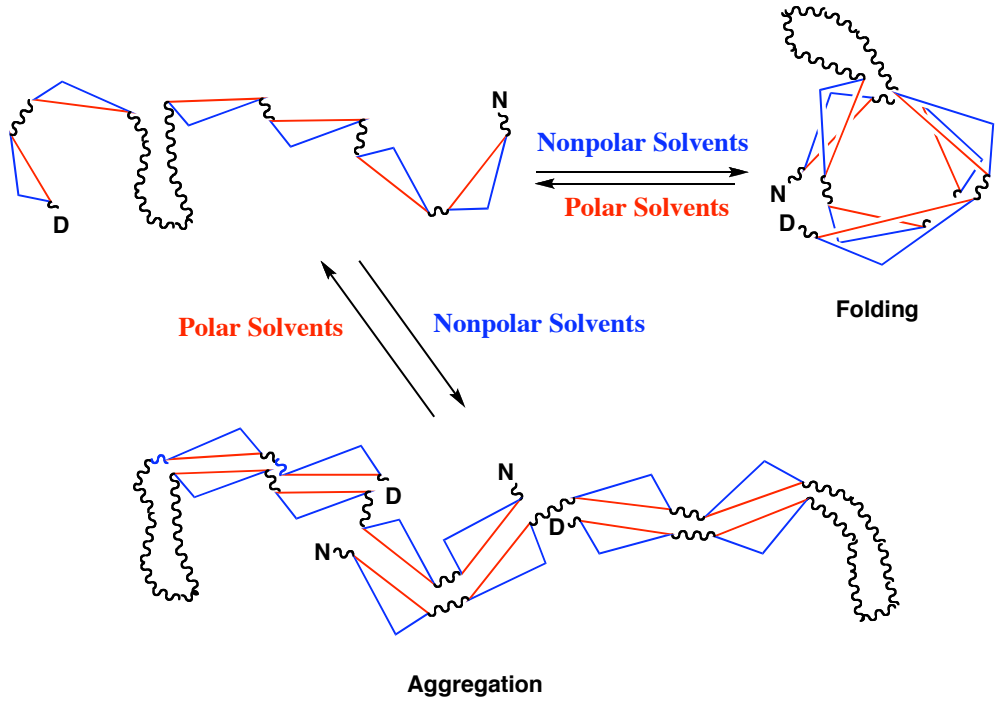

Scheme 12. Conformation change for the 2,3-spaced oligomers in different solvents

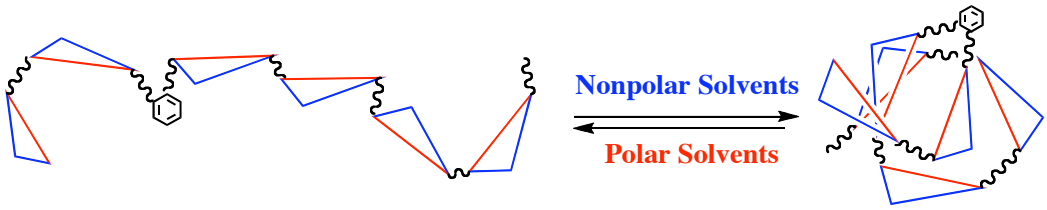

Scheme 13. The proposed folding structure of spaced oligomer **15**

The dansyl and naphthalene groups in oligocholates **12, 13, 14** and **15** are designed to allow the use of fluorescence resonance energy transfer (FRET) to study its conformational behavior. Fluorescence resonance energy transfer (FRET) is a powerful technique for conformational analysis. The energy-transfer efficiency (E) is related to the donor-acceptor (D-A) distance (r) by the following equation: $E = R_o^6/(R_o^6 + r^6)$, in which R_o is the Förster distance for a specific D-A pair. Because a typical R_o (2-6 nm) is comparable to the diameters of proteins, FRET has been widely used in the conformational study of biomolecules. On the other hand, when the donor and acceptor are in proximity (1-10 nm) due to the interaction of the two fluorophores, the acceptor emission is enhanced because of the intermolecular FRET from the donor to the acceptor. According to the CPK model, the end-to-end distance of the fully folded hexamer is 1-1.5 nm. Separated by six cholates in between, the distance between dansyl group and naphthalene group are reasonably close in space to allow the observation of acceptor emission. The donor molecule naphthyl absorbs at 300 nm and emits around 360 nm, where the acceptor dansyl has strong absorption. In FRET, one ideally wants to irradiate the donor at a wavelength where the acceptor does not absorb at all (to avoid direction excitation of the acceptor), but such selectivity is rarely found. Because the largest difference in absorbance for dansyl and naphthyl occurs at 287 nm, fluorescence spectra should be first collected with the compounds excited at this wavelength.

To evaluate the folding of these spaced oligocholates, we could study the emission of the oligomers in 2:1 hexane/ethyl acetate (EA) with 1-10% MeOH. This solvent system represents one of the most "folding-friendly" for the parent foldamer. Since hexane is not miscible with methanol but EA is; having hexane in the mixture facilitates the phase-

separation of methanol. The solvent mixture, with the polar solvent to microphase-separate from the bulk, has a lower energetic cost in the demixing and is beneficial to the helix folding.

4. Conclusions

The attempted synthesis showed the synthetic potential of this project, and possible results of the experiments have been discussed. Further effort is needed to complete the project. However, improvements have been made to the synthesis of the monomer, which will benefit the research group in the future.

5. Acknowledgements

Is made to the Prof. Yan Zhao and the research group at Iowa State University for the training and helpful discussion. A special thanks is also given to the Chinese Evangelical Free Church for the great support in every way.

6. Experimental

6.1. General method

Anhydrous tetrahydrofuan (THF) and methylene chloride (CH_2Cl_2) were dried by passage through a column of activated alumina under compressed nitrogen. Methanol, hexanes, and ethyl acetate were of HPLC grade and were purchased from Fisher Scientific. All other reagents and solvents were of A. C. S. certified grade or higher, and were used as received from commercial suppliers. All glassware and syringes were dried in an oven at least overnight prior to use. Routine ^{1}H and ^{13}C NMR spectra were recorded on Bruker 400 or Varian VXR-400 spectrometer.

6.2. Synthesis of Compounds

The syntheses of compounds **2**, **3**, **4**, **7**, **A** and **B** were reported previously.[4]

6.2.1. Synthesis of Compound 1:

β-cholate **1C** (1.51 g, 3.57 mmole) was purged with nitrogen for 30 min, and dissolved in anhydrous THF (40 mL). Triethylamine (TEA, 1.10 mL, 5.36 mmole) was added dropwise via a syringe. The reaction was cooled with ice-water bath, and methanesulfonyl chloride (MsCl, 1.10 mL, 5.36 mmole) was slowly added to the reaction with a syringe. The ice-water bath is removed, and the reaction mixture was stirred at room temperature under nitrogen, and monitored with TLC and diluted in ethyl acetate after 3 hours. Hydrochloric acid was added (1M, 5.36 mL) to neutralize triethylamine. The solvent was removed in *vacuo*, giving a solid product **1D**.

The solid product and NaN_3 (1.38 g, 2.13 mmol) were dissolved in 10 mL DMF. The reaction was stirred at 40 ^oC and monitored by TLC. The reaction mixture was slowly added to a stirred solution of ice water (30 mL), the crude product was extracted using ethyl acetate, and was purified by column chromatography over silica gel with hexane/ethyl acetate (3:1) as the eluent to give an ivory powder product (**1**). (1.10 g, 69%). ^1H NMR (400 MHz, $CDCl_3/CD_3OD$, δ): 3.92 (br, 1H), 3.79 (br, 1H), 3.64 (s, 3H), 3.13 (m, 1H), 2.38–1.00 (series of m, 25H), 0.96 (d, J = 6.0Hz, 3H), 0.90(s, 3H), 0.67(s, 3H).

6.2.2. Synthesis of Compound 5:

A mixture of dimer acid **3** (0.99 g, 1.21 mmol), dimer amine **4** (0.98 g, 1.22 mmol), 1H-benzotriazol-1-yloxytris-(dimethylamino)phosphonium hexafluorophosphate (BOP, 0.64 g, 1.46 mmol) and HOBt (0.212 g, 1.57 mmol) was dissolved in anhydrous DMF. Diisopropylethylamine (DIPEA, 0.6 mL, 3.63 mmol) was added via a syringe, and the reaction was stirred at 70 ^oC for 14 h under nitrogen. The reaction mixture was then slowly

added to a stirred solution of ice water (30 mL). The crude product was collected by suction filtration, washed with water, dried in air, and purified by column chromatography over silica gel with ethyl acetate/methanol (10/1) as the eluent to give an ivory powder product **5** (2.09 g, 100%). ^{1}H NMR (400 MHz, $CDCl_3/CD_3OD$, δ): 3.97 (br, 4H), 3.80 (s, 4H), 3.70 (br, 3H), 3.48(m, 1H), 3.18 (m, 1H), 2.38–1.00 (series of m, 48H), 1.35 (br, 12H), 0.95(br, 12H), 0.71(br, 12H).

6.2.3. Synthesis of Compound 6:

(a) Tetramer **5** (0.7 g, 0.44 mmol) was dissolved in 20 mL MeOH, and 2M LiOH (5mL) was added dropwise. The reaction mixture was allowed to stir overnight, and monitored with TLC. Solvent was removed *in vacuo*, and neutralized with 2M HCl. An ivory powder product tetramer acid was isolated via vacuum filtration (0.64 g, 92%). ^{1}H NMR (400 MHz, $CDCl_3/CD_3OD$, δ): 3.97 (br, 4H), 3.80 (s, 4H), 3.48 (m, 1H), 3.18 (m, 1H), 2.38–1.00 (series of m, 98H), 1.03 (br, 12H), 0.94 (br, 12H), 0.70 (br, 12H).

(b) Tetramer acid (0.67g, 0.42 mmole), 1H-benzotriazol-1-yloxytris-(dimethylamino) phosphonium hexafluorophosphate (BOP, 0.40g, 1.26 mmol) and HOBt (0.07 g, 0.42 mmol) was dissolved in 20 mL DMF. Diisopropylethylamine (DIPEA, 0.43g, 3.36 mmol) was added to the reaction mixture dropwise, and the reaction stayed overnight. 1-aminonaphathaline (0.31 g, 2.10 mmol) was then added. The reaction mixture was stirred for 6 days under nitrogen, and monitored with TLC. The reaction mixture was then slowly added to a stirred solution of ice water (30 mL). The crude product was collected by suction filtration, washed with acetonitrile, dried in air, and purified by column chromatography over silica gel with ethyl acetate/methanol (20/1) as the eluent to give an ivory powder product **6** (0.36 g, 50%). ^{1}H NMR (400 MHz, $CD_3OD/CDCl_3$, δ): 3.97 (br, 4H), 3.80 (s, 4H), 3.48 (m, 1H), 3.18 (m, 1H), 2.38–1.00 (series of m, 98H), 1.03 (br, 12H), 0.94 (br, 12H), 0.70 (br, 12H). ^{13}C NMR (400 MHz, $CD_3OD/CDCl_3$, δ): 174.94, 174.73, 174.65, 134.60, 133.13, 128.88, 128.73, 126.66, 126.47, 126.36, 125.87, 122.94, 122.41, 73.40, 73.34, 68.48, 68.29,

61.96, 46.90, 46.81, 46.60, 42.02, 36.24, 34.95, 31.97, 26.85, 22.93, 17.52, 12.85, 12.74, 12.69.

6.2.4. Synthesis of Compound 7:

Dimer amine **4** (0.10 g, 0.38 mmol) was dissolved in 4 mL CH_2Cl_2, and 0.10 mL Et_3N was added to the mixture dropwise via syringe, dansyl chloride (0.10 g, 0.38 mmol) was then added to the solution. The reaction was allowed to stir at room temperature under nitrogen for 6 h. The product was purified by column chromatography over silica gel, with CH_2Cl_2 / MeOH (12/1) as the eluent to give an ivory powder product **7**. (0.11 g, 58 %). ^{1}H NMR (400 MHz, $CDCl_3$, δ): 0.85 (d, J = 8.8 Hz, 2H), 8.34 (d, J = 8.4 Hz, 2H), 8.20 (d, J = 6.4Hz, 2H), 7.53 (m, 2H), 7.44 (d, J = 7.6Hz, 1H), 3.95 (br, 1H), 3.88 (br, 1H), 3.79 (br, 1H), 3.70 (br, 1H), 3.64 (br, 1H), 3.48 (br, 1H), 2.85 (br, 7H), 1.00 (br, 6H), 0.92 (br, 3H), 0.80 (br, 3H), 0.70 (br, 3H), 0.64 (br, 3H). ^{13}C NMR spectrum (400 MHz, $CDCl_3$, δ):175.13, 174.56, 174.47, 151.68, 137.02, 129.67, 127.59, 122.99, 119.57, 115.07, 114.98, 105.05, 72.53, 67.62, 67.47, 50.79, 46.16, 42.48, 41.64, 37.31, 35.60, 34.49, 32.94, 30.57, 27.42, 26.44, 21.92, 16.36, 11.77, 11.75.

6.2.5. Synthesis of Compound 8:

(a) Dansyl dimer **7** (0.10 g, 0.02 mmol) was dissolved in 10 mL MeOH, and 2M LiOH (1 mL) was added to the solution dropwise. The reaction mixture was allowed to stir overnight, and monitored with TLC. Solvent was removed *in vacuo*, and neutralized with 2M HCl. Ivory powder product dansyl dimer acid was isolated via vacuum filtration (0.10 g, 100%). ^{1}H NMR (400 MHz, $CDCl_3$, δ): 8.52 (d, J = 8.4Hz, 1H), 8.46 (br, 1H), 8.24 (d, 1H), 7.63 (br, 2H), 7.42 (br, 1H), 3.97 (br, 1H), 3.90 (br, 1H), 3.80 (br, 1H), 3.71 (br, 1H), 3.48 (br, 1H), 3.00 (br, 1H), 2.85 (br, 1H), 1.00 (br, 6H), 0.94 (br, 3H), 0.82 (br, 3H), 0.72 (br, 3H), 0.66 (br, 3H).

(b) Dansyl dimer acid (0.10 g, 0.22 mmol), 1H-benzotriazol-1-yloxytris-(dimethylamino) phosphonium hexafluorophosphate (BOP, 0.29 g, 0.65 mmol) and HOBt (0.056 g, 0.44 mmol) was dissolved in 20mL DMF. Diisopropylethylamine (DIPEA, 0.298 mL, 1.73 mmol) was added to the reaction mixture dropwise, and the reaction was allowed to stir for 20 min. Propargyl amine (0.040 mL, 0.65 mmol) was then added. The reaction mixture was stirred for 12 h under nitrogen, and monitored with TLC. The reaction mixture was then slowly added to a stirred solution of ice water (30 mL). The crude product was collected by suction filtration, washed with water, dried in air, and purified by column chromatography over silica gel with ethyl acetate/methanol (10/1) as the eluent to give a greenish yellow powder product **8** (0.70 g, 65%). ^{1}H NMR (400 MHz, $CD_3OD/CDCl_3$, δ): 8.85 (d, J = 8.8 Hz, 2H), 8.34 (d, J = 8.4 Hz, 2H), 8.20 (d, J = 6.4Hz, 2H), 7.53 (m, 4H), 7.44 (d, J = 7.6Hz, 1H), 3.96 (br, 1H), 3.89 (br, 1H), 3.79 (br, 1H), 3.70 (br, 1H), 3.64 (br, 1H), 3.48(br, 1H), 3.27 (br, 2H), 2.95 (br, 2H), 2.88 (br, 7H), 2.72 (br, 2H), 1.00 (br, 6H), 0.92 (br, 3H), 0.80 (br, 3H), 0.70 (br, 3H), 0.64 (br, 3H). ^{13}C NMR (400 MHz, $CD_3OD/CDCl_3$, δ): 209.94, 175.89, 175.87, 175.22, 152.49, 152.46, 138.89, 137.23, 130.62, 129.53, 128.62, 128.58, 127.51, 123.93, 120.14, 120.10, 115.88, 80.23, 80.20, 73.66, 73.58, 72.39, 71.68, 68.75, 68.62, 54.79, 54.27, 50.27, 47.61, 47.43, 47.09, 45.89, 43.55, 42.95, 42.77, 42.49, 42.39, 40.15, 40.08, 38.15, 36.31, 35.31, 35.01, 34.05, 33.42, 32.59, 30.36, 29.33, 28.00, 27.13, 24.99, 24.34, 23.90, 23.82, 23.20, 23.00, 19.90, 17.95, 17.92, 17.67, 17.64, 12.98, 12.92.

6.2.6. Synthesis of Compound 9:

Dansyl dimer **7** (0.20 g, 0.42 mmol) was dissolved in 2 mL ethylenediamine. The reaction mixture was allowed to reflux for 12 h, and monitored with TLC. The extra ethylenediamine was removed *in vacuo*. The product was purified by column chromatography over silica gel, with ethyl acetate / methanol (1/ 6) as the eluent to give an ivory powder product **9** (0.04 g, 19 %). ^{1}H NMR (400 MHz, CDCl3/CD_3OD, δ): 0.85 (d, J = 8.8 Hz, 2H), 8.34 (d, J = 8.4 Hz, 2H), 8.20 (d, J = 6.4Hz, 2H), 7.53 (m, 4H), 7.44 (d, J = 7.6Hz, 1H), 3.96 (br, 1H), 3.89 (br, 1H), 3.79 (br, 1H), 3.70 (br, 1H), 3.64 (br, 1H), 3.48(br,

1H), 3.27 (br, 2H), 2.95 (br, 2H), 2.88 (br, 7H), 2.72 (br, 2H), 1.00 (br, 6H), 0.92 (br, 3H), 0.80 (br, 3H), 0.70 (br, 3H), 0.64 (br, 3H).

7. References

1 For several recent reviews, see: (a) Gellman, S. H. *Acc. Chem. Res.* **1998**, *31*, 173-180. (b) Kirshenbaum, K.; Zuckermann, R. N.; Dill, K. A. *Curr. Opin. Struct. Biol.* **1999**, *9*, 530-535. (c) Stigers, K. D.; Soth, M. J.; Nowick, J. S. *Curr. Opin. Chem. Biol.* **1999**, *3*, 714-723. (d) Hill, D. J.; Mio, M. J.; Prince, R. B.; Hughes, T. S.; Moore, J. S. *Chem. Rev.* **2001**, *101*, 3893-4012. (e) Cubberley, M. S.; Iverson, B. L. *Curr. Opin. Chem. Biol.* **2001**, *5*, 650-653. (f) Sanford, A. R.; Gong, B. *Curr. Org. Chem.* **2003**, *7*, 1649-1659. (g) Martinek, T. A.; Fulop, F. *Eur. J. Biochem.* **2003**, *270*, 3657-3666. (h) Cheng, R. P. *Curr. Opin. Struct. Biol.* **2004**, *14*, 512-520. (i) Huc, I. *Eur. J. Org. Chem.* **2004**, 17-29. (j) Licini, G.; Prins, L. J.; Scrimin, P. *Eur. J. Org. Chem.* **2005**, 969-977. (k) Foldamers: Structure, Properties, and Applications. (Eds.: S. Hecht, I. Huc), Wiley-VCH,. Weinheim, **2007.** (l) Bautista, A. D.; Craig, C. J.; Harker, E. A.; Schepartz, A. *Curr. Opin. Chem. Biol.* **2007**, *11*, 685-692. (m) Saraogi, I.; Hamilton, A. D. *Chem. Soc. Rev.,* **2009**, 38, 1726 – 1743.

2 For some of selected research from Iverson's group, see: (a) Lokey, R. S.; Iverson, B. L. *Nature* **1995**, *375*, 303-305. (b) Nguyen, J. Q.; Iverson, B. L. *J. Am. Chem. Soc.* **1999**, *121*, 2639-2640. (c) Zych, A. J.; Iverson, B. L. *J. Am. Chem. Soc,* **2000***, 122,* 8898-8909. (d) Guelev, V. M.; Harting, M. T.; Lokey, R.S.; Iverson, B. L. *Chem. Bio.* **2000**, *7*, 1-8. (e) Cubberley, M. S.; Iverson, B. L. *J. Am. Chem. Soc,* **2001**, 123, 7560-7563. (f) Guelev, V.; Lee, J.; Ward, J.; Sorey, S.; Hoffman, D. W.; Iverson, B. L. *J. Am. Chem. Soc,* **2002**, *124,* 2864-2865. (g) Gabriel, G. J.; Iverson, B. L. *J. Am. Chem. Soc,* **2002,** *124*, 15174-15175. (h) Lee, J.; Guelev, V.; Sorey, S.; Hoffman, D. W.; Iverson, B. L. *J. Am. Chem. Soc,* **2004,** *126*, 14036-14042. (i) Gabriel, G. J.; Sorey, S.; Iverson, B. L. *J. Am. Chem. Soc,* **2005,** *127*, 2637- 2640.

3 Stone, M. T.; Heemstra, J. M.; Moore, J. S. *Acc. Chem. Res.* **2006**, *39*, 11-20.

4 Zhao, Y.; Zhong, Z. *J. Am. Chem. Soc.* **2005**, *127*, 17894-17901.

5 Meldal, M.; Tornøe, C. W.; *Chem. Rev.* **2008,** *108,* 2952–3015.

6 Pan, X.; and Zhao, Y. *Org. Lett.* **2009,** *11*, 69-72.

7 (a) Zhao, Y.; Zhong, Z. *J. Am. Chem. Soc.* **2006**, *128*, 9988-9989. (b*)* Zhao,Y.; Zhong, Z.; Ryu, E.-H. *J. Am. Chem. Soc.* **2007**, *129,* 218-225.

8 Zhao, Y. J. *Org. Chem.* **2009,** *74,* 834-843.

9 Davis, A. P.; Dresen, S.; Lawless, L. J. *Tetrahedron Lett.* **1997**, *38*, 4305-4308.

10 Montalbetti, C. A. G. N.; Falque, V. *Tetrahedron*, **2005,** *61*,10827–10852.

11 H. Staudinger, J. Meyer, *Helv. Chim. Acta,* **1919**, *2*, 635.

12 Rodionov, V. O.; Fokin, V. V.; Finn, M. G. *Angew. Chem., Int. Ed.* **2005**, *44*, 2210.